REMOVAL OF TRACE CONTAMINANTS FROM COAL-DERIVED SYNTHESIS GAS

TOPICAL REPORT

March 2003

Prepared by

Air Products and Chemicals, Inc.
Allentown, Pennsylvania

and

Eastman Chemical Company
Kingsport, Tennessee

for the
Air Products Liquid Phase Conversion Company, L.P.

Prepared for the United States Department of Energy
National Energy Technology Laboratory
Under Cooperative Agreement No. DE-FC22-92PC90543

Patents cleared by Chicago on 12 December 2002.

DISCLAIMER

This report was prepared by Eastman Chemical Company and Air Products and Chemicals, Inc. for the Air Products Liquid Phase Conversion Company, L.P., pursuant to a Cooperative Agreement partially funded by the U.S. Department of Energy, and neither Air Products & Chemicals, Inc., Eastman Chemical Company, the Air Products Liquid Phase Conversion Company, L.P., nor any of their subcontractors nor the U.S. Department of Energy, nor any person acting on behalf of either:

(A) Makes any warranty or representation, express or implied, with respect to the accuracy, completeness, or usefulness of the information contained in this report, or that the use of any information, apparatus, method, or process disclosed in this report may not infringe privately owned rights; or
(B) Assumes any liabilities with respect to the use of, or for damages resulting from the use of, any information, apparatus, method, or process disclosed in this report.

Reference herein to any specific commercial product, process, or service by trade name, trademark, manufacturer, or otherwise, does not necessarily constitute its endorsement, recommendation, or favoring by the U.S. Department of Energy. The views and opinions of authors expressed herein does not necessarily state or reflect those of the U.S. Department of Energy.

Abstract

The Liquid Phase Methanol (LPMEOH™) Demonstration Project at Kingsport, Tennessee, is a $213.7 million cooperative agreement between the U.S. Department of Energy (DOE) and Air Products Liquid Phase Conversion Company, L.P. (the Partnership) to produce methanol from coal-derived synthesis gas (syngas). Air Products and Chemicals, Inc. (Air Products) and Eastman Chemical Company (Eastman) formed the Partnership to execute the Demonstration Project.

A key challenge for the LPMEOH™ Demonstration Unit has been the identification and removal of potential catalyst poisons from the coal-derived synthesis gas (syngas) feed to the reactor system. This report describes the effort to identify, quantify, and remove chemical components that were found to reduce catalyst performance in the laboratory. Laboratory studies are described, which were used to evaluate the impact of various contaminants on catalyst deactivation. Additional laboratory studies considered the effectiveness of several adsorbents in the removal of the identified catalyst poison species. Trials were conducted in the LPMEOH™ Demonstration Unit 29C-40 catalyst guard bed using identified adsorbents to remove targeted catalyst poisons.

Table of Contents

Abstract ii
Acronyms and Definitions iv
Executive Summary 1
A. Introduction 3
B. Results and Discussion 5
  1. Evaluation of Various Classes of Syngas Contaminants as Methanol Catalyst Poisons 5
    1.1 General Procedures for Syngas Contaminant Evaluation 5
    1.2 Arsenic-Containing Contaminants 6
    1.3 Phosphorus-Containing Contaminants 9
    1.4 Sulfur-Containing Contaminants 10
    1.5 Nitrogen-Containing Contaminants 13
    1.6 Halide-Containing Contaminants 15
    1.7 Volatile Metal Carbonyls 17
    1.8 Evaluation of "Self-Poisoning" 20
    1.9 Poison Comparison 20
  2. Adsorbents for the Removal of Catalyst Poisons from Syngas 23
    2.1 Adsorbent Screening 23
    2.2 Evaluation of Copper-Impregnated Carbon (CuO/C) Adsorbent 27
    2.3 Evaluation of Cu/C for Other Syngas Contaminants. 34
    2.4 Alternate Adsorbents. 36
  3. Analytical Results from Kingsport Samples 39
    3.1 Kingsport Catalyst Campaign 1 40
    3.2 Kingsport Catalyst Campaign 2 40
      3.2.a Catalyst Analysis 41
      3.2.b Mineral Oil Analysis 49
    3.3 Kingsport Catalyst Campaign 3 51
    3.4 Kingsport Catalyst Campaign 4 55
  4. LPMEOH™ Demonstration Unit Contaminant Removal Configurations and Trials 55
    4.1 Impurity Removal Upstream of the LPMEOH™ Demonstration Unit 55
    4.2 LPMEOH™ Demonstration Unit Catalyst Guard Bed (29C-40) Configuration 56
    4.3 Catalyst Guard Bed Adsorbent Trial 59
    4.4 Catalyst Guard Bed Analysis 59
  5. Effect of Trace Contaminants on Catalyst Life in the LPMEOH™ Demonstration Unit 65
    5.1 Overview of Trace Contaminant Issues at the LPMEOH™ Demonstration Unit 65
    5.2 Catalyst Performance: Catalyst Campaign 1 66
    5.3 Catalyst Performance: Catalyst Campaign 2 67
    5.4 Catalyst Performance: Catalyst Campaign 3 70
    5.5 Catalyst Performance: Catalyst Campaign 4 71
C. Conclusions 72
D. References 76

APPENDICES

  APPENDIX A - Experimental Techniques 77

ACRONYMS AND DEFINITIONS

Term:	**Definition:**
AEM	Analytical Electron Microscopy
Air Products	Air Products and Chemicals, Inc.
AFDU	Alternative Fuels Development Unit - The "LaPorte PDU"
atm	Atmosphere (pressure)
Balanced Gas	A synthesis gas with a composition of hydrogen (H_2), carbon monoxide (CO) and carbon dioxide (CO_2) in stoichiometric balance for the production of methanol (approximately 2:1)
Carbon Monoxide Gas	A syngas containing primarily carbon monoxide (CO); also called CO Gas
Catalyst Age (η - eta)	the ratio of the rate constant at any point in time to the rate constant for a freshly reduced catalyst (as determined in the laboratory autoclave)
DOE	United States Department of Energy
DSC	Differential Scanning Calorimeter
Eastman	Eastman Chemical Company
EDS	Energy Dispersive Spectroscopy
FTIR	Fourier Transform Infrared
GC	Gas chromatograph
GHSV	Gas hourly space velocity, defined as standard flow rate (standard cubic centimeters per hour) divided by adsorbent volume (cubic centimeters)
Hydrogen Gas	A syngas containing an excess of hydrogen (H_2) over the stoichiometric balance for the production of methanol; also called H_2 Gas
ICP-AES	Inductively Coupled Plasma Atomic Emission Spectroscopy
IGCC	Integrated Gasification Combined Cycle, a type of electric power generation plant
IR	Infrared Spectroscopy
lb	Pound
Kingsport Gas	See Balanced Gas
LPMEOH™	Liquid Phase Methanol (the technology to be demonstrated)
mL	Milliliter
MS	Mass Spectrometer
na	Not available
nd	Not detected
nm	Nanometer
Partnership	Air Products Liquid Phase Conversion Company, L.P.
ppb	Parts per billion (volume basis)
ppm	Parts per million (volume basis)
ppmw	Parts per million (weight basis)
psig	Pounds per square inch (gauge)
sccm	Standard cubic centimeters per minute
sT/D	Short ton(s) per day
Shell Gas	A syngas rich in carbon oxides (approximately 30 vol% H_2, 66 vol% CO, 3 vol% CO_2, 1 vol% N_2)
Syngas	Abbreviation for Synthesis Gas
Synthesis Gas	A gas containing primarily hydrogen (H_2), carbon monoxide (CO), or mixtures of H_2 and CO; intended for "synthesis" in a reactor to form methanol and/or other hydrocarbon products (Synthesis gas may also contain carbon dioxide (CO_2), water, and other gases)
TGA	Thermal Gravimetric Analysis
TOS	Time on stream
UV	Ultraviolet Spectroscopy (analysis method)

ACRONYMS AND DEFINITIONS (cont'd)

Term:	**Definition:**
vol%	Volume %
wt%	Weight %
XAS	X-ray Absorption Spectroscopy
XPS	X-ray Photoelectron Spectroscopy
XRD	X-ray Diffraction
XRF	X-ray Fluorescence

Executive Summary

The Liquid Phase Methanol (LPMEOH™) Demonstration Project at Kingsport, Tennessee, is a \$213.7 million cooperative agreement between the U.S. Department of Energy (DOE) and Air Products Liquid Phase Conversion Company, L.P. (the Partnership) to produce methanol from coal-derived synthesis gas (syngas). Air Products and Chemicals, Inc. (Air Products) and Eastman Chemical Company (Eastman) formed the Partnership to execute the Demonstration Project. The LPMEOH™ Demonstration Unit was designed, constructed, and operates at a site located at the Eastman chemicals-from-coal complex in Kingsport.

The project involves the operation of an 80,000-gallons-per-day (260-short-tons-per-day (sT/D)) methanol unit utilizing coal-derived syngas from Eastman's integrated coal gasification facility. The new equipment consists of syngas feed preparation and compression facilities, the liquid phase reactor and auxiliaries, product distillation facilities, and utilities.

One of the long-term goals for the LPMEOH™ Demonstration Unit is the determination of the change in catalyst performance with time due to exposure to the trace contaminants present in coal-derived syngas. This topical report examines the identification of potential catalyst poisons and their effects on catalyst performance, the selection of suitable adsorbents to be used in a fixed catalyst guard bed configuration for the removal of targeted catalyst poisons, and the implementation and evaluation of the performance of the adsorbents in the LPMEOH™ Demonstration Unit.

Laboratory studies were used to evaluate the effect of various potential catalyst poisons in the syngas on the methanol synthesis catalyst deactivation rate. A relative ranking of these poisons was developed and used to determine which contaminant species needed to be targeted for removal. Based on the results of this study, the following ranking of methanol synthesis catalyst poison strength was obtained: nickel carbonyl ($Ni(CO)_4$) > iron carbonyl ($Fe(CO)_5$) > thiophene $\cong$ arsine (AsH_3) > methyl chloride (CH_3Cl) > methyl thiocyanate (CH_3SCN) > carbon disulfide (CS_2) > carbonyl sulfide (COS) > phosphine (PH_3) > methyl fluoride (CH_3F). The nitrogen containing species methyl amine (CH_3NH_2), acetonitrile (CH_3CN), and hydrogen cyanide (HCN) were determined to not be catalyst poisons during this study. Mercury was determined not to be present in the syngas supplied to the LPMEOH™ Demonstration Unit and, therefore, was not considered as part of this laboratory evaluation.

Initially, iron and nickel carbonyl were targeted as the main poisons of concern at the LPMEOH™ Demonstration Unit based on their relative ranking and expected occurrence in the coal-derived syngas. However, after several years of operation at the facility, both iron and nickel carbonyl were not determined to be appreciably present in the fresh syngas supplied. However, arsenic (most likely in the form of arsine) and to a lesser degree hydrogen sulfide and carbonyl sulfide (forms of sulfur) were all determined to be present in the fresh syngas supplied to the LPMEOH™ Demonstration Unit. This led to the requirement to identify adsorbents with particular affinity for arsenic and potential affinity for sulfur.

Ten adsorbents were screened for effectiveness for arsenic removal and for safe usage under syngas in the laboratory. The adsorbents consisted of various metal oxides supported on alumina or carbon and, in one case, carbon alone. A copper oxide on carbon (CuO/C) adsorbent was judged to be the most suitable adsorbent and it was evaluated more thoroughly.

The arsenic affinity of CuO/C was very high with a minimum capacity of 3.0 weight % arsenic. The reduced adsorbent, Cu/C, was much less effective for AsH_3 removal and at 30 °C its capacity was 1.74 weight % but its effectiveness was substantially better at elevated temperature with a minimum arsenic capacity of 4.31 weight % at 140 °C. (In this case, reduction refers to the reaction of the copper oxide with a reductant such as CO or hydrogen (H_2) to copper metal and either carbon dioxide (CO_2) or water (H_2O)).

Two different adsorbents to target arsenic were evaluated at the LPMEOH™ Demonstration Unit during Catalyst Campaigns 2 through 4. During Catalyst Campaign 2 (December 1997 – July 2001), the 29C-40 catalyst guard bed was charged with 50% manganese dioxide and 50% activated carbon. The manganese dioxide adsorbent displayed affinity for arsenic removal but the adsorbent exhibited breakthrough (based on gas phase arsine analysis) after approximately one month of service. During Catalyst Campaigns 3 and 4 (August 2001 – present), a copper oxide impregnated activated carbon adsorbent was reduced and placed into service. This adsorbent was effective in arsenic removal as determined by gas phase analysis and catalyst sample results. Reduced copper oxide impregnated activated carbon had a service life of about two months based on gas phase analysis of arsine. An innovative thermal treatment was employed to extend the service life of the adsorbent two additional months.

Catalyst Campaign 4 at the LPMEOH™ Demonstration Unit was the second campaign to use an in-situ activation procedure. Catalyst performance during this campaign was excellent with an approximate catalyst deactivation rate of 0.1 to 0.2 % per day during the first 6 months of operation. In addition, during this time, the initial LPMEOH™ reactor temperature of 215 °C was not changed. This improved result may have been related to the performance of the adsorbent in the 29C-40 catalyst guard bed, to the removal of carbon steel components from the reactor internals, and to the operation of the LPMEOH™ reactor at reduced temperature (temperature programming).

Although several different adsorbents were evaluated in the LPMEOH™ Demonstration Unit, it was difficult to positively correlate catalyst performance, as measured by catalyst activity or eta, with the adsorbent performance. This was due to the presence of other variations in operation not related to the adsorbent, such as upstream gas composition, which can result in variations in the kinetic model predictions of eta. The copper oxide-impregnated activated carbon was found to be effective for arsenic removal at ambient temperature based on results from gas phase arsine analysis (in and out of the 29C-40 catalyst guard bed) and also based on analysis of catalyst samples from the LPMEOH™ reactor.

A. Introduction

The Liquid Phase Methanol (LPMEOH™) Demonstration Project at Kingsport, Tennessee, is a \$213.7 million cooperative agreement between the U.S. Department of Energy (DOE) and Air Products Liquid Phase Conversion Company, L.P., a partnership between Air Products and Chemicals, Inc. (Air Products) and Eastman Chemical Company (Eastman), to produce methanol from coal-derived synthesis gas (syngas)[1]. Construction of the LPMEOH™ Demonstration Unit at Eastman's chemicals-from-coal complex in Kingsport was completed in January 1997. Following commissioning and shakedown activities, the first production of methanol from the facility occurred on 02 April 1997. Nameplate capacity of 260 short tons per day (sT/D) was achieved on 06 April 1997, and production rates have exceeded 300 sT/D of methanol during test periods. Since startup, overall availability has exceeded 97.5%. Eastman has accepted all of the greater than 103.9 million gallons of methanol produced to date at the LPMEOH™ Demonstration Unit for use in downstream chemical processes.

Sponsored under the DOE's Clean Coal Technology Program, the LPMEOH™ Demonstration Project culminates an extensive cooperative development effort by Air Products and DOE in a program that began in 1981. By the late 1980s, the technology was proven in over 7,400 hours of test operation at a 10-sT/D rate in the DOE-owned Alternative Fuels Development Unit (AFDU) in LaPorte, Texas. Developed to enhance electric power generation using integrated gasification combined cycle (IGCC) technology, the LPMEOH™ Process exhibits several features essential for the economic coproduction of methanol and electricity in the IGCC scenario.

The slurry bubble column reactor differentiates the LPMEOH™ Process from conventional technology. Conventional methanol reactors use fixed beds of catalyst pellets and operate in the gas phase. The LPMEOH™ reactor uses catalyst in powder form, slurried in an inert mineral oil. The mineral oil acts as a temperature moderator and heat removal medium, transferring the heat of reaction away from the catalyst surface to boiling water in an internal tubular heat exchanger. Since the heat transfer coefficients on both sides of the exchanger are relatively large, the heat exchanger occupies only a small fraction of the cross-sectional area of the reactor. As a result of this capability to remove heat and maintain a constant, highly uniform temperature throughout the entire length of the reactor, the slurry reactor can achieve much higher syngas conversion per pass than its gas-phase counterparts.

Furthermore, because of the LPMEOH™ reactor's unique temperature control capabilities, it can directly process syngas rich in carbon oxides (carbon monoxide (CO) and carbon dioxide (CO_2)). Gas-phase methanol technology would require that syngas feedstocks with similar compositions undergo stoichiometry adjustment by the water-gas shift reaction, to increase the hydrogen content, and subsequent CO_2 removal. In a gas-phase reactor, temperature moderation is achieved by recycling large quantities of hydrogen (H_2)-rich gas, utilizing the higher gas velocities around the catalyst particles and minimizing the conversion per pass. Typically, a gas-phase process is limited to CO concentrations of about 16 volume % (vol%) in the reactor feed, as a means of constraining the conversion per pass to avoid excess heating. In contrast, for the LPMEOH™ reactor, CO concentrations in excess of 50 vol% have been tested in the laboratory, at the AFDU in LaPorte, and at Kingsport, without any adverse effect on catalyst activity. As a result, the LPMEOH™ reactor can achieve approximately twice the conversion per pass of the gas-phase process, yielding lower recycle gas compression requirements and capital savings.

A second distinctive feature of the LPMEOH™ reactor is its robust character. The slurry reactor is suitable for rapid ramping, idling, and even extreme stop/start actions. The thermal moderation provided by the liquid inventory in the reactor acts to buffer sharp transient operations that would not normally be tolerable in a gas-phase methanol synthesis reactor. This characteristic is especially advantageous in the environment of electricity demand load following in IGCC facilities.

A third differentiating feature of the LPMEOH™ Process is that a high quality methanol product is produced directly from syngas rich in carbon oxides. Gas-phase methanol synthesis, which must rely on H_2-rich syngas feedstocks, yields a crude methanol product with 4 weight % (wt%) to 20 wt% water. The product from the LPMEOH™ Process, using CO-rich syngas, typically contains only 1 wt% water. As a result, raw methanol coproduced in an IGCC facility would be suitable for many applications at a substantial savings in purification costs. The steam generated in the LPMEOH™ reactor is suitable for purification of the methanol product to a higher quality or for use in the IGCC power generation cycle.

Another unique feature of the LPMEOH™ Process is the ability to withdraw spent catalyst slurry and add fresh catalyst on-line periodically. This facilitates uninterrupted operation and also allows perpetuation of high production rate of methanol from the reactor. Furthermore, choice of catalyst replacement rate permits optimization of methanol production rate versus catalyst replacement cost.

Figure 1 provides a simplified process flow diagram of the LPMEOH™ Demonstration Unit in Kingsport. Three different feed gas streams (hydrogen gas or H_2 Gas, carbon monoxide gas or CO Gas, and the primary syngas feed known as Balanced Gas) are diverted from existing operations to the LPMEOH™ Demonstration Unit, thus providing the range of coal-derived syngas ratios (H_2 to CO) needed to meet the technical objectives of the demonstration project. Syngas enters the bottom of the slurry reactor, which contains solid particles of catalyst suspended in liquid mineral oil. The syngas dissolves through the mineral oil, contacts the catalyst surface, and reacts to form methanol. The highly exothermic heat of reaction is absorbed by the slurry and removed from the reactor by steam coils. The product methanol vapor diffuses from the catalyst surface through the mineral oil, and exits the reactor with unreacted syngas, is condensed to a liquid, and sent to distillation columns for removal of higher alcohols, water, and other impurities. Most of the unreacted syngas is returned to the reactor by the syngas recycle compressor, improving overall cycle efficiency.

This report describes the identification and removal of trace contaminants from syngas in the LPMEOH™ Process. Laboratory studies were used to evaluate the effect of various classes of poisons on catalyst performance. Additional laboratory studies determined adsorbent effectiveness in removing these contaminants from the syngas feed stream. Selected adsorbents were incorporated in the LPMEOH™ Demonstration Unit to evaluate commercial-scale trace contaminant removal.

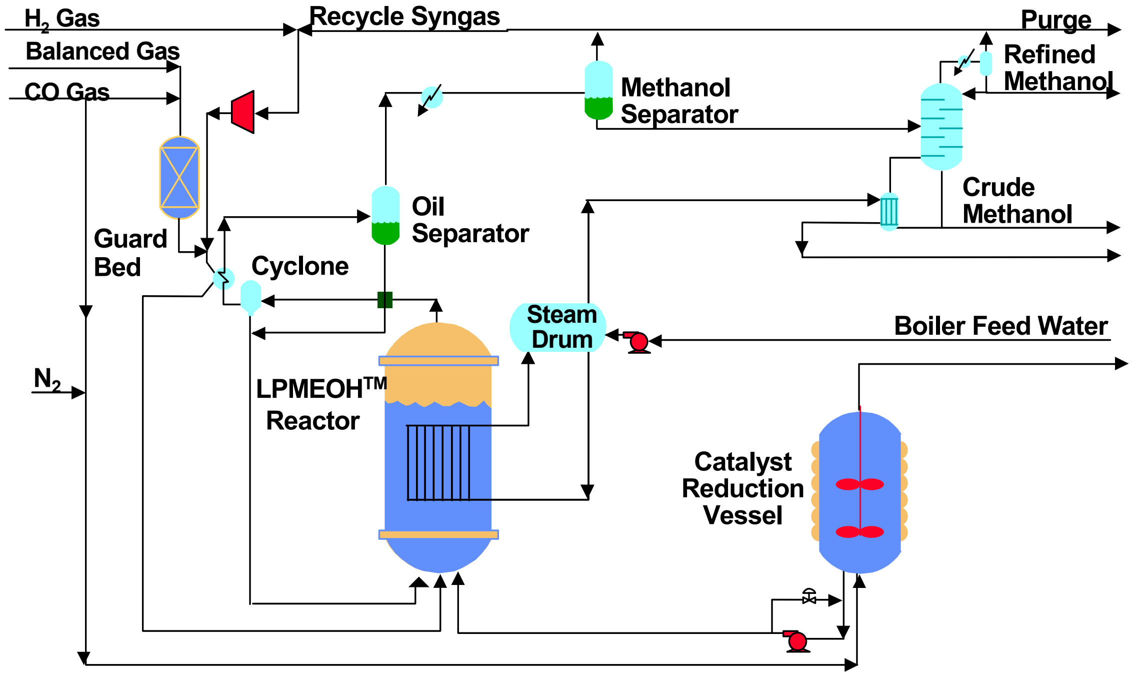

Figure 1. Kingsport LPMEOH™ Demonstration Unit Process Flow Diagram.

B. Results and Discussion

1. Evaluation of Various Classes of Syngas Contaminants as Methanol Catalyst Poisons

1.1 General Procedures for Syngas Contaminant Evaluation

The details of the equipment used to study the effects of syngas contamination on catalyst activity are described in Appendix A. The effects of a syngas contaminant on catalyst activity were determined by comparing the methanol catalyst deactivation rate in the presence and absence of the contaminant in the laboratory. The catalyst was initially exposed to clean syngas until a baseline deactivation rate could be calculated, usually 150 hours or longer. Approximate syngas feed compositions tested included: Kingsport Gas, a syngas with a composition approaching the stoichiometric balance for methanol synthesis (68 vol% H_2, 23 vol% CO, 5 vol% CO_2, 4 vol% nitrogen [N_2]); and Shell Gas, a syngas rich in carbon oxides (30 vol% H_2, 66 vol% CO, 3 vol% CO_2, 1 vol% N_2). The contaminant was then introduced into the feed by blending with a pre-mixed cylinder gas containing part per million by volume (ppm) levels of the contaminant in 5 vol% CO and 95 vol% H_2. Following exposure to the contaminant, the catalyst was again exposed to clean syngas to determine if the poisoning effects continued after the contaminant was eliminated from the feed. All of the experimental studies presented in this report used the alternative methanol synthesis catalyst that has been used at the LPMEOH™ Demonstration Unit since October of 1998.

1.2 Arsenic-Containing Contaminants

A wealth of analytical data from the analysis of adsorbent from the catalyst guard bed, catalyst from the LPMEOH™ reactor, and Balanced Gas have conclusively shown that an arsenic containing species is the most significant syngas contaminant, and hence the most likely catalyst poison, at the LPMEOH™ Demonstration Unit. Although the identity of the gas phase species was not determined experimentally, arsine, AsH_3, is the most reasonable. Coal contains arsenic in various, predominantly oxidized forms. Gasification of arsenic oxides or related nonmetallic oxides results in formation gaseous hydrides, specifically arsine in the case of arsenic.[2] Arsine has generally been viewed as a methanol catalyst poison even though no supporting experimental evidence is in the literature. An earlier, unpublished investigation at Air Products indicated that AsH_3 concentrations as high as 200 parts per billion by volume (ppb) had no effect on methanol synthesis catalyst activity even though arsenic was found on the spent catalyst. Thus, an experimental program was instituted to evaluate the effects of arsine on methanol synthesis catalyst activity and to understand AsH_3-catalyst chemistry.

Catalytic Activity in the Presence of Arsine. Table 1 lists the catalyst deactivation rates in the presence and absence of arsine (AsH_3). In each of the runs (except 16655-58, see below), exposure to AsH_3 resulted in a deactivation rate greater than that of clean syngas. In each case when AsH_3 exposures were ended, the resulting deactivation rates were statistically the same as the initial deactivation rate of clean syngas; that is, AsH_3 poisoning stopped when it was removed from the feed. This implies that binding of arsenic to the catalyst is irreversible under methanol synthesis conditions. Results for run 16655-44 (Figure 2) show that, as expected, the deactivation rate depends on the AsH_3 concentration in the feed. The dependence is not linear; rather, as shown in Figure 3, the data can be fitted to a Langmuir-like expression. For comparable AsH_3 concentrations, deactivation rates were approximately the same at 235 °C (run 16655-97) and 250 °C (see below).

Table 1 also lists the arsenic concentrations found on each of the spent catalysts. Considering the long run times, small errors in feed AsH_3 concentrations can have significant impact on a calculation of total exposure. Although agreement was not perfect, the calculated arsenic loading based on the arsine feed concentration, flow rates, and exposure times were generally about the same as the arsenic loading determined by elemental analysis. This implies that arsine reacted quantitatively with the catalyst under methanol synthesis conditions.

In an attempt to evaluate the deactivation rate at AsH_3 concentrations typical of the LPMEOH™ Demonstration Unit, still lower AsH_3 concentrations were evaluated (run 16655-58). Exposure to 38 ppb and 76 ppb AsH_3 resulted in deactivation rates that were not statistically different from those obtained under clean syngas; that is, no poisoning effect was observed. This does not mean that AsH_3 poisoning does not occur at these concentrations; rather, because of scatter in the data, the effects are obscured by the baseline rate of deactivation in the autoclave. These concentrations represent a lower limit for observing laboratory deactivation resulting from arsenic poisoning.

Characterization of Catalyst/Arsine Reaction Product. Complete analytical results for catalyst samples following AsH_3 exposure are provided in Tables 2 and 3. X-ray Absorption

Spectroscopy (XAS) was used to further characterize spent catalyst sample 16655-28 containing 5,670 parts per million by weight (ppmw) arsenic. XAS provides oxidation state and structural information with high elemental selectivity and has been shown to be a powerful technique in numerous applications.[3] These results were consistent with the presence of a phase most similar to the mineral domeykite, Cu_3As.

Table 1. Methanol synthesis catalyst deactivation rates for exposure to AsH_3-containing syngas.

				deactivation rate, % per hour			As conc. spent catalyst, ppmw	
run number	AsH_3 conc, ppb	syngas comp.[a]	T, °C	initial, syngas only	AsH_3/ syngas	final, syngas only	experimental	calculated[b]
16655-28	660	Shell	250	0.0775	0.140	~0	5,670	4,899
	310			~0	0.153	-		
16655-44	578	Kingsport	250	0.0840	0.325	0.0784	5,980	3,290
	248			0.0784	0.206	0.0850		
	150			0.0850	0.190	-		
16655-58	38	Kingsport	250	0.0354	0.0667	0.0651	378	674
	76			0.0651	0.0691	-		
16655-97	458	Kingsport	235	0.0953	0.312	-	1,720	1,029

a. Approximately 750 psig.

b. Arsenic loading calculated from AsH_3 concentration in secondary feed, gas flow rates, and exposure times.

Table 2. Elemental analysis for catalysts exposed to AsH_3-containing syngas.

	concentration, ppmw				
run number	As	S	Fe	Ni	Cl[a]
16655-28	5,670	≤71	137	14.3	60
16655-44	5,980	<100	106	14.8	80
16655-58	378	<100	48.2	120[b]	40
16655-97	1,720	<100	215	54.9	40
16655-101[c]	2,560	<100	244	62.7	50

a. Cl analysis by XRF.

b. High Ni level likely due to contamination.

c. Continuation of run 16655-97, calculated 1,088 ppmw As additional or total calculated As 2,114 ppmw.

Table 3. XRD and surface areas properties of catalysts exposed to AsH_3-containing syngas.

		crystallite size, Å		surface	relative
run no.	XRD phases	Cu [111]	ZnO	area, m^2/g	Cu SA[a]
16655-28	Cu, ZnO[b]	148	85.0		0.552
16655-44	Cu, ZnO	250	63.9	71	0.504
16655-58	Cu, ZnO	101	73.6		0.885
16655-97	Cu, ZnO	148	75.0		-
16655-101[c]	Cu, ZnO	163	80.7	73	0.571

a. Relative Cu SA = observed Cu surface area/ Cu surface area of freshly reduced catalyst.

b. Possible trace Zn_3As_2.

c. Continuation of run 16655-97.

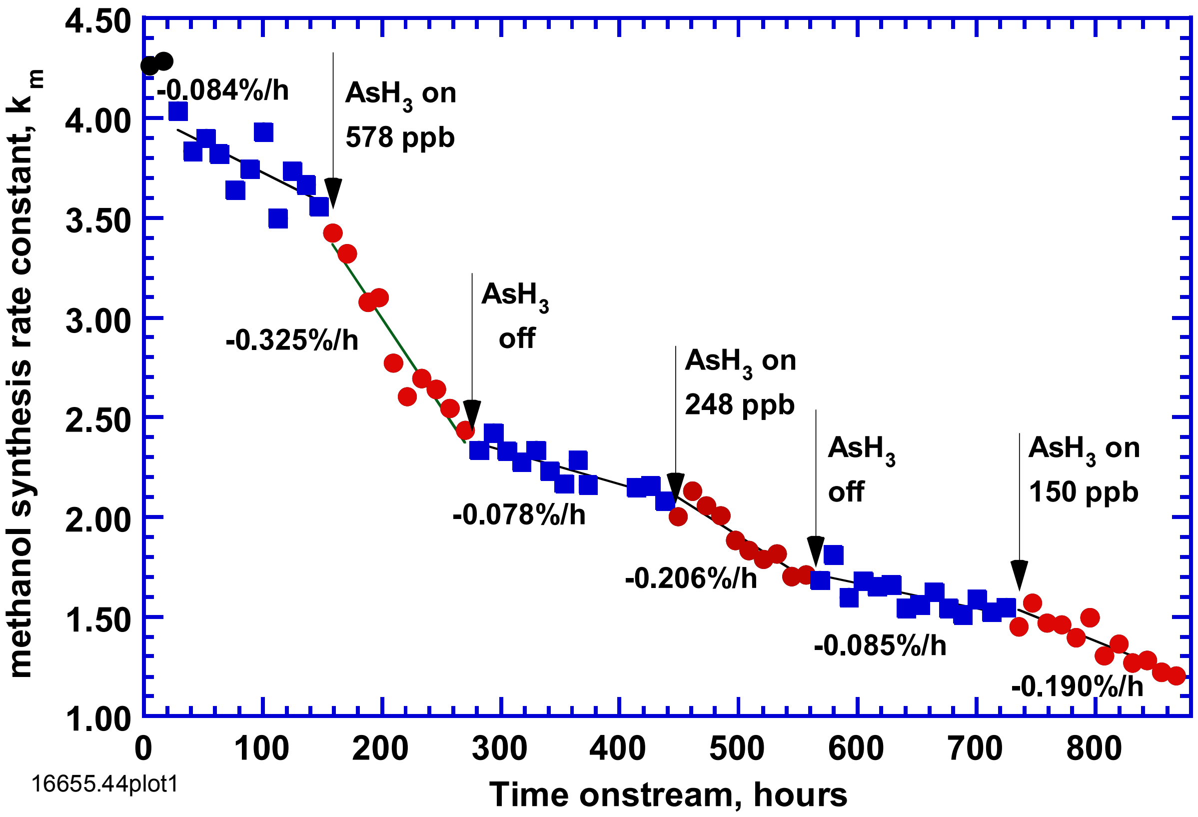

Figure 2. Alternative catalyst at 250°C; 750 psig; Kingsport feed gas; approx. conc.: 68.2 vol% H_2, 22.8 vol% CO, 4.7 vol% CO_2, 5.2 vol% N_2. Secondary feed: 12.6 ppm AsH_3 in 5 vol% CO, 95 vol% H_2. Feed arsine concentrations as indicated.

Based on the experimental evidence, the most reasonable poisoning mechanism is dissociative adsorption of AsH_3 on the copper (Cu) surface accompanied by formation of Cu_3As. The result is a loss of methanol synthesis sites on the copper surface or, more simply, a decrease in copper surface area for catalysis. The reaction of copper and arsine (reaction 1) is thermodynamically very favorable with an equilibrium constant value of $3.3\text{x}10^8$ and a heat of reaction of -17.7 kcal/mol AsH_3 at 250 °C.[4] Even at the relatively high H_2 pressures encountered during methanol synthesis, about 31 atmospheres (atm), the equilibrium AsH_3 concentration based on reaction 1 is only 10 ppb AsH_3, illustrating the high arsine affinity of the catalyst. The observed AsH_3-catalyst reactivity is consistent with that reported for copper metal surfaces.[5]

	K, 250 °C	
$3Cu + AsH_3(g) = Cu_3As + 1.5H_2(g)$	$3.3\text{x}10^8$	(1)

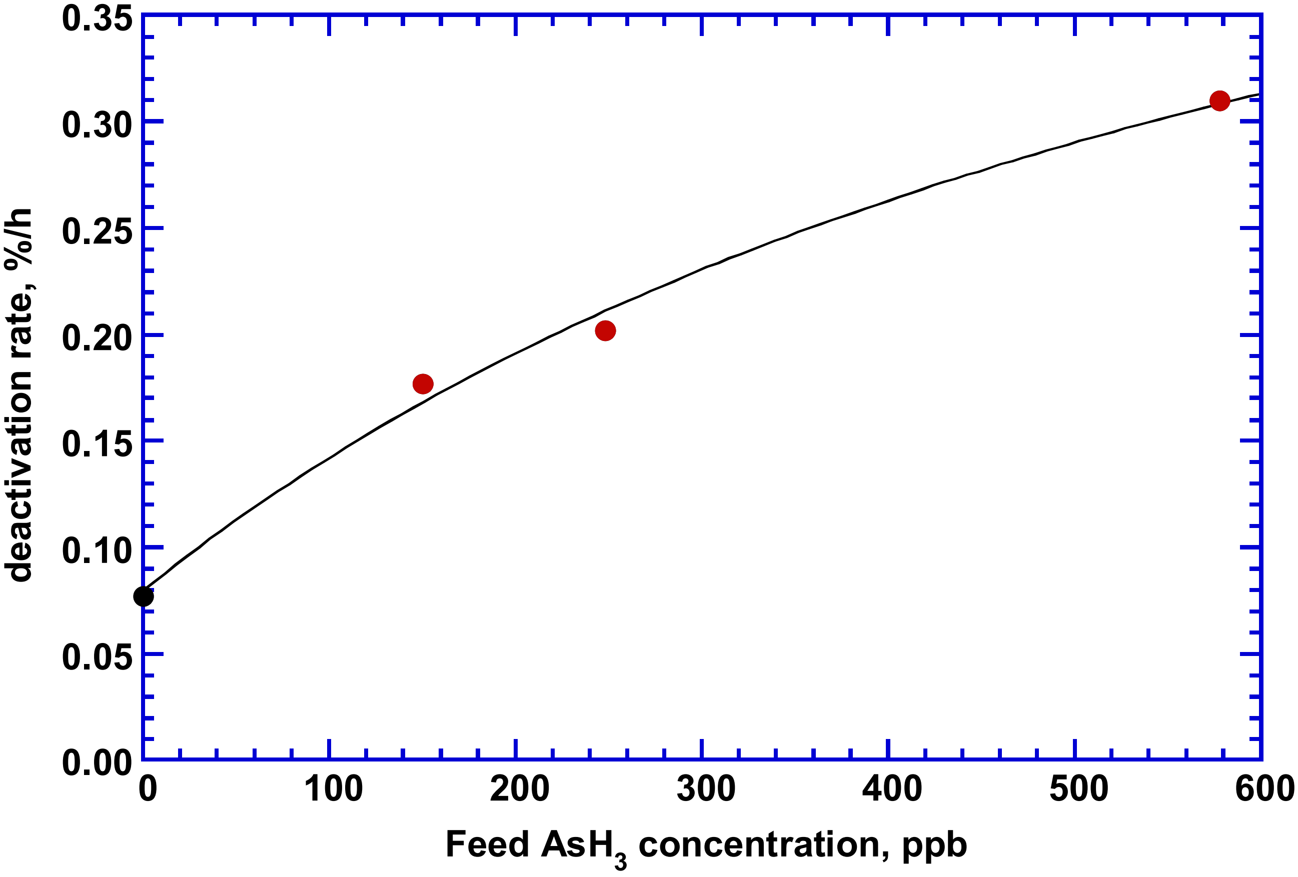

Figure 3. Fit of catalyst deactivation rate to the concentration of AsH_3 in the syngas feed.

1.3 Phosphorus-Containing Contaminants

Another class of contaminants, which may function as catalyst poisons, is phosphines including phosphine itself, PH_3, and substituted phosphines (PR_3) such as trimethyl phosphine, $P(CH_3)_3$. Phosphine can be formed by hydrogenation of phosphorus during coal gasification. Phosphorus concentrations on spent catalyst samples from the LPMEOH™ reactor were consistently below its limit of detection (<100 ppmw).

Catalytic Activity in the Presence of Phosphine. Results for exposure of catalyst to PH_3-containing syngas are listed in Table 4. The presence of PH_3 had a substantial effect on the deactivation rate. Upon returning to clean syngas, the poisoning effects of PH_3 stopped and over a 48-hour period there was no evidence of catalyst deactivation.

Table 4. Methanol synthesis catalyst deactivation rates for exposure to PH_3-containing syngas. Kingsport Gas feed, 750 psig, 250 °C.

		deactivation rate, % per hour			P conc. spent catalyst, ppmw	
run number	PH_3 conc, ppm	initial, clean syngas	contaminant/ syngas	final, clean Syngas	experimental	calculated*
17716.81	1.91	0.0096	0.256	~0	1,580	1,628

* Based on contaminant feed concentration, flow rate, and exposure time.

The phosphorus concentration (by elemental analysis, Table 5) on the spent catalyst was comparable to the calculated P loading of 1,628 ppmw, consistent with quantitative reaction of PH_3. As detailed in Table 6, X-ray Diffraction (XRD) analysis of the spent catalyst slurry revealed the expected phases and crystallite sizes. The copper surface area was greater than generally found for poisoned laboratory catalysts and the BET surface area was unusually low.

Table 5. Elemental concentrations by elemental analysis and XRF for catalyst exposed to PH_3-containing syngas.

	concentration,[a] ppmw				
17716-81	P	S	Fe	Ni	Cl
Elemental analysis	1,580	<40	60.5	≤21	-
XRF	-	-	-	-	nd

a. nd = not detected.

Table 6. XRD and surface areas properties of catalyst exposed to PH_3-containing syngas.

		crystallite size, Å		surface	relative
run no.	XRD phases	Cu [111]	ZnO	area, m^2/g	Cu SA[a]
17716-81	Cu, ZnO	96.5	86.6	59	0.637

a. Relative Cu SA = observed Cu surface area/ Cu surface area of freshly reduced catalyst.

Poisoning by phosphine likely occurs by a reaction analogous to that proposed for AsH_3. Reaction 2 is extremely favorable with an equilibrium constant value of 1.2×10^{16} at 250 °C. The calculated equilibrium PH_3 concentration in Kingsport Gas under methanol synthesis conditions is essentially zero (3×10^{-7} ppb).

	K, 250 °C	
$3Cu + PH_3(g) = Cu_3P + 1.5H_2(g)$	1.2×10^{16}	(2)

1.4 Sulfur-Containing Contaminants

There is ample evidence that a wide variety of sulfur-containing species are reactive with metals and, thus, are potential methanol catalyst poisons. Most reasonable sulfur-containing species for evaluation are hydrogen sulfide (H_2S), carbonyl sulfide (COS), carbon disulfide (CS_2), and organosulfur compounds. Of the later, thioethers (RSR) and thiocyanates (RSCN) were chosen for study using thiophene (C_4H_4S) and methyl thiocyanate (CH_3SCN). Thiols (RSH) were not examined but experimental results for other sulfur-containing species (see below) indicate that these will be potent methanol synthesis catalyst poisons. The decision as to which sulfur-containing contaminants to evaluate was based in part on those found in typical syngas feed from coal gasification.

Catalytic Activity in the Presence of Sulfur-Containing Contaminants. The results for catalyst runs involving exposure to sulfur-containing species in syngas are summarized in Table 7. All four sulfur-containing species were found to be methanol catalyst poisons as shown by the greater deactivation rate in the presence of each species versus initial value under clean syngas. For COS, CS_2 and CH_3SCN, returning to clean syngas after contaminant exposure resulted in deactivation rates significantly greater than for the initial clean syngas exposure. Thus, the poisoning effects of these species continued after the contaminant flow was stopped. The deactivation rate following thiophene exposure was not statistically different from the initial clean syngas value. For each species, the calculated sulfur concentration on the spent catalyst and that determined experimentally by elemental analysis were in reasonable agreement. This implies that each species reacted quantitatively with the catalyst under methanol synthesis conditions. Conspicuously absent from Table 7 is H_2S. Unfortunately, at the ppm levels of H_2S in the syngas feed most of the H_2S reacted with metal surfaces before entering the methanol synthesis reactor. Thus, meaningful results could not be obtained with the existing apparatus.

Table 7. Methanol synthesis catalyst deactivation rates for exposure to sulfur-containing contaminants in syngas. Kingsport Gas, 750 psig, 250 °C.

			deactivation rate, % per hour				
run number	species	conc, ppm	initial, clean syngas	contaminant/ syngas	final, clean syngas	S conc. spent catalyst, ppmw experimental	calculated[a]
17716-60	COS	2.75	0.0717	0.5714	0.1899	3,196	3,320
17716-45	CS_2	2.07	0.0660	1.330	0.999	4,510	3,851
17716-40	thiophene	1.61	0.0803	1.000	0.0988	-	-
	thiophene	0.48	0.0988	0.576	na	2,280	1,624
17716-49	CH_3SCN	2.14	0.0374	0.674	0.323	1,930	2,080

a. Sulfur loading calculated from contaminant concentration in secondary feed, gas flow rates, and exposure time; for CS_2 calculation assumes that both sulfur atoms react with catalyst; na = not available.

Complete analytical results for catalyst samples following contaminant exposure are provided in Tables 8 and 9. One noteworthy result is the unusually large ZnO crystallite size, 117.1 Å, following CH_3SCN exposure.

Table 8. Elemental analysis for catalysts exposed to sulfur-containing species in syngas.

		Concentration, ppmw[a]				
run no.	species	S	As	Fe	Ni	Cl
17716-60	COS	3,320	na	339	24.6	30
17716-45	CS_2	4,510	<20	343	44.9	nd
17716-40	thiophene	2,280	<20	223	<10	nd
17716-49	CH_3SCN	1,930	≤32	241	50.6	60
-	fresh catalyst[b]	<100	<10	14.4	<5	-

a. Cl analysis by XRF.
b. Alternative catalyst, oxide form.
na = not available, nd = not detected.

Table 9. XRD and surface areas properties of catalysts exposed to sulfur-containing species in syngas.

			crystallite size, Å			
run no.	species	XRD phases	Cu [111]	ZnO	surface area, m^2/g	relative Cu SA[a]
17716-60	COS	Cu, ZnO	104.9	71.5	76	0.504
17716-45	CS_2	Cu, ZnO	130.0	67.3	89	0.353
17716-40	thiophene	Cu, ZnO	103.5	71.6	109	0.745
17716-49	CH_3SCN	Cu, ZnO, Cu_2O(t)	116.5	117.1	79	-

a. Relative Cu SA = observed Cu surface area/Cu surface area of freshly reduced catalyst.
(t) = trace.

Rationalizing catalyst-sulfur reactivity is more complicated than in the case of AsH_3 or PH_3 because these species can undergo hydrogenation or hydrolysis reactions under methanol synthesis conditions and/or react with either the Cu metal or the zinc oxide (ZnO) portion of the catalyst. Reaction of COS, CS_2, thiophene, and CH_3SCN likely involves, at least initially, hydrogenation catalyzed by the copper metal surface. Because of its proximity to Cu (versus ZnO), the sulfur containing product (formally H_2S) will react to yield Cu_2S. For example, the overall reaction involving hydrogenation of COS over copper metal results in Cu_2S and CO as products (reaction 3). In addition to Cu_2S, hydrogenation of CS_2, thiophene, and CH_3SCN will likely result in methane (CH_4), n-butane, and hydrogen cyanide (HCN), respectively, as represented by reactions 4, 5, and 6.

	K, 250 °C	
$2Cu + COS(g) = Cu_2S + CO(g)$	2.76×10^{6}	(3)
$4Cu + CS_2(g) + 2H_2(g) = CH_4(g) + 2Cu_2S(g)$	2.23×10^{14}	(4)
$2Cu + C_4H_4S(g) + 3H_2(g) = Cu_2S + C_4H_{10}(g)$	1.59×10^{16}	(5)
$2Cu + CH_3SCN(g) + H_2(g) = Cu_2S + HCN(g) + CH_4(g)$	-	(6)

The Cu_2S product in reactions 3 through 6 can undergo subsequent reduction to copper metal and gaseous H_2S as in reaction 7. Although this reaction is not particularly favorable (K is very small), the relatively high H_2 pressure under methanol synthesis conditions results in an equilibrium H_2S concentration of 4.8 ppm. This concentration of gaseous H_2S exceeds its equilibrium concentration above ZnO (0.36 ppm) and reaction to zinc sulfide (ZnS) will occur (reaction 8). Perhaps it is this transfer of sulfur from the copper to the ZnO that resulted in the observed continuation of poisoning after sulfur contaminants were removed from the feed. When COS, for example, is present in the feed, sulfur deposition on Cu, hydrogenation to H_2S, and formation of ZnS all occur simultaneously and the result is a net or steady state deactivation rate. Sulfur deposition on Cu stops when COS is removed from the feed but the other two process continue. Once poisoning at the catalytic copper surface stops, the rate of deactivation will likely decrease, as has been observed, and eventually return to the clean syngas deactivation rate.

	K, 250 °C	equilibrium H_2S conc., ppb	
$Cu_2S + H_2(g) = 2Cu + H_2S(g)$	$8.06\text{x}10^{-6}$	4,839	(7)
$ZnO + H_2S(g) = ZnS + H_2O(g)$	$1.33\text{x}10^{7}$	0.19	(8)

1.5 Nitrogen-Containing Contaminants

Most reasonable nitrogen-containing species for evaluation are amines, nitriles, and inorganic cyanides. In the present study, methyl amine (CH_3NH_2), acetonitrile (CH_3CN), and HCN were evaluated. An extensive literature review failed to reveal any reports on the effect of amines, nitriles, hydrogen cyanide or other nitrogen-containing species on methanol synthesis catalyst activity. This was particularly surprising for HCN because it is generally assumed to be a catalyst poison and is regarded as a species that must be removed from syngas feeds. HCN is known to poison Fischer-Tropsch catalysts, particularly those containing Group VIII metals (e.g. Fe, Co, Ni),[6] but none of the literature references to copper-based catalyst poisoning by HCN offer any evidence to support this claim.

Catalytic Activity in the Presence of Nitrogen-Containing Contaminants. The results of catalyst runs involving exposure to nitrogen-containing species in syngas are summarized in Table 10. Acetonitrile and methyl amine had no effect on catalyst deactivation. However, the apparent inactivity of HCN was a surprise that was investigated more thoroughly. Exposure to Kingsport or Shell Gas containing 2.3 to 6.6 ppm HCN resulted in no significant change in the

Table 10. Methanol synthesis catalyst deactivation rates for exposure to nitrogen-containing contaminants in syngas. All at 250 °C and 750 psig.

				deactivation rate, % per hour	
run number	species	conc, ppm	feed gas	initial, clean syngas	contaminant/ syngas
16655-39	HCN	2.27, 4.24	Kingsport	0.0420	0.039
		4.21	Shell	~0	~0
16655-50	HCN	6.57	Kingsport	0.0438	0.059
16655-68	HCN	101.5	Kingsport	0.0426	0.0569
17203-38	CH_3CN	11.5	Kingsport	0.0870	0.0895
17716-49	CH_3NH_2	2.52	Kingsport	0.0803	0.0374

catalyst deactivation rate. Even at a feed HCN concentration of 101.5 ppm, catalyst deactivation rates in the presence and absence of HCN were not statistically different (Table 10). These unexpected results show that HCN is not a poison under methanol synthesis conditions.

Analytical data for the spent catalyst (Tables 11 through 13) make a convincing case for the inactivity of these species. In particular, nitrogen and cyanide analysis (Table 11) indicate that very little of either was incorporated into the catalyst even though the catalyst had been exposed to very large amounts of contaminants. Most striking are the results for run 16655-68 for which the spent catalyst contained 97 ppmw CN^- but had been exposed to 1,000 times that quantity (99,500 ppmw HCN). These analytical results show that cyanide was not incorporated into the catalyst under methanol synthesis conditions. Either the catalyst has little affinity for HCN under the experimental conditions or, as discussed below, HCN is unstable under methanol synthesis condition. XRD analysis (Table 12) identified only the expected phases; no cyanide containing phases were found. Cu and ZnO crystallite sizes indicated that no unusual crystallite growth had occurred during HCN exposure. Likewise, X-ray Fluorescence (XRF) and elemental analysis (Table 13) indicated no unexpected concentrations of trace contaminants.

Table 11. N and CN^- analysis of catalyst slurries exposed to nitrogen-containing contaminants in syngas.

run number	species	wt% solid	conc., ppmw N	conc., ppmw CN^-	N conc. on catalyst, ppmw[a] exper.	N conc. on catalyst, ppmw[a] calculated[b]	CN^- conc. on catalyst, ppmw[a] exper.	CN^- conc. on catalyst, ppmw[a] calculated[b]
16655-39	HCN	18.01	<15	0.8	<83	5,739	4.4	10,658
16655-50	HCN	36.61	30	<23	82	11,012	<58	20,451
16655-68	HCN	31.91	195	31	611	53,558	97	99,465
17203-38	CH_3CN	39.49	30	<29	76	12,160	<73	22,582
17716-49	CH_3NH_2	100	64	-	64	1,051	-	-
17200-41-1	none[c]	100	<1.5	28	-	-	-	-

a. Assumes all N or CN^- on the catalyst.
b. Based on contaminant feed concentration, flow rate, and exposure time.
c. Fresh alternative catalyst in oxide form.

Table 12. XRD and surface areas properties of catalysts exposed to HCN in syngas.

run no.	species	XRD phases	crystallite size, Å Cu [111]	crystallite size, Å ZnO	surface area, m^2/g
16655-39	HCN	Cu, ZnO	124.5	74.9	
16655-50	HCN	Cu, ZnO	111.0	60.7	63
16655-68	HCN	Cu, ZnO	114.6	75.8	

Table 13. Elemental analysis for catalysts exposed to HCN in syngas.

sample	ppmw, elements* As	S	Fe	Ni	Cl
16655-39	<20	<100	182	22.5	60
16655-50	≤19	<100	260	38.3	40

* Cl analysis by XRF.

Amines and nitriles, such as methyl amine and acetonitrile, are not expected to act as methanol catalyst poisons. Neither will bind to metallic copper and at best only weakly to Cu (I, II) formed during the catalytic cycle. Surprising, however, was the apparent inactivity of HCN. Although thermodynamics implies that copper-HCN reactions are unfavorable, the reaction of HCN with ZnO is expected to be quite favorable. Thus, not observing $Zn(CN)_2$ on the spent catalyst was surprising.

An alternative explanation is that HCN undergoes hydrogenation to methyl amine, CH_3NH_2. Under methanol synthesis conditions, conversion of HCN to CH_3NH_2 expected to be quantitative with an equilibrium HCN concentration of only 0.01 ppb (reaction 9). Thus, the apparent "inertness" of HCN can be attributed to it conversion to an inert species, methyl amine. This conclusion was supported by the reactivity of methanol synthesis catalyst under syngas at 30 °C, a temperature at which HCN hydrogenation is expected to be slow. Under these conditions, the 51.3 ppm HCN in the syngas feed were quantitatively adsorbed onto the catalyst.

	K, 250 °C	
$HCN(g) + 2H_2(g) = CH_3NH_2(g)$	9.87×10^3	(9)

1.6 Halide-Containing Contaminants

Poisoning of methanol synthesis catalyst by hydrogen chloride (HCl) is well established.[7,8] The presence of chlorine reportedly caused an immediate decrease in catalytic activity which continued even after the HCl source has been removed.[9] The primary effect of Cl poisoning has been ascribed to increased sintering due to the formation of low-melting CuCl.[7-10] In contrast, no published catalyst performance data exists for exposure to alkyl chlorides (RCl) even though such species are likely poisons.

Catalytic Activity in the Presence of Halide-Containing Contaminants. The chlorine and fluorine containing hydrocarbons methyl chloride (CH_3Cl) and methyl fluoride (CH_3F) both proved to be methanol catalyst poisons (Table 14). Methyl chloride was a much more active poison and exposure to 2.01 ppm in syngas resulted in a high deactivation rate, 0.657 % per hour. Following CH_3Cl exposure and a return to clean syngas, the deactivation rate remained high, 0.169 % per hour indicating that poisoning continued even after the contaminant was removed. After approximately 84 hours, the deactivation rate returned to a value typical for

Table 14. Methanol synthesis catalyst deactivation rates for exposure to halide-containing contaminants in syngas. Kingsport Gas, 750 psig, 250 °C.

			deactivation rate, % per hour			Cl or F conc. spent catalyst, ppmw	
Run Number	species	conc, ppm	initial, clean syngas	contaminant/ syngas	final, clean syngas	experimental	calculated[a]
17716-34	CH_3Cl	2.01	0.0311	0.657	0.169[b]	2,650	2,505
17716-52	CH_3F	2.55	0.0853	0.272	0.0498	344[c]	1,637

a. Expected halide loading calculated from contaminant concentration in secondary feed, gas flow rates, and exposure time.
b. Initial value after return to clean syngas; after 84 hours, deactivation rate was 0.059 % per hour over next 200 hours.
c. 337 ppm as F, 7 ppm as F^-.

clean syngas. This would seem to be consistent with typical HCl poisoning of copper-based catalyst in other industrial applications, for which continued exposure to HCl reflected increased sintering. Not surprisingly, CH_3F was a less active poison and, unlike CH_3Cl, the poisoning effects of CH_3F stopped when the contaminant was removed from the syngas feed.

The calculated and experimental Cl concentrations on the spent catalyst were nearly identical implying quantitative reaction of CH_3Cl. In contrast, only a fraction (~20% by weight) of the expected F concentration was found on the spent catalyst, meaning that most of the CH_3F simply passed through the reactor without reacting. The analytical results for the catalyst following CH_3Cl exposure (Tables 15 and 16) indicated that the catalyst had not undergone any unusual sintering as is often associated with Cl poisoning. The relative copper surface area of 0.424 for the Cl poisoned sample was comparable to those of other poisoned catalyst samples. Because of the possibility that CH_3Cl can be hydrolyzed to HCl upon storage, care was taken to insure that poisoning resulted from CH_3Cl. Analysis by Gas Chromatograph Mass Spectrometer (GCMS) of the feed cylinder used to supply CH_3Cl (55 ppm CH_3Cl, 5 vol% CO in H_2) unequivocally showed the presence of CH_3Cl. No HCl was detected; thus, CH_3Cl hydrolysis to HCl prior to use was not a concern.

Table 15. Elemental analysis and estimated elemental concentrations by XRF for catalyst exposed to CH_3Cl.

	ppmw, elements[a]		
17716-34	Cl	Fe	Ni
Elemental anal.	2,650	204	21.6
XRF[b]	1,600	-	nd

a. nd = not detected.
b. Data obtained for slurries and corrected for presence of oil.

Table 16. XRD and surface areas properties of catalyst exposed to CH_3Cl in syngas.

			crystallite size, Å		surface	relative
run no.	species	XRD phases	Cu [111]	ZnO	area, m^2/g	Cu SA[a]
17716-34	CH_3Cl	Cu, ZnO	124.3	83.0	84	0.424

a. Relative Cu SA = observed Cu surface area/Cu surface area of freshly reduced catalyst.

Alkyl halide poisoning likely results from hydrogenation over the methanol synthesis catalyst. Hydrogenation of CH_3Cl is quite favorable and it has been demonstrated over a platinum/carbon catalyst.[11] It is theorized that, as for sulfur-containing species, copper supplies a catalytic surface for hydrogenation resulting in copper chloride (CuCl) and CH_4 (reaction 10). Under methanol synthesis conditions, however, CuCl can be reduced to metallic Cu and HCl(g) (reaction 11) followed by its reaction with ZnO to form $ZnCl_2$ (reaction 12). As described above, perhaps it is this Cl^- transfer from the Cu to ZnO that is the source of continued CH_3Cl poisoning after its removal from the feed. Following removal of CH_3Cl from the syngas feed, chlorine deposition on Cu stops while the transfer of HCl to ZnO continues. The result is a greater than baseline deactivation rate but one lower than for poisoning at the copper catalytic surface. Poisoning continues at ZnO sites until transfer of HCl from CuCl is complete and, as observed, the deactivation rate returns to the baseline value.

	K, 250 °C	
$Cu + CH_3Cl(g) + 0.5H_2(g) = CuCl + CH_4(g)$	4.03×10^{11}	(10)
$CuCl + 0.5H_2(g) = Cu + HCl(g)$	1.29×10^{-3}	(11)
$ZnO + 2HCl(g) = ZnCl_2 + H_2O(g)$	1.21×10^{6}	(12)

Methyl fluoride, like CH_3Cl, can undergo hydrogenation over Cu to form CH_4 and CuF (reaction 13). However, because of the strong C-F bond (108 kcal vs C-Cl, 84 kcal),[12] reaction of CH_3F will likely be slower and this may explain why much of the feed CH_3F does not react under the experimental conditions. Copper fluoride can be reduced to Cu and hydrogen fluoride (HF) (reaction 14) but its reaction is much more favorable than for CuCl. Thus, any CuF formed will likely be quantitatively converted to HF with its subsequent reaction with ZnO (reaction 15). This reaction pathway is consistent with the observed stoppage of poisoning when CH_3F was removed from the syngas feed.

	K, 250 °C	
$Cu + CH_3F(g) + 0.5H_2(g) = CuF + CH_4(g)$	3.08×10^{8}	(13)
$CuF + 0.5H_2(g) = Cu + HF(g)$	1.35×10^{3}	(14)
$ZnO + 2HF(g) = ZnF_2 + H_2O(g)$	2.20×10^{4}	(15)

1.7 Volatile Metal Carbonyls

Poisoning of methanol catalyst by gaseous metal carbonyls is well established.[7] Previous laboratory evaluations at Air Products showed that both iron carbonyl ($Fe(CO)_5$) and nickel carbonyl ($Ni(CO)_4$) were very potent poisons.[13,14] Air Products has also experienced firsthand catalyst deactivation due to deposition of iron and nickel from a CO-rich syngas feed at the LaPorte AFDU.[15] Both $Fe(CO)_5$ and $Ni(CO)_4$ are generally found in syngas, particularly those rich in CO. Iron carbonyl can form when syngas is in contact with carbon steel while $Ni(CO)_4$ results from contact with 304 and 316 stainless steel. An optimum temperature for metal carbonyl formation is about 200 °C.[15]

Catalytic Activity in the Presence of $Fe(CO)_5$ and $Ni(CO)_4$. The current evaluation of carbonyl reactivity was inadvertent but beneficial. Following a run to evaluate PH_3, the spent catalyst was found to contain usually high Fe and Ni concentrations. These contaminants were subsequently traced to the PH_3 gas mixture used for which GC analysis showed 0.73 ppm $Ni(CO)_4$ and 81 ppm $Fe(CO)_5$. Kingsport Gas was blended with this gas mixture to give a reactor feed containing 5.63 ppm $Fe(CO)_5$. The result was an extremely high deactivation rate of 7.12 % per hour (Table 17). Because $Fe(CO)_5$ concentration was much greater than that of $Ni(CO)_4$, all of the poisoning effect can be attributed to $Fe(CO)_5$. After the contaminant exposure, insufficient catalyst activity remained to obtain meaningful activity data for a clean syngas feed. Notable is that exposure to metal carbonyls resulted in a dramatic loss of activity rather than the loss of selectivity frequently noted in the literature. Deposition of Fe or Ni has reportedly resulted in selectivity for methane and other hydrocarbons at the expense of methanol synthesis. Such hydrocarbon products were not observed in the current experiments; in fact, no change in methanol selectivity was observed.

Table 17. Methanol synthesis catalyst deactivation rates for exposure to $Fe(CO)_5$ in syngas. Kingsport Gas, 750 psig, 250 °C.

			deactivation rate, % per hour		
run number	species	conc, ppm	initial, clean syngas	$Fe(CO)_5$/ syngas	Fe conc. spent catalyst, ppmw
17716-52	$Fe(CO)_5$	5.63	0.0498	7.12	4,290

Table 18 lists the elemental concentrations on the catalyst following $Fe(CO)_5$/syngas exposure. Iron was the most significant contaminant followed by a minor amount of nickel. XRD analysis of the spent catalyst slurry revealed the expected phases and crystallite sizes (Table 19). The relative copper surface area, 1.13, was unexpected high, even for a catalyst only exposed to clean syngas. Such a high copper surface area following poisoning is contrary to results for other poisons (see below). It is believed that this is an artificial increase resulting from iron deposited on the catalyst. Copper surface area is determined by reaction of Cu with nitrous oxide (N_2O) as in reaction 16. It is likely that Fe results in an artificially high surface area value because of its reaction with the N_2O (reaction 17). At a minimum, one mole of Fe will consume 1 mole of N_2O to form FeO[16] so that each surface Fe atom will result in a minimum of twice the area for each Cu atom.

$$2Cu + N_2O = Cu_2O + N_2 \quad (16)$$
$$xFe + yN_2O = Fe_xO_y + yN_2 \quad (17)$$

Table 18. Elemental concentrations by elemental analysis and XRF for catalyst exposed to $Fe(CO)_5$ in syngas.

	ppmw, elements			
	Fe	Ni	S	Cl
Elemental anal.[a]	4,290	41.7	282	-
XRF[b]	5,400	-	-	nd

a. nd = not detected.
b. Data obtained for slurries and corrected for presence of oil.

Table 19. XRD and surface areas properties of catalysts exposed to $Fe(CO)_5$ in syngas.

		crystallite size, Å		surface	relative
run no.	XRD phases	Cu [111]	ZnO	area, m^2/g	Cu SA[a]
17716-52	Cu, ZnO	100.1	73.7	88	1.13

a. Relative Cu SA = observed Cu surface area/Cu surface area of freshly reduced catalyst.

Another aspect of $Fe(CO)_5$ or $Ni(CO)_4$ poisoning is the potential for generation of these gaseous contaminants within the reactor vessel. A series of laboratory experiments was conducted to address this possibility. For these experiments, Shell Gas, which is rich in CO (~64 vol%), and thus favors metal carbonyl formation, was used as the reactor feed. Based on thermodynamics, a small but significant $Fe(CO)_5$ concentration, 160 ppb, was expected under methanol synthesis conditions. This provides a possible pathway for iron deposition - volatile $Fe(CO)_5$ from reaction of CO with iron in the reactor followed by reaction with the methanol catalyst. Analysis of the reactor product stream under methanol synthesis conditions (250 °C, 754 psig, 17716-15) indicated that $Fe(CO)_5$ was below its detection limit implying that if in situ generated $Fe(CO)_5$ were present, it reacted with the catalyst.

To determine if $Fe(CO)_5$ was formed inside the reactor, a blank run was performed in which only Drakeol-10 mineral oil was present in the reactor. GC analysis of the inlet feed gas, which was passed through a carbon trap upstream of the reactor, showed no detectable concentrations of $Fe(CO)_5$ (<1 ppb) or $Ni(CO)_4$. Initiating Shell Gas flow at 250 °C and 750 psig resulted in an initial burst of 100 ppb $Fe(CO)_5$ in the reactor product stream. The $Fe(CO)_5$ concentration quickly decreased to 4 ppb after 20 hours and 3 ppb when the run was stopped at 33 hours (Figure 4). Thus, although $Fe(CO)_5$ levels are initially quite high, concentrations decreased rapidly with time. This is in fact what happens during a so-called carbonyl burnout prior to catalyst loading – exposure to CO-rich syngas passivates the reactor by removal of reactive surface iron. Subsequent investigation showed that this passivated reactor surface is lost or damaged during exposure of the reactor to air or during the cleaning process. The mechanism by

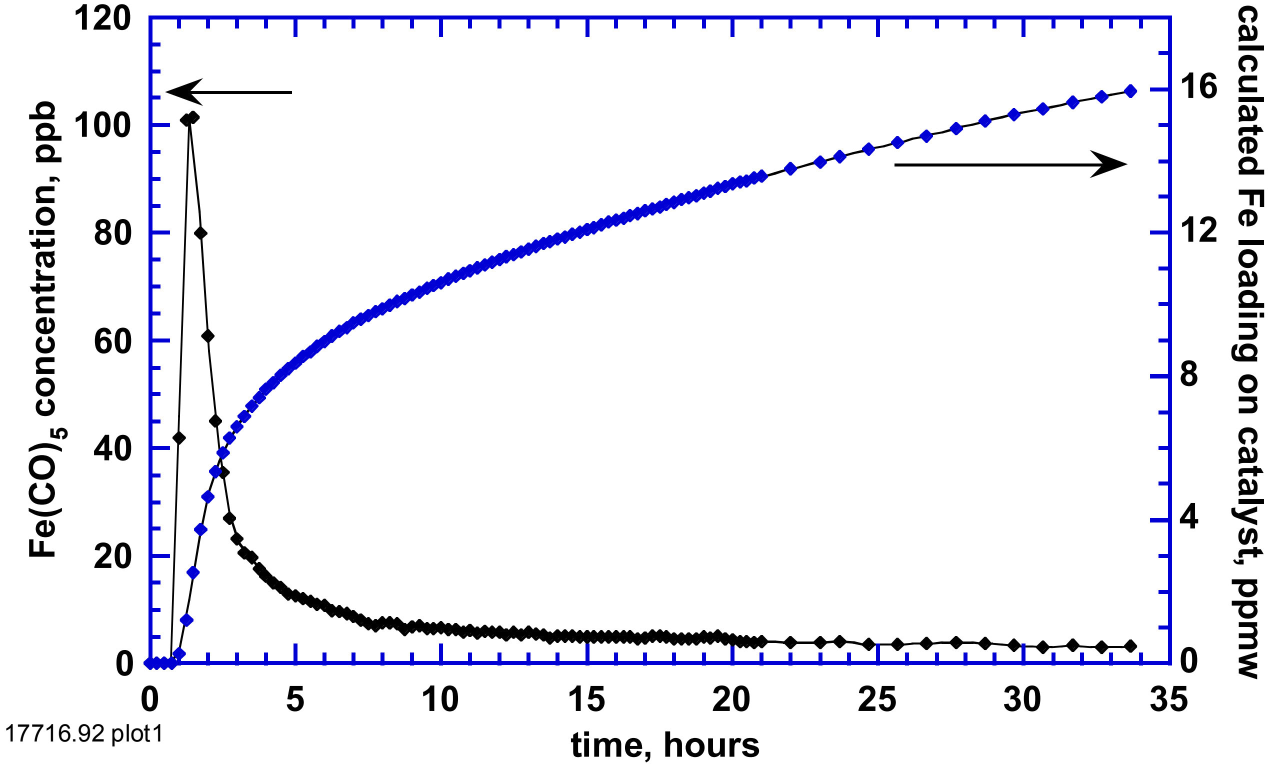

Figure 4. $Fe(CO)_5$ in reactor exit for trailer autoclave containing only oil after exposure to air and normal cleaning. Shell Gas at 750 psig and 250 °C (17716.92). Second Y-axis is the calculated Fe loading if all $Fe(CO)_5$ reacted with the catalyst.

which air or water exposure results in loss of the passivation layer is unclear. Nonetheless, this will not be a concern in an industrial reactor such as the one at Kingsport and iron poison via in-situ generated $Fe(CO)_5$ is unlikely.

1.8 Evaluation of "Self-Poisoning"

One potentially important issue is whether it is possible that poisons from a contaminated catalyst can be transferred to uncontaminated catalyst and thus impact the catalyst activity. This is a particularly important consideration when the liquid phase process operates in the addition/withdrawal mode. Aliquots of "spent" catalyst are removed from the reactor and replaced with fresh reduced, uncontaminated catalyst. If poison transfer occurs, fresh catalyst will be poisoned by contact with aged catalyst in the reactor resulting in a greater than anticipated deactivation rate.

A laboratory evaluation of "self-poisoning" was performed as follows. Initially, the deactivation rate for half the normal catalyst charge (5 g) was determined using a Kingsport Gas feed. The run was temporarily stopped and an amount of spent Kingsport slurry sample K9906-1 was added. The catalyst in the added slurry contained the following contaminants concentrations in ppmw: As, 1,680; S, 316; Fe 109; Cl, 40; Ni, 20. The mixture of fresh and K-9906-1 catalyst exhibited a methanol synthesis rate constant about 60% that of the fresh catalyst alone. More importantly, the deactivation rate prior to addition of the K9906-1 catalyst was 0.0335 % per hour while that after its addition it was 0.0406 % per hour. These values are statistically indistinguishable and the result implies that addition of poisoned catalyst had no effect on the catalyst deactivation rate. It can therefore be concluded that poisons do not migrate under methanol synthesis conditions, especially arsenic, the most abundant contaminant on sample K9906-1. This result is also consistent with those of laboratory experiments which showed that when AsH_3 was removed from the syngas feed, the deactivation rate returned to that for clean syngas.

1.9 Poison Comparison

A ranking of the relative potency of methanol catalyst poisons is valuable information and literature methods were used for this purpose.[14] In one approach, the change in "reduced rate constant" versus the concentration of poison deposited on the catalyst was considered. The reduced rate is the ratio of the actual rate constant, k', to that predicted in the absence of poison, k*, where $k^* = k'(0)e^{-at}$ and k'(0) is the rate at time zero. Values for a and k'(0) were obtained from a plot of ln(k') versus t. The quantity of poison deposited was calculated from the feed poison flow rate and its exposure time. This assumes all of the poison in the feed reacts with and is bound to the catalyst. Plots of k'/k* vs. ppmw poison deposited were linear as shown for thiophene as an example in Figure 5. The slope of such a plot, (k'/k*)/ppmw, represents the effect of the weight of bound contaminant. A comparison on a molar basis, (k'/k*)/ppm, is provided in Table 20. The more potent the poison the greater will be the value of (k'/k*)/ppm.

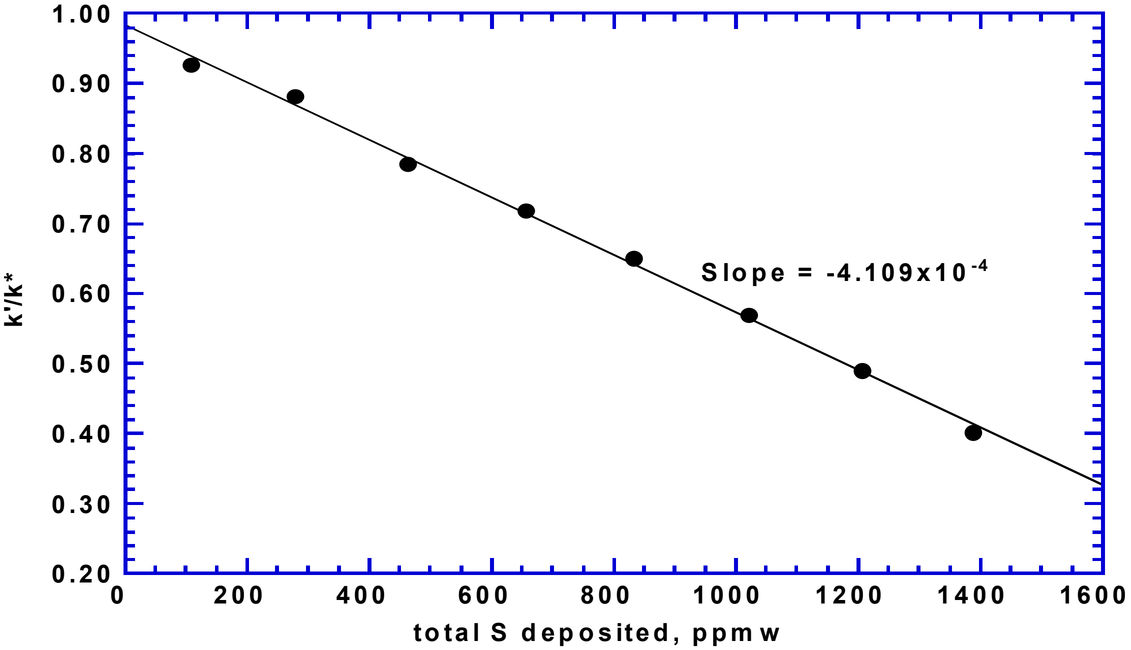

Figure 5. Reduced rate constant versus sulfur deposition for alternative catalyst exposed to 1.61 ppm thiophene.

A second approach, as detailed in the above reference, is based on the assumption of a linear relationship between the reduced rate constant and the concentration of poison on the catalyst surface.[14] A parameter, α_p, the amount of catalyst surface area poisoned per unit weight of poison, was calculated as described in the reference. Again, the greater the value of α_p, the more effectively was a poison in consuming catalyst surface area and thus, the more potent was the poison. Table 20 lists molar values of α_p. For either model, the following order of decreasing poison strength was obtained:

$Ni(CO)_4 > Fe(CO)_5 >$ thiophene $\cong AsH_3 > CH_3Cl > CH_3SCN > CS_2 > COS > PH_3 > CH_3F$.

Perhaps the most significant surprise is the relative low potency of PH_3 when compared to AsH_3.

Another illuminating comparison is that of copper surface area of poisoned catalysts. These are summarized in Table 21 and plotted versus contaminant concentration (ppm not ppmw) in Figure 6. With the exception of $Fe(CO)_5$ (discussed above), results for laboratory catalysts show an approximate linear relationship between contaminant concentration and copper surface area. Significantly, there appears to be no unusual loss of copper surface area associated with Cl poisoning as is often claimed in the literature.

Table 20. Reduced rate constants and α_p for various methanol synthesis catalyst poisons.

contaminant	feed conc, ppm	T, °C	$10^2 \cdot k'/k^*/$ ppm[c]	$10^{-5} \cdot \alpha_p$, m^2/mole
PH_3	1.91	250	0.33	3.25
COS	2.75	250	0.51	3.95
CH_3F	2.55	250	0.25	2.20
CH_3SCN	2.14	250	0.72	7.05
CS_2[b]	2.07	250	0.59	5.23
thiophene	1.61	250	1.33	11.6
CH_3Cl	2.01	250	0.82	7.59
AsH_3	0.578	250	0.82	7.30
	0.248	250	1.28	11.4
	0.150	250	1.64	14.7
	0.458	235	1.49	13.9
$Fe(CO)_5$	5.63	250	1.43	12.4
COS[a]	5.0	250	-	4.17
$Fe(CO)_5$[a]	1.0	250	-	30.2
$Ni(CO)_4$[a]	1.0	250	-	57.5

a. Literature data for a catalyst other than alternative catalyst.
b. Assumes both S atoms of CS_2 are incorporated into catalyst.
c. mole x 10^6/g catalyst.

Table 21. Relative copper surface area of laboratory catalysts following exposure to various contaminants in syngas.

run number	sample no.	contaminant	total run time, h	contaminant conc., ppmw[a]	contaminant conc., ppm	relative Cu SA, m^2/g
17716-40	17475-94-3	thiophene	676	2,280 (S)	71.1	0.745
17716-45	17475-101-2	CS_2	447	4,510 (S)	140.7	0.353
17716-60	18141-17-6	COS	380	3,320 (S)	103.6	0.505
17716-34	17475-90-1	CH_3Cl	668	2,650 (Cl)	74.7	0.456
17716-81	17716-81	PH_3	306	1,580 (P)	51.0	0.636
16655-58	17200-97-1	AsH_3	1,003	378 (As)	5.0	0.883
16655-44	16655-44	AsH_3	867	5,980 (As)	80.1	0.505
16655-101	17475-45-2	AsH_3[b]	534	2,560 (As)	34.2	0.572
17716-52	18141-13-2	$Fe(CO)_5$	589	4,290 (Fe)	76.8	1.13[c]

a. As determined by elemental analysis.
b. Catalyst run at 235 °C.
c. See explanation in section 1.7.

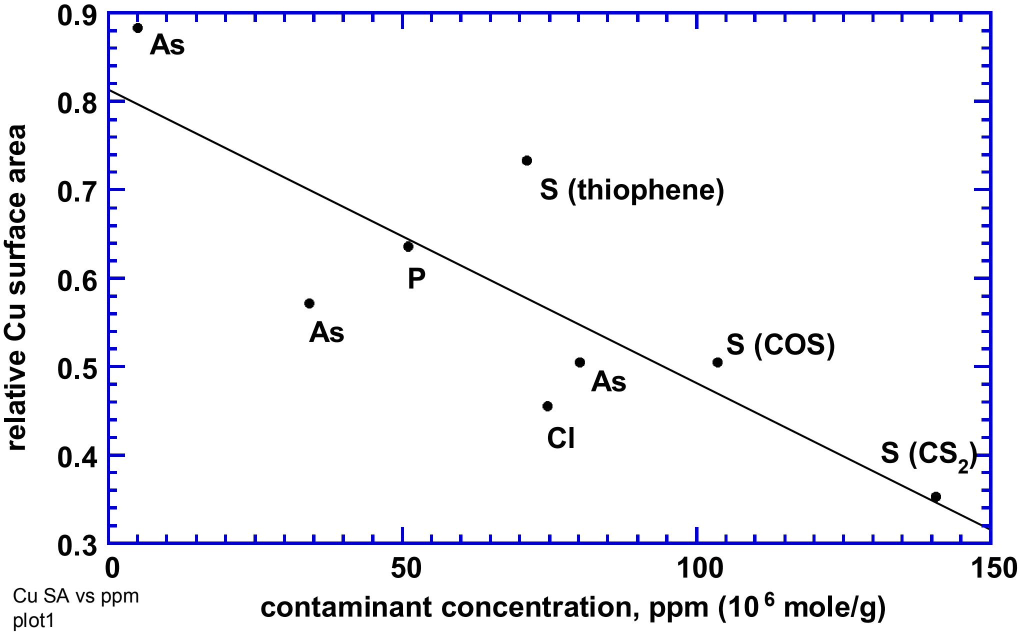

Figure 6. Relative copper surface area versus contaminant concentrations on spent laboratory catalysts.

2. Adsorbents for the Removal of Catalyst Poisons from Syngas

2.1 Adsorbent Screening

The initial round of adsorbent testing was directed toward evaluation of the syngas reactivity and the AsH_3 removal ability of each adsorbent. In-house testing for AsH_3 removal became critical when it was found that adsorbents advertised as effective for AsH_3 removal were actually ineffective. Syngas reactivity was principally a safety issue. Many of the adsorbents contained metal oxide that could be reduced under syngas and/or function as methanol synthesis catalysts. (In this case, reduction refers to the reaction of the metal oxide with a reductant such as CO or H_2 to the base metal and either CO_2 or H_2O). In either case, high bed temperatures and potential runaway reaction could occur.

Exposure to Syngas. Packed beds of adsorbent were used to determine temperature changes upon exposure to syngas. Internal bed temperatures were monitored by thermocouples placed in the inlet, middle, and outlet portions of the bed. Maximum temperature changes upon exposure to syngas and experimental conditions are summarized in Table 22. A representative temperature versus time profile in shown in Figure 7 for lead oxide impregnated alumina (PbO/Alumina). The largest temperature changes were observed for the Pb-based adsorbents and a Cu/Cr-containing carbon. None of the adsorbents appeared to undergo strongly exothermic or runaway reactions upon exposure to syngas. Only H_2, CO, CO_2, N_2, and trace H_2O were found in the bed exit for each adsorbent. No methanol or other organics products were observed implying that none of the adsorbents acted as methanol synthesis catalysts under the experimental conditions.

Table 22. Maximum temperature changes in the presence of syngas.
Approximate feed gas composition and pressure: 67.0 vol% H_2, 29.0 vol% CO, 2.5 vol% CO_2, 1.5 vol% N_2 or 68 vol% H_2, 21 vol% CO, 4.5 vol% CO_2, 5 vol% N_2; 750-760 psig.

composition	space velocity, h^{-1}	initial external T, °C	maximum temperature change, °C inlet	middle	outlet
PbO/Al_2O_3 -1[c]	2,612	31.0	10.7	13.5	11.5
PbO/Al_2O_3 -1	2,612	69.6	12.3	9.4	7.3
PbO/Al_2O_3 -2	2,918	30.6	10.3	13.5	8.8
PbO/Al_2O_3 -2	2,714	29.6[a]	3.3[a]	1.6[a]	3.6[a]
MnO_2/Al_2O_3	2,984	30.9	2.8	3.2	3.0
CuO/C -1	2,999	29.8	3.7	2.4	2.7
CuO/C -2	2,861	30.8	4.5 (5.2)[b]	4.5 (6.8)	3.0 (4.4)
CuO/Al_2O_3	3,038	29.4	3.7	5.0	3.8
$CuO/MnO_2/Al_2O_3$	3,012	29.9	4.4	5.5	4.1
$Ag/AgO/Al_2O_3$	2,875	30.4	8.9	12.0	8.8
$CuO/CrO_3/C$	3,499	29.9	15.1	16.2	13.7
carbon	3,043	30.1	-	1.1 (3.4)	-

a. Data for feed not containing CO_2: 66.9 vol% H_2, 29.1 vol% CO, 3.9 vol% N_2.
b. Values in parenthesis are relative to slight temperature drop upon initial switching from N_2 to syngas.
c. Hyphenated numbers refer to alternate suppliers of similar composition adsorbents.

Temperatures at which metal oxide reduction occurred were determined by Thermal Gravametric Analysis/Infrared Spectroscopy/Differential Scanning Calorimeter (TGA/IR/DSC) (Table 23). Samples were exposed to a N_2 or 3 vol% H_2 in N_2 atmosphere from 30 to 1000 °C. TGA weight losses below 400 °C are summarized in Table 23. By IR, H_2O and CO_2 were the primary species liberated into the gas phase. Reduction under 3 vol% H_2 in N_2 typically occurred in a series of steps at the indicated temperatures. For example, reduction of copper oxide on carbon (CuO/C) gave three exotherms at 210, 245, and 285 °C that totaled 24.68 kcal/mol Cu (164.3 J/g adsorbent). For PbO/Al_2O_3, no significant exotherms were observed under 3 vol% H_2 in N_2 meaning that PbO was not reduced to metallic Pb under the experimental conditions. With the exception of the Ag/AgO adsorbent, experimental and literature heats were in reasonable agreement. It is probable that a significant fraction of the silver in the as received adsorbent was in the metallic state.

Evaluation of enhanced activated carbon was of special interest because of the possibility that syngas exposure might eliminate oxidized sites on the carbon that were thought responsible for AsH_3 removal. TGA/IR scans were run by pretreating the sample at 100 °C under N_2 for 1 hour followed by heating from 100 to 800 °C under N_2 or 3 vol% H_2 in N_2. The following differences in weight losses under H_2 in N_2 versus N_2 were observed: H_2O, 2.70 wt%; CO_2, -0.66 %; 1.74 wt%. These results do not show conclusively that oxidized sites are consumed because of exposure to H_2. In the absence of H_2, evolved CO_2 and CO result from loss of surface COOH, C=O, or C-O-C groups. The higher concentrations of CO and H_2O at the expense of CO_2 in the presence of 3 vol% H_2 in N_2 could result from the water gas shift reaction or a different reaction pathway for reduction. In any case, the literature implies that oxidized sites on carbon are removed by reducing atmospheres or by heating to elevated temperatures under inert gas.[17]

Table 23. TGA weight loss, reduction temperatures and heats as determined by TGA/DSC for a 3 vol% H_2 in N_2 atmosphere.

Composition	wt% metal	reduction temp., °C	experimental kcal/mol	lit. heat,[a] kcal/mol	wt% loss < 400 °C for:	
					3 vol% H_2 in N_2	N_2
PbO/Al_2O_3 -1	17.94	none	-	-6.71	6.02	6.36
CuO/C -2	10.11	210, 245, 285	-24.68	-21.57	9.11	6.61
CuO/Al_2O_3	8.792	240, 290	-16.13	-21.57	6.71	5.94
$CuO/CrO_3/C$	4.01 (Cu) 1.73 (Cr)	220, 280	-37.27	-21.57 -87.26	4.91	3.60
MnO_2/Al_2O_3	24.06	290, 407, 475	-20.74	-19.37	9.61	4.64
$CuO/MnO_2/Al_2O_3$	13.82 (Mn)	280, 340	-13.23	-19.37	10.51	3.64
$Ag/AgO/Al_2O_3$	11.23 (Cu)			-21.57		
	5.78	275	-11.00	-55.92	6.06	5.31
Carbon (enhanced)	0	none	-	-	2.20	3.17

a. At 300 °C for CuO to Cu; MnO_2 to Mn_2O_3; CrO_3 to Cr_2O_3; AgO to Ag.

Arsine Removal. Once a constant temperature under syngas was obtained, each adsorbent was exposed to an arsine-containing syngas feed for approximately 24 hours. An activated carbon trap was placed downstream of the adsorption bed to collect any AsH_3 which passed through the adsorbent. Elemental arsenic analysis results for spent adsorbent from the inlet, middle, and outlet portion of the bed and for the activated carbon trap are listed in Table 24.

Table 24. Elemental analysis results for spent and fresh adsorbents and carbon trap.

adsorbent	AsH_3 feed conc, ppb	run time, h	As conc., ppmw fresh	inlet	middle	outlet	As, mg, C trap	total As, mg[b]
PbO/Al_2O_3 -1	145	24.9	≤35	≤37	≤40	≤35	1.11	1.59
PbO/Al_2O_3 -2	171	24.0	<10	36.97	25.34	21.13	0.62	1.79
PbO/Al_2O_3[a] -2	154	24.0	-	277	≤39	≤22	0.013	1.65
MnO_2/Al_2O_3	144	23.3	≤11	289	≤13	≤12	<0.01	1.47
CuO/C -1	291	11.4	10.2	425	8.96	6.79	<0.01	1.45
CuO/Al_2O_3	157	24.0	≤21	359	≤16	≤19	nd	1.70
$CuO/MnO_2/Al_2O_3$	131	24.0	≤13	456	≤23	≤23	nd	1.42
$CuO/CrO_3/C$	159	24.0	≤35	681	≤34	≤41	<0.005	1.43
$Ag/AgO/Al_2O_3$	133	24.0	≤13	145	≤17	≤12	nd	1.72
CuO/C –2	169	91.5	≤19	3,240	≤19	≤20	nd	6.55

a. Data for feed not containing CO_2: 66.9 vol% H_2, 29.1 vol% CO, 3.9 vol% N_2.
b. Total weight of As entering the adsorbent bed based on flow rates and run times.
nd = not detected.

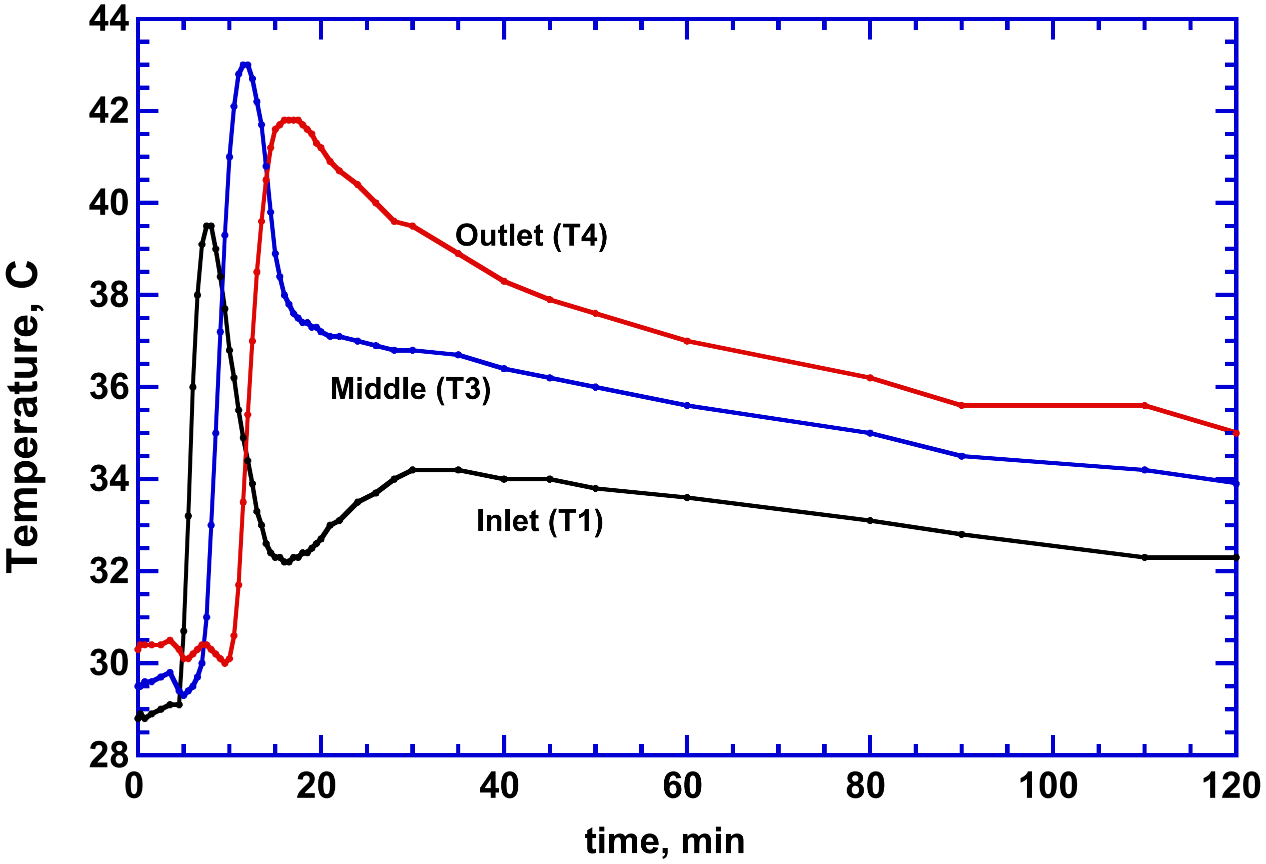

Figure 7. Temperature changes for exposure of PbO / alumina adsorbent to syngas. See Table 22 for conditions.

Results of these AsH_3 exposure experiments do not give AsH_3 adsorption capacities but did indicate which adsorbents were unacceptable. For example, manganese dioxide/alumina (MnO_2/Al_2O_3) trapped all arsine (analyzed as arsenic) at the inlet end of the bed; none was found downstream or on the carbon trap. Thus, MnO_2/Al_2O_3 was acceptable under the experimental conditions. However, MnO_2/Al_2O_3 has been shown to be ineffective for AsH_3 removal at Kingsport. The most significant result of this screening was that neither PbO-based adsorbent removed AsH_3 from syngas. For PbO/Alumina - type 1, arsenic on the spent adsorbent was below its limit of detection (~40 ppmw) even at the bed inlet. More troubling, 1.11 mg of arsenic were found on the carbon trap compared with the total arsenic exposure of about 1.6 mg. The adsorbent simply does not remove AsH_3 under the experimental conditions. The PbO/alumina - type 2 adsorbent was only marginally better but arsine breakthrough still occurred.

That two PbO-based adsorbents were ineffective for AsH_3 removal was quite surprising since both adsorbent suppliers had promoted them as being very effective for AsH_3 removal. Furthermore, the patent and open literature describe PbO/Al_2O_3 as an excellent AsH_3 adsorbent.[18-20] However, all earlier applications involved hydrocarbon or hydrocarbon/H_2/CO streams and none contained CO_2 as in our testing. The PbO results reinforce the absolute need for evaluating adsorbents in the presence of syngas.

It is believed that reaction of PbO with CO_2 to form $PbCO_3$ is responsible for the observed inactivity with respect to AsH_3. Formation of $PbCO_3$ is quite favorable at ambient temperature (reaction 18) with an equilibrium CO_2 pressure of only $5.5\text{x}10^{-7}$ psia. The resulting $PbCO_3$ will be far less reactive with AsH_3 than PbO as shown by comparing reactions 19 and 20. XRD and X-ray photoelectron spectroscopy (XPS) analysis of the Pb-based adsorbents following syngas exposure failed to find $PbCO_3$ present. These results do not preclude the presence of $PbCO_3$; rather, it could be amorphous or it might decompose upon removal of CO_2 (see below).

	ΔH (kcal/mol)	K	
$PbO + CO_2 = PbCO_3$	-20.92	$2.66\text{x}10^{7}$	(18)
$8PbO + 2AsH_3(g) = 5Pb + Pb_3(AsO_4)_2 + 3H_2(g)$	-40.30	$8.18\text{x}10^{31}$	(19)
$8PbCO_3 + 2AsH_3(g) = 5Pb + Pb_3(AsO_4)_2 + 3H_2(g) + 8CO_2(g)$	+127.07	$3.29\text{x}10^{-28}$	(20)

TGA/DSC analysis clearly showed that PbO/alumina - type 1 absorbed CO_2 reversibly, which would explain why $PbCO_3$ was not found when the adsorbent was removed from the CO_2-containing atmosphere. Exposure to CO_2 in the TGA resulted in a rapid weight increase of 1.73 % corresponding to reaction of about half of the available PbO. Purging with N_2 resulted in a more gradual weight loss due to CO_2 desorption. As expected, CO_2 absorption was exothermic, 23.3 kcal/mole CO_2, a value close to heat of reaction of CO_2 with PbO, 20.8 kcal/mole at 100 °C.

Finally, exposure of PbO/alumina - type 2 to syngas containing no CO_2 had a dramatic effect on AsH_3 removal. In the absence of CO_2, nearly 1 mg arsenic was trapped on the inlet portion of the bed versus only 0.15 mg arsenic in the presence of CO_2. Furthermore, only 0.013 mg arsenic was found on the carbon trap downstream of the absorption bed while 0.62 mg arsenic was deposited for the CO_2 containing feed (0.8% vs 35% of total arsenic feed).

2.2 Evaluation of Copper-Impregnated Carbon (CuO/C) Adsorbent

Of the adsorbents examined, CuO/C was viewed as the material most likely to remove AsH_3 and other contaminants from the Balanced Gas feed. It was reasoned that the CuO portion would remove AsH_3, COS, and H_2S while the carbon portion would function as it did previously to remove contaminants such as $Fe(CO)_5$, $Ni(CO)_4$, and trace organics. The most reasonable alternative, enhanced activated carbon, was reasoned to have insufficient AsH_3 affinity to achieve a desired 5 ppb AsH_3 concentration. An extensive evaluation of CuO/C was therefore performed including (1) safety related issues (2) AsH_3 removal properties and (3) other contaminant removal properties. Two similar CuO/C adsorbents from different suppliers were evaluated and labeled type 1 and type 2. The CuO/C from the alternate supplier (type 2) was used for all evaluations in this test program.

Safety Related Issues. For any copper oxide-based adsorbent used under reducing conditions, exothermic reduction to metallic copper is a potential safety concern. Moreover, metallic copper can function as a catalyst for methanol synthesis, a highly exothermic reaction that could cause a rapid increase in temperature within the catalyst guard bed. The initial experimentation concentrated on the catalytic properties of Cu/C. The reduction of CuO/C was initially and mistakenly dismissed as unlikely because (as shown below) reduction was not observed at ambient temperature.

As detailed in Table 25, exposure of CuO/C to Kingsport Gas at 750 psig and 30 °C resulted in relatively minor temperature increases of 4.5 °C or less implying that no significant reduction to metallic copper occurred at near ambient temperature. No methanol or other organics were observed in the bed exit gases implying that the adsorbent had no methanol synthesis catalytic activity. Following reduction to Cu/C using dilute H_2 in N_2, temperature increases upon syngas exposure were almost the same as for CuO/C. Again, the bed outlet showed no sign of methanol or other organics meaning that Cu/C had negligible catalytic activity at near ambient temperatures. Additional testing with other syngas compositions containing higher CO concentrations (see Table 25) resulted in maximum temperatures lower than those for Kingsport Gas exposure, perhaps reflecting the lower CO_2 concentration in these feeds. Methanol or other organics were not detected in the bed exit gases.

Table 25. Maximum temperature changes for as received and reduced[e] type 2 CuO/C exposed to syngas. Approximate feed gas compositions: (A) Kingsport Gas, 68 vol% H_2, 21 vol% CO, 4.5 vol% CO_2, 5 vol% N_2 (B) 35.3 vol% H_2, 61.4 vol% CO, 2.4 vol% CO_2, 1.5 vol% N_2 (C) 50.9 vol% H_2, 47.6 vol% CO, 2.5 vol% CO_2, 1.4 vol% N_2.

Adsorbent	Feed gas composition	Feed P, psig	GSHV, h^{-1}	initial external T, °C	maximum temperature change, °C inlet	middle	outlet
Oxide form	A	750	2,861	30.8	4.5 (5.2)[d]	4.5 (6.8)	3.0 (4.4)
reduced[e]	A	751	3,017	30.7	5.0 (5.4)	4.3 (6.5)	3.1 (5.2)
reduced[e]	B	759	3,132	30.6	2.6	1.5	1.3
reduced[e]	C	756	3,199	30.0	1.9	1.4	2.9

d. Values in parenthesis are relative to slight temperature drop upon initial switching from N_2 to syngas.

e. Reduced using 2.06 vol% H_2 in N_2 at 100 psig.

The catalytic activity of Cu/C was evaluated between 125 and 250 °C for a Kingsport Gas feed at 750 psig. No methanol or other organics were detected at 125 °C and 150 °C. At 175 °C and 200 °C, traces of methanol were observed, ~15 and 30 ppm, respectively. Even at 250 °C, only 220 ppm of methanol and 40 ppm methylformate were detected, showing that Cu/C was a very poor catalyst. As shown by XRD, elemental copper was the only copper containing phase found on the adsorbent. Copper crystallite sizes were 151 Å and 377 Å for the inlet and outlet samples, respectively, which are large relative to methanol synthesis catalysts and indicative of having poor catalytic performance.

Further proof of the non-catalytic properties of Cu/C was obtained by determining its methanol synthesis activity using standard liquid phase methanol catalyst testing. The powdered adsorbent in mineral oil slurry was reduced in an autoclave under standard conditions. At 250 °C and 750 psig, exposure to Kingsport Gas feed, resulted a methanol concentration of 1,790 ppm methanol, corresponding to an estimated methanol synthesis rate constant of 0.009. A normal alternative catalyst run using Kingsport Gas yields 16 to 17 vol% methanol. Again, XRD analysis of the spent slurry confirmed the presence of metallic Cu (crystallite size, 571 Å) and CuO was not found. These results clearly demonstrate that methanol synthesis catalysis by Cu/C is not a concern.

Although initially discounted as unlikely, the reduction of CuO/C upon exposure to syngas is a serious safety concern. This was illustrated by an unanticipated, significant temperature rise that occurred at the LPMEOH™ Demonstration Unit when the 29C-40 catalyst guard bed filled with CuO/C was initially exposed to syngas. Exposure at 750 psig resulted in a bed temperature greater than 200 °C. Based on the above laboratory results, methanol synthesis appeared to be an unlikely heat source. Calculations further showed that complete conversion of the syngas in the bed to methanol supplied insufficient heat for the observed temperature rise. The only reasonable alternative was exothermic CuO reduction. Calculations showed that reduction via CO (30.3 kcal/mol at 25 °C) could result in a temperature increase of 190 °C while the temperature rise for a H_2 reduction (20.5 kcal/mol at 25 °C) is somewhat lower, 129 °C. Hence, a series of experiments to investigate CuO/C reduction were performed.

To determine the lowest temperature at which CuO/C was reduced under syngas, powdered adsorbent were exposed to syngas at internal bed temperatures of 40, 60, and 80 °C. As listed in Table 26, the maximum temperature increases were only 2.3-2.7 °C and the bed inlet and outlet gas compositions were nearly identical. Upon completion of each run, the spent adsorbents were handled so as to avoid contact with the air (see Appendix A). XRD analysis clearly indicated the present of metallic copper for each sample. Although the extent of reduction is difficult to determine by XRD, these results clearly showed that significant reduction occurred even at 40 °C. XPS analysis of the sample exposed to syngas at 60 °C indicated that 40 atomic % of the <u>surface</u> copper was in the metallic state (Table 27). This value was probably lower than the actual since some surface oxidation due to handling in air was inevitable. Once the sample was exposed to air, reoxidation of surface Cu to CuO and Cu_2O occurred (Table 27).

Table 26. Results for exposure of CuO/C to Kingsport Gas.
Approx. composition: 67 vol% H_2, 29 vol% CO. 2.5 vol% CO_2, balance N_2; 750 psig.

syngas space velocity, h^{-1}	internal bed T, °C	maximum ΔT upon syngas exposure	syngas exposure time, h	XRD Cu containing phases, spent adsorbent
3,809	40	2.7	73.2	Cu (major), CuO (low minor)
3,332	60	2.4	18.8	Cu (major), CuO (trace); Cu_2O (trace?)
3,724	80	2.3	18.8	Cu (major), CuO (trace?); Cu_2O (trace?)

Table 27. XPS of CuO/C following exposure to syngas at 60 °C.

	sample	atomic %, surface			atomic % surface Cu oxidation states		
sample no.	handled under:	C	O	Cu	Cu(II)	Cu(I)	Cu(0)
17475-57-1	N_2	88.4	8.6	3.0	60		40
17475-57-1	air	88.3	9.0	2.6	80	20	-
17475-24-1, -57-3	fresh*	88.7	9.1	2.4	100	-	-

*as received adsorbent; average of two determinations.

A Procedure for CuO/C Reduction. The above experimental evidence shows that, even at modest temperatures, CuO/C will be reduced if exposed to syngas and, thus, there is no safe way in which CuO/C can be used at typical syngas operating pressures. If CuO/C is to be used to remove AsH_3 or other impurities from syngas, a safe, controlled reduction procedure will be required. Laboratory experiments were conducted to evaluate the feasibility of reducing CuO/C using dilute syngas. It was found that exposure to 1 vol% of reductant ($CO+H_2$) in N_2 at 100 °C resulted in a fully reduced adsorbent.

The CuO/C adsorbent at 100 °C was exposed to 1.09 vol% ($CO+H_2$) in N_2 at 65 psig. As shown in Figure 8, reduction proceeded smoothly and was complete in about 1,985 minutes (33 hours). The quantity of CuO reduced based on the total consumption of both CO and H_2 was greater than expected, 0.145 g Cu/g adsorbent versus 0.10 g Cu/g. This difference may reflect the low outlet H_2 and CO concentrations relative to the GC calibration standards. In any case, XRD analysis indicated that metallic Cu was the major phase (crystallite size, 508 Å) with a minor amount of CuO, most likely from air oxidation during sample handling.

Reduction was also evaluated at 80 °C over 88.5 hours and, predictably, it proceeded much more slowly (Figure 8). Unfortunately, a GC failure occurred at 52.8 hours and data to show complete

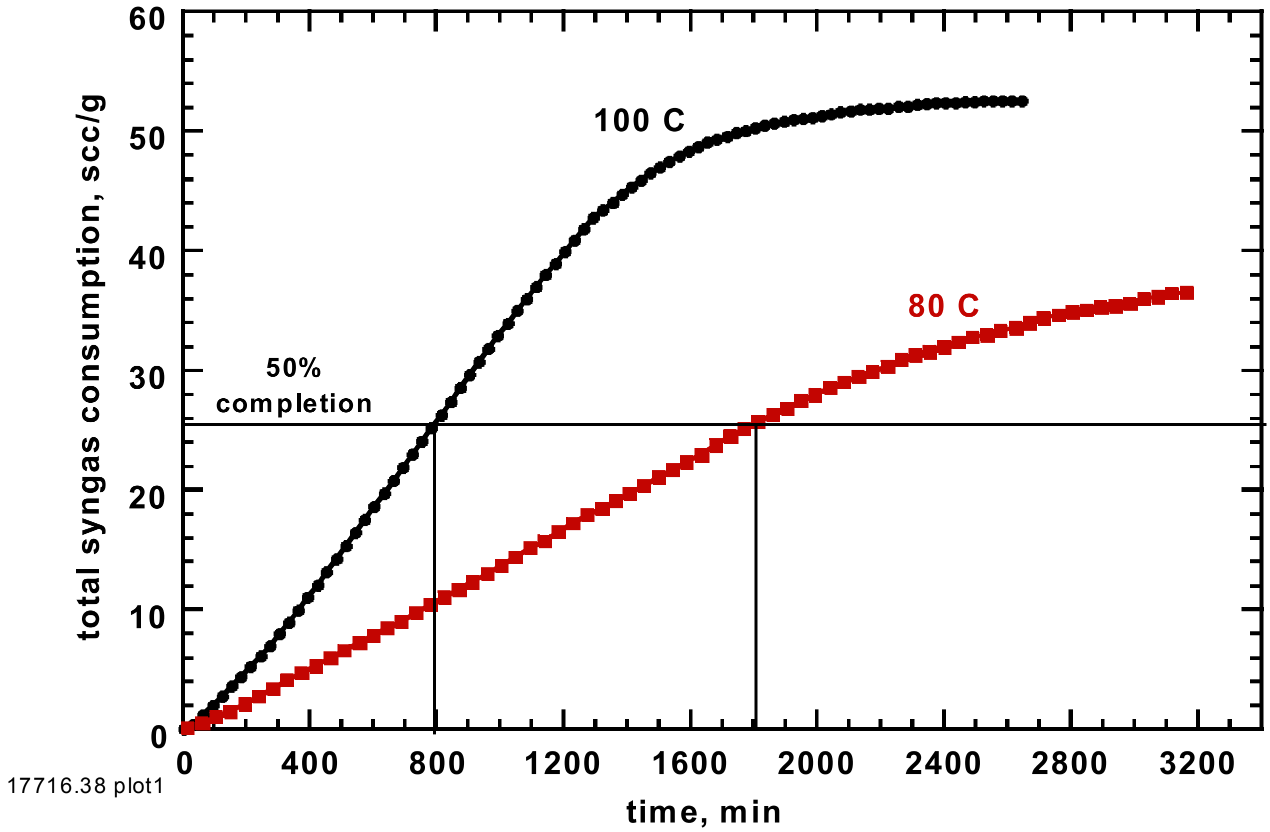

Figure 8. Reduction of CuO/C at 80 °C and 100 °C using 1.09 vol% ($CO+H_2$) in N_2; 65 psig; Gas Hourly Space Velocity (GHSV) = 390 h^{-1}.

reduction was not available. Nonetheless, using the total syngas consumption for the 100 °C run, 51.18 scc/g, the 80 °C reduction was 71% complete in 52.8 hours. Times to 50 % completion were 30.1 hours at 80 °C versus 13.2 hours at 100 °C. XRD analysis following syngas exposure showed the presence of metallic Cu (crystallite size, 318 Å) as the major phase with minor amounts of Cu_2O and CuO. As the target CuO/C reduction time at the LPMEOH™ Demonstration Unit was 2 days or less, a reduction temperature of 100 °C would be required.

AsH_3 Removal Properties. Both the as received and the reduced adsorbent were evaluated for arsine removal. Examination of the reduced adsorbent became necessary once it was clear that CuO/C will undergo reduction under syngas at near ambient temperatures (see above). The adsorbent vendor believed that only CuO/C and not metallic Cu will react with AsH_3. Air Products has shown, however, that exposure of a $Cu/ZnO/Al_2O_3$ methanol synthesis catalyst to syngas containing AsH_3 resulted in the quantitative reaction of metallic Cu with AsH_3 at 235 °C and 250 °C. Furthermore, thermodynamic calculations support a strong driving force for forming Cu_3As at ambient temperature ($K = 1.9 \times 10^{14}$ at 25 °C).

Experimental conditions and results for exposing CuO/C to arsine-containing syngas are listed in Table 28. Beyond the initial screening experiment (Table 27 above), CuO/C proved effective for quantitative removal of 0.418 ppm AsH_3 from a syngas feed over 11.73 days. As detailed in Table 28, most of the arsenic was trapped on the inlet portion of the bed and no arsenic was found on the downstream trap. The agreement between the weight of arsenic found on the adsorbent and the quantity calculated from gas flows and concentrations was excellent implying quantitative adsorption. The arsenic loading on the inlet sample, 3.03 wt%, is approaching the maximum thermodynamic capacity. If quantitative reaction of Cu occurred, the expected As/Cu molar ratios are 0.42 and 0.33 for reactions 21 and 22, respectively, versus the experimental value of 0.26 on the inlet sample. Support for reaction 22 comes from the literature.[21] Exposure of CuO to 1 vol% AsH_3 in N_2 at ambient pressure and temperature resulted in the exothermic adsorption of 2 mmol AsH_3/g adsorbent.

.

$$11CuO + 4.67AsH_3 = 2.67Cu_3As + Cu_3(AsO_4)_2 + 3H_2O + 4H_2 \qquad (21)$$

$$3CuO + 2AsH_3(g) = Cu_3As + 3H_2O(g) + As \qquad (22)$$

Identified reaction products were Cu_3As and H_2O but elemental arsenic was not found by XRD, presumably because it was amorphous. The difference between the observed capacity and that expected based on reaction 20, 8.3 mmol/g, was proposed to be due to limited diffusion of CuO to the adsorbent surface as Cu_3As formed.[21]

XRD analysis of the spent inlet (3.03 wt% As) and outlet (no As) samples from the above run showed that both contained amorphous carbon, CuO, and possibly elemental Cu but contaminant phases such as Cu_3As or $Cu_3(AsO_4)_2$ were not detected. The presence of elemental Cu indicates that, even at only 30 °C, some reduction occurred over the 11.7 day run. XPS analysis (Table 27) of the inlet sample surface indicated the presence of C, O, Cu, and 0.4 atomic % As. Since the sample had been exposed to air during analysis, the surface copper and arsenic were present in the expected oxidized forms, Cu(II) and As(III). By XPS analysis, the outlet sample contained no detectable surface arsenic. The presence of surface Cu(I) in the outlet sample implies that some reduction to Cu(0) upon exposure to syngas at 30 °C had occurred following by air

Table 28. Arsine removal by CuO/C and Cu/C at 30 and 140 °C using Kingsport Gas feed. GHSV = standard flow rate (standard cubic centimeters per hour)/adsorbent volume (cc); Contact time = adsorbent volume (cc)/actual rate (cc/min).

adsorbent run number	CuO/C 16655-98	Cu/C 17716-13	Cu/C 17716-30	Cu/C 17716-43	Cu/C 17716-63	Cu/C calculated
internal bed temperature, °C	30	30	30	140	30	30
bed pressure, psig	750	750	738	748		
AsH_3 feed conc, ppm	0.418	0.668	0.715*	0.737	0.065	0.065
contact time, min	0.910	0.875	0.407	0.41	0.410	0.410
GHSV, h^{-1}	3,098	3,215	6,800	6,847	6,875	6,875
calculated arsenic exposure, mg	50.737	7.313	65.67	61.75	4.83	4.83
AsH_3 exposure time, d	11.73	2.9	9.99	8.670	10.00	10.00
As conc., ppmw, on spent bed:[a]						
inlet	30,300	2,930	17,389	43,100	2,350	2,150
2nd	1,310	53.1	9,007	529	≤20[b]	650
3rd	64.2	≤8.6	7,206	≤12		200
4th	≤19		3,214	<10	≤12[b]	60
5th	≤15					
6th	≤13					
7th	≤15					
outlet	≤14	<2	496	<10		20
downstream trap	<0.005 mg		58.4	<10	<10	
total As, mg, absorbed on bed	48.50	6.665	75.944	79.257	3.69	
adsorbent wt., g						
inlet	1.53	2.230	1.886	1.814	1.570	
2nd	1.56	2.460	2.040	2.030	1.567	
3rd	1.54	1.142	2.214	2.070	1.552	
4th	1.51	none	2.373	2.057	1.564	
5th	2.53					
6th	2.51					
7th	4.51					
outlet	8.29	2.600	2.042	2.156	1.529	
downstream trap	carbon	none	3.066	3.140	1.816	

a. For reference, the arsenic concentration of the fresh CuO/C adsorbent was ≤19 ppmw.

b. 2nd and 3rd; 4th and outlet layers combined.

reoxidation.

Elemental mapping by Analytical Electron Microscopy (AEM) was used to ascertain the location of arsenic on the inlet sample. Surprisingly, arsenic was more or less uniformly distributed on the adsorbent with only a modest correlation of arsenic to copper. Thus, both CuO and C appear to have reacted with AsH_3. There was, as expected, a correlation between Cu-rich and O-rich regions consistent with the presence of an oxidized copper state, Cu_2O or CuO, in the spent adsorbent.

Because the probability that metallic copper will be present when CuO/C is exposed to syngas, even at ambient temperatures, evaluation of the reduced adsorbent for AsH_3 removal was undertaken. The Cu/C adsorbent was obtained by dilute H_2 or syngas reduction of CuO/C as described above and detailed in Appendix A. The H_2 reduced adsorbent had a copper surface area of 24.3 m^2/g, a relatively high value considering that the copper concentration was 10 wt%.

In an initial test (17716-13), the reduced adsorbent was shown to be effective at relatively low space velocities and AsH_3 loadings (Table 28). Arsine exposure was continued over a 10-day period in a second experiment (17716-30). Although a significant portion of the feed AsH_3 was deposited on the inlet portion of the bed, arsenic was found down the full length of the bed and on the downstream trap indicating that AsH_3 had broken through the bed. A larger percentage of the adsorbed arsenic was found on the inlet portion of the bed for the longer contact time run. This implies that AsH_3 adsorption is limited by kinetics; that is, the reaction of elemental copper with AsH_3 is relatively slow.

To determine conclusively if AsH_3 adsorption was kinetically limited, Cu/C was exposed to AsH_3 at a higher temperature, 140 ^{o}C, while keeping the contact time approximately the same. Nearly all the arsenic was trapped on the inlet portion of the bed, consistent with the proposed kinetic limitation. The inlet loading of 4.31 wt% arsenic was much larger than that for Cu/C at 30 ^{o}C, 1.74 wt% (Table 28). The As/Cu molar ratio for the inlet sample was 0.37 versus 0.33 if all arsenic was bound by copper and AsH_3 reacted as in reaction 23 implying that 4.31 wt% is close to the thermodynamic AsH_3 capacity.

$$3Cu + AsH_3(g) = Cu_3As + 1.5H_2(g) \qquad (23)$$

Additional analysis by AEM and Electron Dispersive Spectroscopy (EDS) of a pellet cross section of the inlet Cu/C sample showed that copper was uniformly dispersed throughout the pellet but arsenic was concentrated on the outer surface. This means that only a fraction of the copper was utilized for arsine removal. Arsenic was associated with copper on the outer surface; that is, arsenic reacted preferentially with copper but only on the pellet surface. Elemental concentrations were determined to be approximately 60 wt% Cu and 40 wt% As. These concentrations correspond to an empirical formula of $Cu_{1.77}As$, a composition approaching the maximum arsenic concentration in a copper alloy, $Cu_{1.5}As$ (44 wt% As).**[22]** The greater than anticipated arsenic to copper ratio may explain how high arsenic loadings can be achieved even when only the pellet surface was utilized.

The use of a heated catalyst guard bed at the LPMEOH™ Demonstration Unit was not possible and, therefore, an additional evaluation (17716-63) was conducted at AsH_3 feed concentrations comparable to the AsH_3 concentrations (50 to 60 ppb) measured at Kingsport (Table 28). For 65 ppb AsH_3 in syngas, arsenic was found only on the inlet portion of the bed. To judge the adsorbent's effectiveness, the experimental arsenic gradient in the bed was compared to the gradient calculated based on a first order kinetic adsorption process. The calculation was performed using the bed arsenic concentrations from run 17716-30 to calculate an AsH_3 pressure gradient down the bed. These pressures were used to calculate an average first order rate constant, 4.12×10^{-4} min^{-1}. The rate constant was then used to predict the arsenic gradient for exposure to a 65 ppb AsH_3 feed and these values are listed in Table 28. Based on this model, the inlet sample would contain 2,150 ppmw arsenic with 650, 200, 60, and 20 ppmw on the 2nd through outlet sections of the bed. The experimental results, however, showed no significant arsenic downstream of the inlet sample; that is, Cu/C performed better than expected based on first order kinetics.

A possible explanation for the observed kinetics is that the reaction of Cu with AsH_3 yields the alloy Cu_3As and H_2 (reaction 21). Further, the Cu/C kinetic results are consistent with arsenic migration from the surface as the rate limiting step. That Cu/C removes AsH_3 more efficiently at lower concentrations implies that arsenic migration is not critical when the surface coverage is low. At higher AsH_3, migration from the surface is not fast enough to make free surface available for incoming AsH_3. This analysis also provides a possible explanation for the poor performance of the first Cu/C trial at the LPMEOH™ Demonstration Unit – the bed exotherm caused a significant loss of copper surface area.

An understanding of Cu-AsH_3 kinetics also points to ways in which the effectiveness of Cu/C can be improved. Although it was not feasible to operate the Cu/C catalyst guard bed at the LPMEOH™ Demonstration Unit at elevated temperature, it is possible to expose the catalyst guard bed to flowing N_2 at a modest temperature, about 120 °C maximum. It was reasoned that a "purge" of 120 °C N_2 would warm the bed sufficiently to increase the rate of surface arsenic diffusion into the bulk and thus provide fresh copper surface for AsH_3 adsorption. This "regeneration" provided the predicted result. After 102 days on stream, the AsH_3 concentration in the Cu/C guard bed outlet was 30 ppb. The bed was purged with warm N_2 for 48 hours, returned to ambient temperature, and brought back on stream with syngas. The AsH_3 concentration in the guard bed outlet was below its limit of detection, <3 ppb. It is important to note this is not a traditional "regeneration" process since arsenic or AsH_3 was not desorbed from the bed; rather heating merely increased the rate of diffusion of arsenic.

2.3 Evaluation of Cu/C for Other Syngas Contaminants

Syngas can contain numerous contaminants and, as has been shown, many of these are methanol synthesis catalyst poisons which must be removed from the reactor feed. Adsorption of common syngas contaminant by Cu/C will very likely suffer from the same kinetic limitation (or worse) as does AsH_3. Thus, initial studies involving other contaminants were performed at 140 °C. Results and experimental conditions are summarized in Table 29. The same sample of Cu/C (labeled type 2) from the same supplier was used throughout the evaluation with other syngas contaminants.

PH_3. Two runs involving syngas containing PH_3 were performed with the Cu/C adsorbent (type 2). In the first of these, the PH_3 source was unknowingly contaminated with $Fe(CO)_5$, which may have had some effect on PH_3 removal efficiency (17716-59). Compared to AsH_3, the PH_3 gradient down the bed was less sharp but no breakthrough occurred in either run implying quantitative removal of the contaminant. This may reflect a kinetic limitation resulting from the greater P-H versus As-H bond energy. In the absence of an available bond energy for AsH_3, (PH_3, average bond energy, 76.4 kcal/mol[23]) the diatomic P-H and As-H bond energies, are 79 and 70 kcal/mol, respectively.[24]

Sulfur-Containing Contaminants. The removal of three sulfur-containing contaminants, thiophene, COS, and CS_2, were evaluated using the same Cu/C adsorbent material. The high background sulfur concentration on the adsorbent, about 0.5 wt%, resulted in less certain sulfur loadings and in a much higher detection limit, 1,000 ppmw, than for other contaminants. This makes interpretation of breakthrough more difficult. Nonetheless, the sulfur loadings for thiophene and COS exposure clearly show that Cu/C was ineffective for the removal of these

Table 29. Evaluation of reduced CuO/C for removal of contaminants from Kingsport Gas.

run number: 17716-	59	88	55	56	48	51	59	
contaminant deposited on catalyst (X)	PH_3 P	PH_3 P	thiophene[e] S	COS[e] S	CS_2[e] S	CH_3Cl Cl	$Fe(CO)_5$ Fe	$Ni(CO)_4$ Ni
internal bed temperature, °C	140	140	140	140	140	140	140	140
bed pressure, psig	754	756	751	754	752	749	754	754
contaminant feed conc, ppm	1.915	1.801	1.422	1.846	1.381	1.824	4.717[c]	0.042[c]
contact time, min	0.404	0.388	0.420	0.422	0.428	0.408	0.404	0.404
GHSV, h^{-1}	6,987	7,304	6,710	6,696	6,593	6,893	6,987	6,987
total X exposure, mg (calcd.)	26.12	42.74	25.26	30.28	50.44[b]	60.19	64.78	1.09
contaminant exposure time, d	4.035	6.97	4.778	4.762	5.002	4.000	4.035	4.035
X conc., ppmw, on spent bed:								
inlet	4,879	12,800	2,720	4,120	10,140	490	9,180	115
2nd	4,839	8,450	2,220	4,190	6,270	580	9,576	75.2
3rd	3,035	2,300	3,010	2,590	3,450	780	7,021	45.8
4th	1,871	164	3,430	2,470	<1,000	550	5,046	11.9
outlet	1,824	≤82	1,940	2,000	<1,000	510	4,564	21.4
downstream trap	≤157	≤110	1,510	1,460	<1,000	430	3,034	nd
% of feed X absorbed on bed[a]	~100%	~100%	35.6	47.6	72.9[b]	10.1	55[d]	41[d]
adsorbent wt., g								
inlet	1.605	1.504	1.784	1.648	1.825	1.806	1.605	1.605
2nd	1.755	1.730	1.861	1.820	1.872	1.826	1.755	1.755
3rd	1.759	1.562	1.858	1.702	1.883	1.790	1.759	1.759
4th	1642	1.690	1.872	1.762	1.842	1.824	1642	1642
outlet	1.639	1.599	1.918	1.695	1.861	1.826	1.639	1.639
downstream trap	1.689	1.770	2.042	1.616	2.095	1.845	1.689	1.689

a. Total X on spent bed/calculated X exposure.
b. Based on absorption of both S atoms from CS_2.
c. Feed concentrations were calculated from run 17716-52 spent catalyst metal loadings.
d. Based on calculated feed concentration of $Fe(CO)_5$ or $Ni(CO)_4$.
e. Sulfur loadings corrected for the background sulfur of the fresh adsorbent, 0.5 wt%.

contaminants with breakthrough of both onto the downstream trap. Conclusive evidence for CS_2 breakthrough was not obtained because of the high sulfur detection limit but only about 70% of the expected sulfur was found on the spent adsorbent, suggesting limited effectiveness for CS_2 removal as well.

CH_3Cl. The Cu/C adsorbent (type 2) was almost inert with respect to CH_3Cl. Exposure to 1.8 ppm CH_3Cl in syngas resulted in an approximately uniform distribution of Cl throughout the bed. The total weight of Cl deposited on the bed was much lower than that expected based on the feed CH_3Cl concentration. Clearly, most of the CH_3Cl passed through the bed intact. Since we have shown that CH_3Cl reacts quantitative with methanol synthesis catalyst at 250 °C, it can be concluded that the CH_3Cl/adsorbent reaction was too slow to occur at 140 °C. Higher temperatures will be required for removal of CH_3Cl or other alkyl chlorides using a copper metal-based adsorbent.

Volatile Metal Carbonyls. The fortuitous presence of $Fe(CO)_5$ and $Ni(CO)_4$ in a PH_3-containing gas mixture allowed evaluation of Cu/C (type 2) for removal of these contaminants. Analysis of spent adsorbent samples indicates Fe and Ni gradients for Fe and Ni but, based on the inferred carbonyl concentrations in the feed, the adsorbent removed only a fraction of the contaminants. The adsorbent, therefore, was not very effective for removal of these metal carbonyls. It should be noted, however, that the inlet $Fe(CO)_5$ concentration was extremely large, probably much larger than would be encountered in an industrial setting.

Because of higher than anticipated iron levels on the samples from the LPMEOH™ reactor during catalyst campaign 3, the possibility of $Fe(CO)_5$ breakthrough of the Cu/C adsorbent was considered. A short bed of Cu/C (5.93 g) was exposed to a blend of Shell Gas and H_2 at 30 °C. The Shell Gas (tube trailer) supplied metal carbonyls and H_2 was used to adjust the feed composition to approximately Kingsport Gas. The bed feed contained on average 580 ppb $Fe(CO)_5$ and 112 ppb $Ni(CO)_4$. These concentrations varied depending mostly on the ambient temperature. The gases exiting the bed were monitored by GC and, periodically, the composition of the inlet was checked. After exposure to syngas for 35 days, no breakthrough of $Fe(CO)_5$ or $Ni(CO)_4$ was observed (<1 ppb $Fe(CO)_5$). Based on the average inlet composition, calculated minimum capacities are: Fe, 5.58 wt%; Ni, 1.13 wt% if all metals were absorbed on the inlet ¼ of the bed or Fe, 1.37 wt%; Ni, 0.28 wt% assuming equal distribution throughout the bed. Clearly, Cu/C is much more effective for $Fe(CO)_5$ removal at near ambient temperatures than at 140 °C. This observation implies that the carbon portion of the adsorbent may be responsible for carbonyl removal. As has been shown, in the laboratory and in the field, activated carbons are very effective for $Fe(CO)_5$ removal and adsorption on carbons is expected to be more favorable at lower temperatures. Adsorption on copper, however, will likely be limited by kinetics and, thus, more favorable at high temperatures.[15,25]

2.4 Alternative Adsorbents

Enhanced Activated Carbon. The enhanced activated carbon was suggested by its supplier as an adsorbent specifically for arsine removal. The adsorbent consists of only carbon, no metals, and, hence, its use is not complicated by safety or performance issues associated with the heat of reduction of the metal oxides. The adsorbent is considered to be catalytic in the sense that it binds contaminants and promotes their oxidation on pore surfaces via the presence of low or trace O_2. For example, AsH_3 will be bound and oxidized to an arsenic oxide such as As_2O_3. Gaseous O_2 required for catalytic oxidation is, of course, not present in a syngas feed so experimental verification of AsH_3 removal was required.

Exposure of the enhanced carbon to Kingsport Gas feed containing about 0.8 ppm AsH_3 at two different contact times resulted in favorable performance. As shown in Table 30, no AsH_3 breakthrough was observed for either run. Further, at comparable exposure levels, the amount of arsenic adsorbed on the bed inlet was about the same as for reduced Cu/C (17716-30). In fact, the arsenic profiles of two adsorbents were comparable but breakthrough did not occur for the enhanced carbon. Recall, however, that the Cu/C performance at 140 °C (see Table 28) was far superior to that of the enhanced carbon at 30 °C. Therefore, enhanced carbon would be a reasonable alternative to Cu/C only at near ambient operating temperatures.

MnO_2/Al_2O_3. The enhanced AsH_3 removal efficiency of Cu/C at elevated temperatures prompted an evaluation MnO_2/Al_2O_3 at 140 °C. This adsorbent had been used in the Eastman (19C-30) and 29C-40 catalyst guard beds but it was largely ineffective for AsH_3 removal at ambient temperature. In retrospect, this is not surprising since the AsH_3 capacity for

Table 30. Results for the enhanced carbon versus Cu/C exposed to AsH_3/syngas at 30 °C. Kingsport Gas feed.

adsorbent	Enhanced C	Enhanced C	Cu/C
run number	17716-19	17716-33	17716-30
internal bed temperature, °C	30	30	30
bed pressure, psig	740	757	738
AsH_3 feed conc, ppm	0.803	0.761	0.715
contact time, min		0.505	0.407
GHSV, h^{-1}	3,043	5,620	6,800
total As exposure, mg (calcd.)	9.81	63.10	65.67
contaminant exposure time, d	1.99	7.94	9.99
As conc., ppmw, on spent bed:			
inlet	3,100	17,600	17,389
2nd	799	9,640	9,007
3rd	≤17	4,170	3,214
4th		872	
outlet	<7	51.3	496
downstream trap		≤11	58.4
total As, mg, absorbed on bed	9.07	66.45	75.94
adsorbent wt., g			
inlet	2.121	1.988	1.886
2nd	3.118	2.154	2.040
3rd	2.684	2.078	2.14
4th		2.163	2.373
outlet	3.102	2.059	2.042

MnO_2/Al_2O_3 reported in the literature at ambient temperature was only 0.38 wt%.[26] Its ineffectiveness is almost certainly because arsine reacts slowly with MnO_2 under these conditions.

The adsorbent was evaluated at 140 °C using an AsH_3/syngas feed and the results and a comparison to those for Cu/C are provided in Table 31. Although MnO_2/Al_2O_3 was far more effective at elevated temperature, its reaction with AsH_3 is evidently still too slow to prevent breakthrough. A still higher temperature (or lower gas flow rate) would be required to achieve optimum AsH_3 removal. As shown in Table 31, the performance of Cu/C was superior to that of MnO_2/Al_2O_3. Nearly all of the feed AsH_3 was trapped on the inlet portion of the Cu/C bed while only about 40% was trapped on the MnO_2/Al_2O_3 inlet. Furthermore, no arsenic was detected past the inlet 38% of the Cu/C bed, while the entire MnO_2/Al_2O_3 bed contained at least some arsenic. These results point out the need to test adsorbents prior to their use in industrial applications rather than relying solely on supposed performance data or recommendations provided by adsorbent suppliers. MnO_2/Al_2O_3 is not effective for AsH_3 removal when compared with the Cu/C adsorbent.

Another potential concern involving the use of MnO_2 is its reaction with syngas, a concern that became more real after the exotherm resulting from exposure of CuO/C to syngas at Kingsport. As shown in Table 32, MnO_2 reduction, depending on the product oxidation state, can be at least as energetic as CuO reduction. In organic synthesis, MnO_2 is generally viewed as a strong oxidizing agent and, as shown in Table 32, its potential reactions with syngas are quite favorable. The results of TGA/DSC experiments detailed in Table 23 clearly show that MnO_2 undergoes

Table 31. Arsine removal by MnO_2/Al_2O_3 at 140 °C using Kingsport Gas.
GHSV = standard flow rate (standard cubic centimeters per hour)/adsorbent volume (cc);
Contact time = adsorbent volume (cc)/actual rate (cc/min).

adsorbent run number	MnO_2/Al_2O_3 17716-30	Cu/C 17716-43
internal bed temperature, °C	140	140
feed pressure, psig	755	748
arsine feed conc, ppb	674	737
contact time, min	0.415	0.410
GHSV, h^{-1}	6,829	6,847
total arsenic, mg (calcd.)	40.14	61.75
arsine exposure time, d	9.44	8.67
arsenic conc ppm on spent bed:		
inlet	8,960	43,100
2nd	6,120	529
3rd	3,490	≤12
4th	2,580	<10
outlet	979	<10
downstream trap	400	<10
total As, mg, absorbed on bed	33.33	79.257
Cumulative wt% of bed		
inlet	21.5	17.9
2nd	40.8	38.0
3rd	60.6	58.4
4th	79.9	78.7
outlet	100	100

Table 32. Thermodynamics of CO reduction of MnO_2 and CuO at 25 °C.

oxidation states	reaction	ΔH, kcal/mol M_xO_y	K
IV/III	$MnO_2 + 0.5CO(g) = 0.5CO_2(g) + 0.5Mn_2O_3$	-23.875	$1.089x10^{18}$
IV/II, III	$MnO_2 + 0.67CO(g) = 0.33Mn_3O_4 + 0.67CO_2(g)$	-31.360	$3.079x10^{23}$
IV/II	$MnO_2 + CO(g) = MnO + CO_2(g)$	-35.410	$1.405x10^{27}$
I/0	$CuO + CO(g) = Cu + CO_2(g)$	-30.330	$3.830x10^{22}$

reduction at 290 °C under 3 vol% H_2 in N_2 at 1 atm (CuO/C reduced at 210 °C under same conditions).

Exposure of a test bed containing MnO_2/Al_2O_3 at 40 ^{o}C to Kingsport Gas resulted in maximum temperature changes of only 1.9 ^{o}C (inlet) and 2.5 ^{o}C and, after 73.3 hours syngas exposure, no MnO_2 reduction products such as Mn_2O_3 or Mn_3O_4 were not detected by XRD. The possibility remains that reduction products may be amorphous and, thus, not detectable by XRD. Because the recommended operating temperature for MnO_2/Al_2O_3 is “greater than 80 ^{o}F”, the adsorbent was also evaluated at 100 ^{o}C. After 71.7 hours of exposure to syngas, reduced MnO_2 phases were not found implying that MnO_2/Al_2O_3 was not reduced at 100 ^{o}C under syngas. In addition, no uncontrolled temperature excursions were observed in using this adsorbent at ambient temperature at the LPMEOH™ Demonstration Unit. Nonetheless, care must still be taken to insure that the adsorbent is not exposed to higher temperatures without prior laboratory evaluation under syngas.

Ni-Based Adsorbent. A metallic Ni-containing adsorbent (with an alumina/silica substrate) reportedly has excellent AsH_3 (40.3 wt%) and COS (32 wt%) capacities at ambient temperature.[26] The adsorbent, is supplied in the oxide form, $NiO/SiO_2/Al_2O_3$, and following reduction exhibited impressive capacities for AsH_3 and COS at ambient pressure and 100 ppm each contaminant. The reduced adsorbent might be an alternative for Cu/C for applications in which only an ambient temperature guard bed is available. One significant limitation that needs to be addressed is $Ni(CO)_4$ formation upon syngas exposure. Depending on the $Ni(CO)_4$ concentration generated at ambient temperature, a simple carbon trap might be sufficient. Experiments to determine the extent of $Ni(CO)_4$ formation or the effectiveness of the reduced adsorbent for AsH_3 removal were planned but not completed.

3. Analytical Results from Kingsport Samples

There were four catalyst campaigns, or runs, which characterize the operating program of the LPMEOH™ Demonstration Unit. Kingsport Catalyst Campaign 1 was conducted between April 1997 and November 1997. This run was concluded on 03 November 1997 after 171 days of operation. Kingsport Catalyst Campaign 2 was conducted between December 1997 and August 2001. The run was concluded on 06 August 2001 after 1,325 days of operation. Kingsport Catalyst Campaign 3 was conducted between August 2001 and June 2002. The run was concluded on 04 June 2002 after 284 days of operation. The fourth Kingsport Catalyst Campaign began on 28 June 2002 and included process and analytical data until the end of the operating program on 31 December 2002.

A comparison of the catalyst campaigns is given in Table 33. The first run involved batch-wise catalyst activation along with the addition of fresh slurry to maintain catalyst productivity. The second run involved batch-wise catalyst activation along with withdrawal of spent catalyst slurry and addition of fresh slurry to maintain catalyst productivity. The third and fourth runs used an in-situ activation procedure to prepare a full charge of methanol synthesis catalyst. Temperature programming was used in the third campaigns to maintain productivity. During the fourth

Table 33. Kingsport LPMEOH™ operating program campaigns.

Kingsport Campaign #	Run Start Date	Run End Date	Days Onstream	Catalyst Type Used	Starting Catalyst Charge (lbs)	Activation Method	Productivity Control Method	Operating Temperature (°C)
1	4/6/97	11/3/97	171	Baseline	20,300	Batch	Catalyst Addition Only	250 to 260
2	12/20/97	8/6/01	1,325	Baseline + Alternative	19,500	Batch	Catalyst Addition / Withdrawal	235[a]
3	8/24/01	6/4/02	284	Alternative	41,580	In-situ	Temperature Programming	216 to 242
4	6/28/02	Ongoing[b]	Ongoing[b]	Alternative	40,040	In-situ	-	215

a. Primarily 235 °C with brief operation at other temperatures.
b. The LPMEOH™ Demonstration Unit operating program ended 12/31/02 with 187 days on-stream in Catalyst Campaign 4.

catalyst campaign, productivity was essentially maintained by virtue of the very low catalyst deactivation rates and, therefore, temperature programming was not used during the period of performance. Methanol synthesis catalyst (baseline and alternative) from two different suppliers was used during the operating program.

3.1 Kingsport Catalyst Campaign 1

This campaign used the baseline methanol synthesis catalyst exclusively. Although there were no spent catalyst withdrawals during the campaign, freshly reduced catalyst was added to the LPMEOH™ reactor to maintain productivity starting in July 1997. Analyses of early samples from Kingsport Catalyst Campaign 1 indicated a step-change increase in the concentration of iron on the catalyst surface during the initial six weeks, which could not be correlated to the presence of iron carbonyl in the feed gas streams. This finding was most likely related to the detection of post-construction debris within various parts of the facility. During this run, higher than expected levels of arsenic were also found on the catalyst samples. Tables 34 and 35 list the physical properties and elemental composition of freshly reduced and spent catalyst samples from Kingsport Catalyst Campaign 1.

Table 34. Physical properties of catalyst samples from Kingsport Catalyst Campaign 1.[a]

	TOS	crystallite size, Å		surface	relative Cu
sample	Days	Cu	ZnO	area, m^2/g	surface area[b]
Several	0	80	30	80	1.0
K0597-2	31	273.8	89.2	-	0.387
K0897-1	93	282.8	87	43	0.283
K0997-1	110	280.5	118.1	42	0.247
K1097-1	136	288.9	186.8	45	-
K9711-1b	173	291.6	111.2	40	-

a. No entry means that the data was unavailable
b. Relative Cu SA = observed Cu surface area / Cu surface area of freshly reduced catalyst.

Table 35. Elemental composition of solids from Kingsport Catalyst Campaign 1 slurries.

		concentration, ppmw				
	TOS Days	As	S	Fe	Ni	Cl
Several	0	<25	100	47	25	-
K0597-2	31	446	190	281	61	< 200
K0897-1	93	601	235	169	< 20	-
K0997-1	110	779	575	261	37	-
K1097-	136	711	330	189	28	-
K9711-1b	173	699	340	194	37	

3.2 Kingsport Catalyst Campaign 2

Initially, Catalyst Campaign 2 used the baseline methanol synthesis catalyst. Starting on 29 October 1998 (day 313), an alternative methanol synthesis catalyst was introduced and used thereafter. During the run, there were numerous withdrawals of aged catalyst slurry and additions of freshly reduced catalyst to the reactor resulting in a mixture of aged and fresh catalyst as the run proceeded. This complicated the interpretation of analytical data. Catalyst slurry samples for analysis at Air Products were taken at least monthly and the collected analytical data for these samples is detailed below.

3.2a Catalyst Analysis

Catalyst Physical Properties. Table 36 lists the physical properties of freshly reduced and spent catalyst samples from Kingsport Catalyst Campaign 2. Some additional data for two batches of alternative catalyst (oxide form) used during the run are provided in Table 37. Characterization by XRD was obtained using catalyst slurries. Surface area measurements were determined using solid catalyst obtained from slurries.

XRD analysis indicated that all freshly reduced and spent catalyst samples contained only the expected phases (metallic Cu and ZnO). The only exception was sample K0011-2 which, in addition to these phases, contained a minor amount of Cu_2O and a trace of $ZnCO_3$. As might be expected, Cu crystallite size generally increased with time on stream but, because of numerous catalyst additions and withdrawals, there was not a smooth, continuous increase (Figure 9). Increasing copper crystallite size is usually attributed to thermal sintering. The increase in ZnO crystallite size with time on stream was much more modest than for Cu.

Copper surface area measurements provide valuable information relating to catalyst aging. As would be expected, copper surface area decreased with increasing time on stream. The loss of surface can be ascribed to thermal sintering and the effects of bound poisons.[27] The trend toward lower copper surface area was greatly affected by catalyst addition and withdrawals. However, catalyst activity as represent by eta (the ratio of the observed methanol synthesis rate constant to calculated rate constant for freshly reduced catalyst) closely followed the copper surface area (Figure 10). Decreasing copper surface area resulted in an approximately linear decrease in catalyst activity (Figure 11). The loss of catalyst activity with decreasing copper surface area has been reported in the literature.[27-29]

During the run time for which analysis was performed on a regular basis (> 493 days), the catalyst surface area varied little and was relatively insensitive to time on stream. Detailed particle size distributions are tabulated in Table 37. The particle size data for sample K9906-1 (Figure 12) was typical of that for other spent Kingsport slurries: particles ranging from about 0.1 µm and higher, with three or four particle size maxima. Table 38 data shows that a general decrease in particle size with time on stream but, because of catalyst additions and withdrawals, this was not a smooth, continuous decrease.

Table 36. Physical properties of catalyst samples from Kingsport Catalyst Campaign 2.[a]

sample	TOS days	crystallite size, Å Cu	ZnO	surface area m^2/g	relative Cu surface area	particle size range, μm
Alt. Catalyst batch 1a	-	-	-	103	1.29 [c]	
Alt. Catalyst batch 1a		-	-	98	0.845 [c]	
K9804-1, reduced	-	72.5	84.9	105		
K9909-1, reduced	-	87.2	67.1	93[b]	1.00	
K0009-1, reduced	-	65.7	32.8	97	0.841	
K9712-1	0	95.3	74			
K9712-2	1	100.0	123.8	75		0.17 - 34.25
K9712-3	4	130.9	64			
K9712-4	10	126.8	73.3	73		
K9801-2	37	132.1	98.3			
K9802-1	45	141.1	91.5			
K9802-2	51	158.1	113			
K9802-3	57	145.7	91			0.15 - 2.80
K9802-4	65	176.8	114.5			
K9803-2	80	154.3	95.8	44		
K9803-4	99	169.6	87.9			
K9804-2	115	152.4	89.3			
K9805-2	142	219.2	109.6			
K9806-2	178	272.3	117.2			
K9807-2	200	263.2	108.6			
K9807-3	221	412	112			
K9808-3	237	353.9	124			
K9809-1	278	347.4	129.8		0.534	
K9810-1	289	331.1	130.4			
K9811-2	340	293.9				
K9812-1	374	283.1			0.332	
K9901-1	391	252.5	61.4			
K9902-1	424	474.7	133.6		0.163	0.15 - 15.17
K9904-3	493	418	110	15	0.226	0.17 - 34.25
K9906-1	528	517	105	43	0.229	0.15 - 29.91
K9907-1	570	446	117	60	0.275	0.17 - 22.80
K9908-2	619	632	116	56	0.332	0.20 - 116.2
K9909-2	640	357	109	64	0.534	0.20 - >102
K9910-2	668	134.6	93.6	55	0.422	0.20 - 1020
K9912-1	718	797	120.7	60	0.464	0.15 - 11.56
K0001-1	746	613	104.5	63	0.364	0.15 - 15.17
K0003-1	803	187	88.7	67	0.538	
K0004-1	855	175	114.5	59	0.455	
K0007-1	941	173.5	107.5	69	0.527	
K0008-1	985	384.7	90.4	66	0.509	
K0009-3	1004	157.2	96.0	66		
K0011-1	1053	247.6	79.6	70	0.548	
K0011-2	1073	262.8	109.2			
K0101-1	1110	280.4	110.1	66	0.428	
K0102-1	1145	172.2	103.9	73	0.580	
K0103-1	1173	163.7	137.6	69	0.659	
K0106-1	1263	242.8	103.4	62	0.376	
K0106-3	1285	235.1	83.3	74	0.936	
K0107-1	1299	186.4	159.1	65	0.450	
K0108-1	1325	207.7	127.6	64	0.453	

a. No entry means that the data was unavailable.

b. Oxide form of the catalyst; c. Following reduction.

Table 37. Additional physical properties of alternative catalyst (oxide form) batches used during Kingsport Catalyst Campaign 2.

	Batch 102899	Batch 22812/704/98
Tapped Density	0.66	0.65
TGA weight loss, % (N_2)	16.2	15.2
(H_2, 634°C)	21.1	17.8
Settling, mL: 15 min	40 (92%)	61.5 (61%)
Final	35	38
Viscosity, cP, @37%, 25 °C,		
20.4/sec shear rate	nd	250
10.2/sec shear rate	840	277
4.08/sec shear rate	1480	337

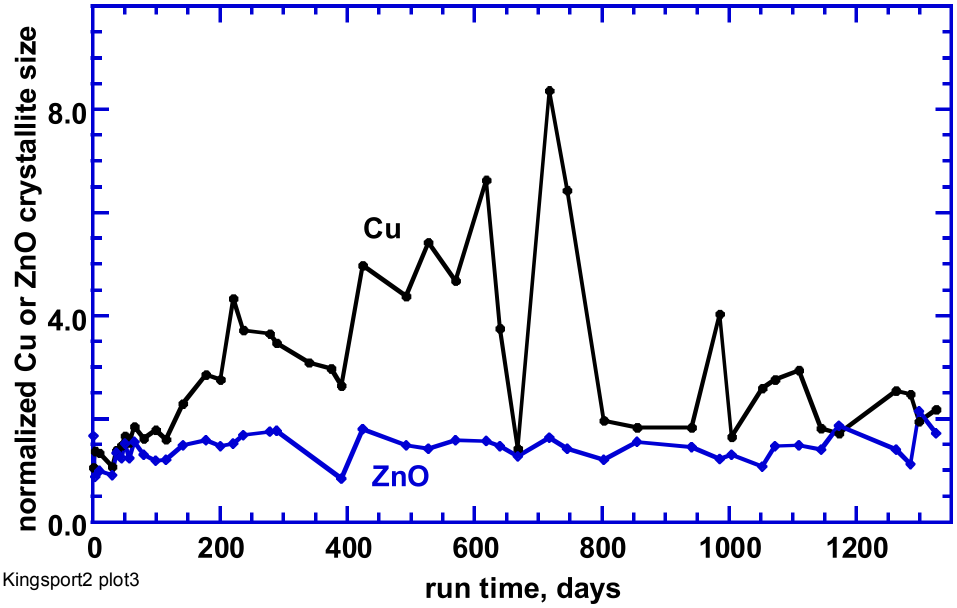

Figure 9. Normalized Cu and ZnO crystallite sizes for Kingsport Catalyst Campaign 2 slurries. The following initial crystallite sizes were used for normalization: Cu, 95.3 Å; ZnO, 74 Å.

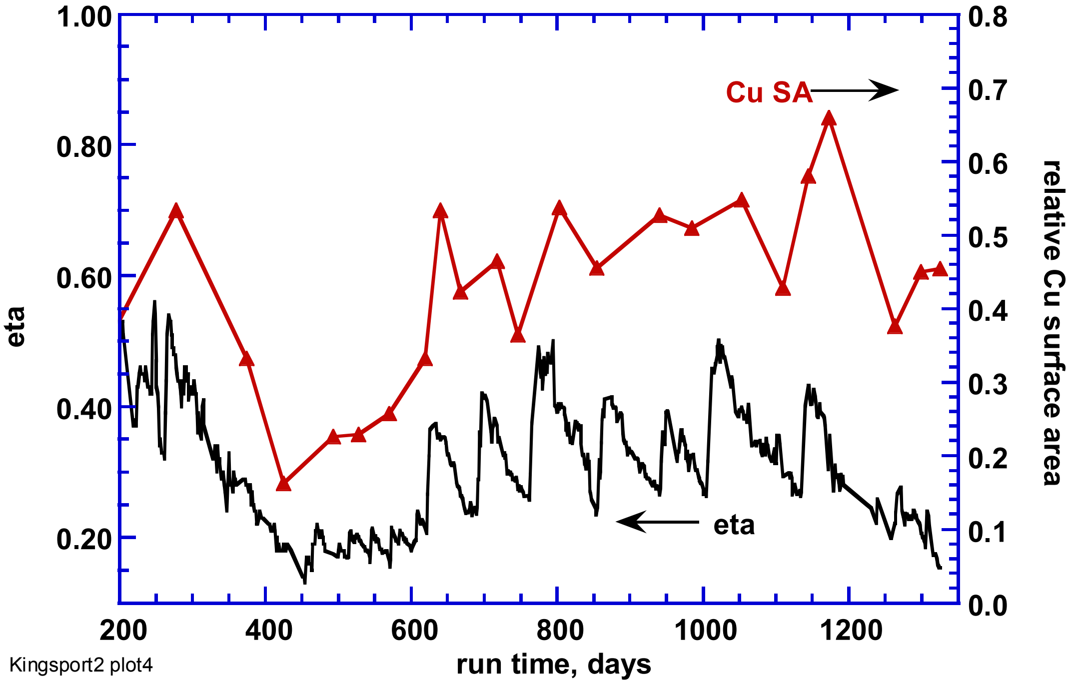

Figure 10. Relative copper surface area and eta versus run time for solids from Kingsport Catalyst Campaign 2 slurries.

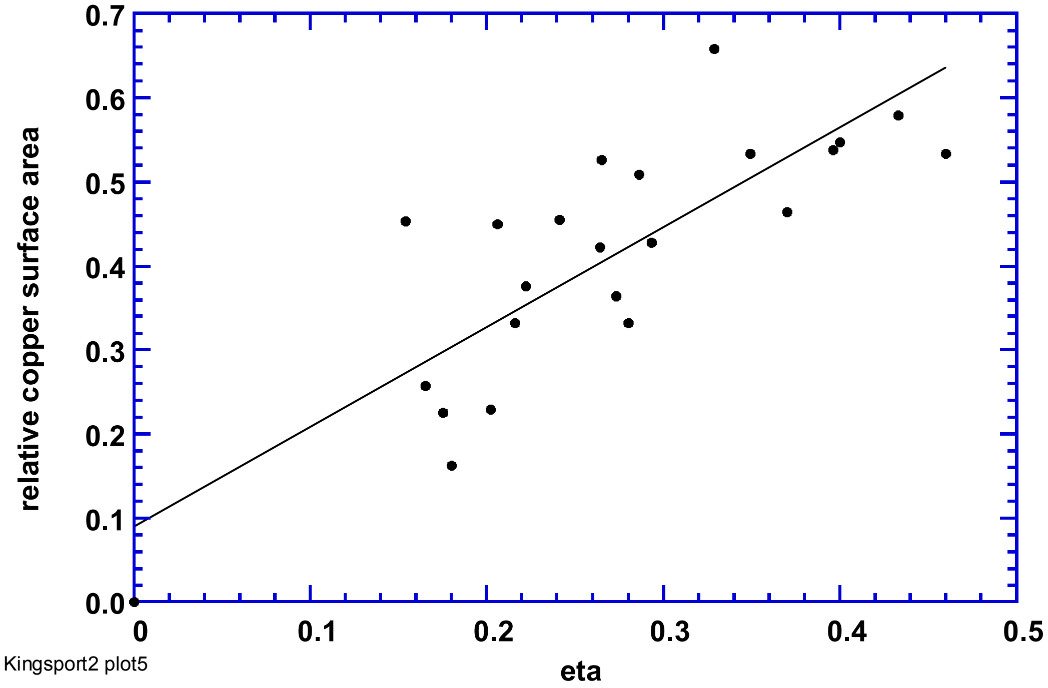

Figure 11. Relative copper surface area versus eta for solids from Kingsport Catalyst Campaign 2 slurries.

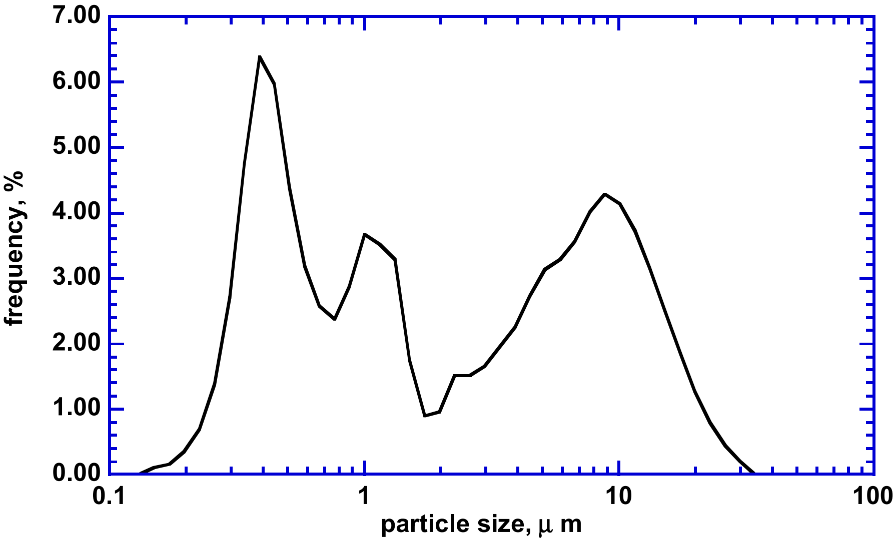

Figure 12. Particle size (μm) versus frequency for spent Kingsport slurry sample K9906-1.

Table 38. Particle size distribution of slurry samples from Kingsport Catalyst Campaign 2.

sample	TOS, days	particle size range, μm	Particle size maxima,[a] μm; (frequency, %)			
K9712-2	1	0.17 - 34.25	10.10 (8.62)	1.32 (1.87)	0.39 (2.45)	
K9802-3	57	0.15 - 22.80	8.82 (6.57)	1.01 (3.07)	0.45 (8.42)	
K9902-1	424	0.15 - 15.17	7.70 (3.39)	1.01 (4.12)	0.45 (10.31)	
K9904-3	493	0.17 - 34.25	10.10 (4.64)	1.01 (3.48)	0.45 (6.65)	
K9906-1	528	0.15 - 29.91	8.82 (4.27)	1.01 (3.67)	0.39 (6.39)	
K9907-1	570	0.17 - 22.80	8.82 (5.05)	1.01 (4.24)	0.45 (6.69)	
K9908-2	619	0.20 - 116.2	10.10 (3.96)	1.01 (3.69)	0.45 (5.05)	
K9909-2	640	0.20 - >102	10.10 (3.70)	1.15 (3.80)	0.45 (3.74)	
K9910-2	668	0.20 - 1020	678.5 (23.7)	10.10 (3.72)	1.01 (4.46)	0.45 (5.59)
K9912-1	718	0.15 - 11.56	5.87 (3.24)	0.77 (7.96)		
K0001-1	746	0.15 - 15.17	7.70 (3.56)	0.77 (7.48)		

a. Distribution frequency based on volume (not number) fraction; a frequency of 5% means that particles of a specified diameter account for 5% of the total particle volume (not number).

Catalyst Composition. The chemical compositions of Kingsport catalyst samples were routinely monitored using XRF and elemental analysis for expected trace contaminants including arsenic, sulfur, chlorine, iron, and nickel. XRF data for chlorine was obtained using a catalyst slurry while a dry, oil-free solid was used for elemental analysis. XRF provides an estimate of concentrations. Concentrations by elemental analysis (Table 39) are more accurate. The combination of the two techniques insured that no elemental contaminant of interest was overlooked. The data in Table 39 shows that the only significant contaminants on the catalyst were As, S, and Fe and, of these, As was by far the most abundant (Figure 13). As with the other analytical properties, catalyst additions and withdrawals caused periodic decreases in arsenic concentration but these values subsequently increase with time on stream. Plotting of the total

Table 39. Elemental composition of solids from Kingsport Catalyst Campaign 2 catalyst slurries.[a]

	TOS	concentration, ppmw				
sample	days	As	S	Fe	Ni	Cl
K9712-1	0	10.2	66.7	362	47.2	
K9712-2	1	<50	≤167	92.1	≤18	
K9712-4	10	<50	≤127	126	≤22	
K9801-1	30	13.2	20.7	98.6	23.1	
K9801-2	37	29.2	42.7	63.5	39.5	
K9802-3	57	209	≤97	67.1	36	
K9803-2	80	408	≤94	61.4	35.8	
K9804-2	115	615	≤170	81.7	30.8	
K9805-2	142	538	163	73.2	35.9	
K9806-2	178	1110	220	86.4	31.3	
K9807-2	200	1045	277	88.7	27.6	
K9807-3	221	1650	211	77.5	35.8	
K9808-3	237	1250	231	107	42.1	
K9809-1	278	1149	326	69.6	29.8	
K9811-2	340	1400	264	57.3	23.4	
K9812-1	374	1300	260	72.3	20.4	
K9902-1	424	1490	385	82.6	22.2	
K9904-1	472	1660	529	136	18.3	
K9904-3	493	1460	348	131	18.2	<30
K9905-2	515	1600	671	158	17.2	
K9906-1	528	1680	316	109	19.7	40
K9907-1	570	1810	488	175	19.7	30
K9908-2	619	1470	406	161	15.1	20
K9909-2	640	1050	253	132	11.2	nd
K9910-1	654	1120	468	181	14.0	
K9910-2	668	1270	343	157	15.4	30
K9911-1	684	1580	335	184	12.8	
K9912-1	718	1400	248	167	13.9	40
K0001-1	746	1190	292	199	10.8	nd
K0001-2	760	1250	432	205	10.0	
K0003-1	803	1010	226	137	8.19	30
K0004-1	855	1240	248	164	6.63	20
K0007-1	941	1270	349	166	≤9.6	30
K0008-1	985	1080	379	186	<10	50
K0009-3	1004	1390	273	145	<10	
K0011-1	1053	1490	237	120	<10	nd
K0011-2	1073	1470	258	128	<10	20
K0012-1	1094	1550	210	110	<10	
K0012-2	1095	1480	410	100	<10	
K0101-1	1110	1980	355	166	<10	30
K0101-4	1133	2260	370	130	<10	
K0102-1	1145	1750	375	121	<10	40
K0103-1	1173	1830	416	89.4	<10	20
K0106-1	1263	1510	527	213	<10	nd
K0106-3	1285	767	≤420	187	<30	nd
K0107-1	1299	1789	640	254	<30	40
K0108-1	1325	1849	774	283	<30	40
MK101	oxide[b]	<10	<100	14.4	<5	<100
MK101	oxide[c]	<10	<55	<10	<10	<100
K9804-1	reduced[d]	≤12	≤110	23	≤11	

Table 39. Continued

K9909-1	reduced[d]	≤19	<100	33.3	<10	nd
K0009-1	reduced[d]	195	106	46.3	<10	30

a. Cl determined by XRF; na = not available; nd = not detected.
b. Batch powder in oxide form.
c. Batch 22812/704/98 powder in oxide form.
d. Freshly reduced catalyst.

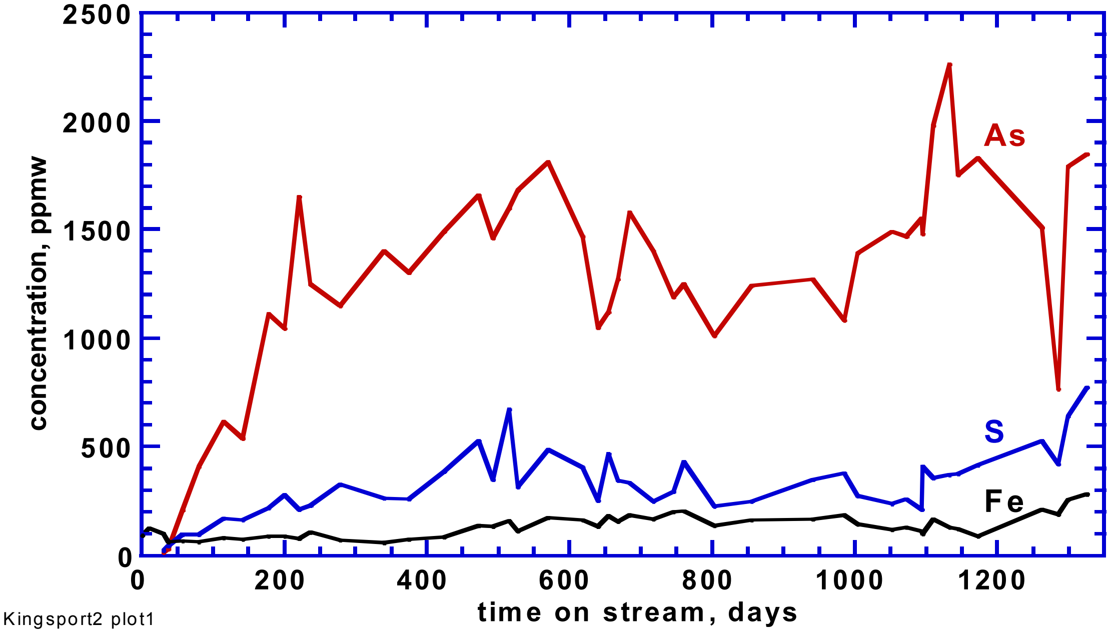

Figure 13. Arsenic, sulfur, and iron concentrations (ppmw) on solids from Kingsport Catalyst Campaign 2 catalyst slurries.

arsenic and sulfur molar concentration against eta (Figure 14), however, showed an exponential relationship between catalyst activity and total contaminant concentration.

One element conspicuously absent from the routine XRF and elemental analysis data is nitrogen. Analytical results for spent guard bed adsorbents indicated that nitrogen-containing contaminants were present in the Balanced Gas and, thus, determining nitrogen concentrations on catalyst samples became critical. Nitrogen (Kjeldhal method) and cyanide testing were performed on a non-routine basis at an external laboratory. A selection of spent catalyst slurries from the first 528 days was examined along with the catalyst in the oxide form and freshly reduced catalyst. The N and CN^- concentrations on the catalyst in each sample were calculated from the analytical results and the weight % catalyst in each sample (by TGA) and by assuming that N and CN^- were present only on the catalyst (Table 40). The spent catalyst slurries were found to contain no significant levels of nitrogen beyond that observed on the freshly reduced catalyst and there was no apparent increase in nitrogen concentration with time on stream. Very low cyanide concentrations were found on the spent catalyst slurries, with a maximum of 31 ppmw on sample

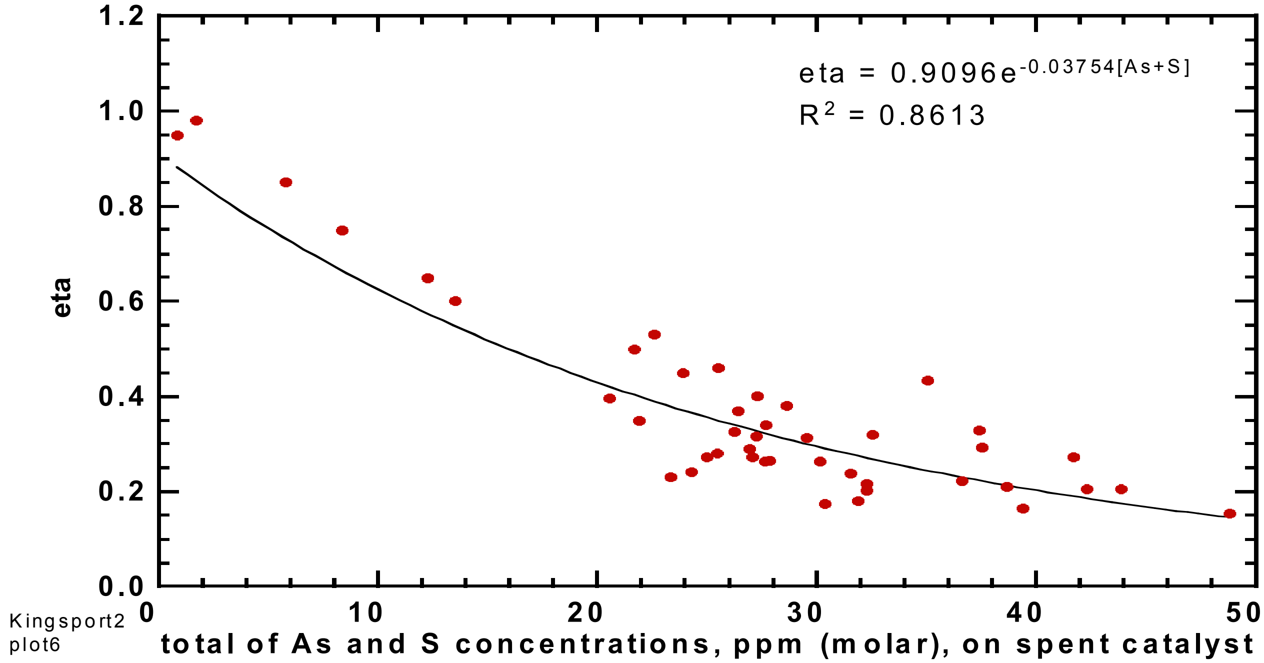

Figure 14. Total of arsenic and sulfur concentrations versus eta for spent Kingsport Catalyst Campaign 2 catalyst samples.

Table 40. Nitrogen and cyanide concentrations for slurry samples from Kingsport Catalyst Campaign 2.

Sample	TOS, days	wt% solid in slurry	conc. N, ppmw, in slurry	conc. N, ppmw, on catalyst[a]	conc. CN$^-$, ppmw, in slurry	conc. CN$^-$, ppmw, on catalyst[a]
spent slurries						
K9712-2	1	15.51	43	271		
K9802-3	57	45.05	32	71		
K9806-1	170	11.50	48	417		
K9902-1	424	31.15	86	276		
K9904-3	472	41.26	43	104		
K9906-1	528	38.8	37	95	-	
K9906-1 (solid)	528	b	-	<300[b]	-	<2.5[b]
K9908-2	619	46.47	30	65	<21	<45
K9909-2	640	40.96			12.6	30.8
K9910-2	668	39.22	50	127	<21	<54
reduced slurries						
K9806-3	-	3.44	30	873		
K9901-2	-	43.42	110	253		
oxide form						
slurry	-	29.5	52	176	<1.5	<1.5
Solid		-	-	<97[c]	-	<1.5

a. Assumes all N or CN$^-$ on the catalyst.
b. Solid used for analysis.
c. Insufficient sample for lower quantitation limit.

K9909-2. These results mean that neither nitrogen or cyanide were bound to the catalyst in any appreciable concentration.

Spent catalyst slurries were routinely screened for Cl by XRF and concentrations were consistently low, 50 ppmw or less. Fluorine, however, cannot be detected by XRF and its routine elemental analysis was not practical. A total fluorine analysis (inorganic and organic fluorine) for a representative spent catalyst slurry (K9909-2, 640 days on stream) indicated no detectable fluorine: < 22 ppmw or < 54 ppmw assuming fluorine was on the catalyst only. Chlorine analysis on the same sample indicated less than 24 ppmw Cl were present, consistent with routine XRF data. For comparison, the oxide form of the catalyst contained <18 ppmw F and 17 ppmw Cl. The solid catalyst from slurry K9909-2 was further characterized by XPS, a technique that is sensitive to the surface composition. As indicated in Table 41, fluorine was not detected (<0.1 atomic %) on the catalyst surface and the surface chlorine concentration was actually lower than that of the fresh catalyst in the oxide form. In fact, Fe was the only contaminant found on the catalyst surface.

The importance of arsenic as a potential catalyst poison led to additional characterization in an attempt to understand catalyst-arsenic chemistry. XAS was used to characterize the nature of arsenic on spent methanol catalyst in slurries K9908-2 (619 days, 1,470 ppmw As) and K9909-2 (640 days, 1,050 ppmw As). Arsenic in both is best characterized as As(0) in a Cu-As intermetallic surface phase structurally related to domeykite, Cu_3As.

Table 41. Relative atomic percent of elements by XPS on catalyst solids.[a]

Sample	Cu	Zn	Al	O	C	F	Cl	N	P	Fe
K9909-2 (solid)	3.8	13.4	15.6	39.6	22.7	nd	2.3	nd	nd	2.6
Alternative Catalyst oxide form	13.2	6.9	20.7	31.2	24.6	nd	2.8	nd	0.6	nd

a. Atomic percents are calculated omitting hydrogen (not detectable XPS) and are normalized to 100%.
nd = not detected; also not detected in either sample: S, As, Na, Ca, Mn.

3.2.b Mineral Oil Analysis

The mineral oil used in the LPMEOH™ Process was analyzed to ascertain the presence of contaminants and to provide information regarding the potential role of mineral oil in catalyst deactivation. This oil is a paraffinic/naphthenic (65/35) mineral oil with an average molecular weight of 366 and an initial boiling point of 283 °C. GCMS analysis of fresh mineral oil from the LPMEOH™ Demonstration Unit indicated a cluster of C_{17} to C_{30} species tailing-off to C_{40} species. Spent mineral oil from a catalyst slurry sample from the LPMEOH™ reactor labeled K9907-1 (570 days) showed only one cluster of C_{30} to C_{44} species implying that the lower molecular weight components were lost with time, perhaps because of volatility or coupling reactions. For comparison, fresh oil used at the Air Products laboratories contained a large cluster of C_{17} to C_{28} species and a second, smaller cluster of C_{28} to C_{40} species.

Elemental analysis of the mineral oil from catalyst slurry sample K9908-2 (619 days) indicated the absence of all inorganic contaminants at the indicated detection limits (ppmw): S <100; Cu ≤1.4, Ni, Cd, Co, Cr, Li, Mg, Mn, V, <1; Zn, Ag, Na, <2; Al, As, <3; Mo, <4; Sn, <10; P, <100;

K, <13; Si, <20; Fe, ≤0.76; Cu, ≤1.4; Ca, ≤5.7; Ti, ≤9.2. Similarly, a sample of mineral oil from the Kingsport fresh oil storage tank showed no Fe or Ni at their limit of detection, 10 ppmw, thus eliminating the oil as the source of these metals on the catalyst. The nitrogen concentrations for both fresh oil from the LPMEOH™ Demonstration Unit and the mineral oil from spent catalyst slurry sample K9906-1 were below the limit of detection, <17 ppmw. Based on these analytical results, the mineral oil does not provide a source of contaminants that can affect catalyst performance.

The possibility of a mineral oil/catalyst reaction leading to diminished activity was considered. In fact, ultraviolet spectroscopy (UV) spectral data for various oil samples was consistent with such a reaction. Fresh oil has very low UV absorbance as expected for a saturated hydrocarbon. However, mineral oil from spent or freshly reduced catalyst slurries exhibited significant UV absorbances with two distinct peaks at about 215 nanometers (nm) and 275 nm (weaker) along with two shoulders (sometimes ill-defined) at about 225 and 240 nm. Such absorbances are expected for unsaturated hydrocarbons. However, ^{13}C nuclear magnetic resonance results showed no resonances due to C=C (olefins) or C=O (limit of detection about 1%) and the Fourier Transform Infrared (FTIR) spectra of fresh and spent mineral oil were identical. Previously at Air Products, mineral oil from freshly reduced and spent catalyst slurries was found to contain 0.6 and 0.3 mol % C=C, respectively, or about 0.015 to 0.008 M C=C.

Table 42 compares the absorbance of the UV maxima near 215 nm normalized for the mineral oil concentration for spent and fresh mineral oil samples. Fresh mineral oil (Air Products) exhibited the expected low UV absorbance but a fresh mineral oil sample from Kingsport exhibited an absorbance almost 5 times greater. Evidently, the Kingsport mineral oil contained a greater fraction of unsaturates. Mineral oil from two freshly reduced Kingsport catalyst slurry samples exhibited absorbances about 5 times that of the fresh oil. Similarly, mineral oil from spent catalyst slurries had UV absorbances greater than for the fresh oil but no increase in absorbance with time on stream was apparent. The implication is that, once reduced, the catalyst

Table 42. UV absorbances of various mineral oil samples.[a]

Source of oil	Time on stream, days	UV peak, nm	absorbance/ wt% oil
Fresh Oil, Air Products	-	212	0.0846
Fresh Oil, Kingsport	-	210	0.401
Fresh Oil, Kingsport; 2nd batch	-	208	0.292
Kingsport freshly reduced	-	217	0.435
Kingsport freshly reduced sample K9909-1	-	219	0.415
Kingsport catalyst slurry sample K9904-3	493	212	0.697
Kingsport catalyst slurry sample K9906-1	528	214	0.746
Kingsport catalyst slurry sample K9907-1	570	212	0.666
Kingsport catalyst slurry sample K9908-2	619	212	0.828
Kingsport catalyst slurry sample K9909-2	640	219	0.572
Kingsport catalyst slurry sample K9910-2	668	215	0.510
Kingsport catalyst slurry sample K9912-1	718	213	0.675
Kingsport catalyst slurry sample K0001-1	746	214	0.462

a. Drakeol-10 mineral oil contains "15 ppm or less" vitamin E as an antioxidant. Vitamin E absorbs at 292 nm with an extinction coefficient of about 3,500 and thus cannot account for the absorbed UV peak position or intensity.

reacts with mineral oil to yield a steady-state concentration of unsaturated hydrocarbon. A possible route to unsaturation is dehydrogenation over Cu metal on the reduced catalyst. The resulting olefins may bind to Cu and compete for methanol synthesis sites or may serve as coke precursors. Unfortunately, evidence to support or refute these possibilities was not obtained but such reactions are thought to have a very minor effect on catalyst activity when compared to poisoning by syngas contaminants.

3.3 Kingsport Catalyst Campaign 3

Unlike previous runs, the third Kingsport catalyst campaign involved an in-situ activation of catalyst. Methanol synthesis catalyst in the oxide form and mineral oil were loaded into the LPMEOH™ reactor without prior activation. The entire contents of the reactor were then reduced, or activated, using dilute Balanced Gas in N_2. In previous runs at the LPMEOH™ Demonstration Unit, catalyst had been reduced with dilute CO in N_2 in smaller batches in the catalyst preparation system and transferred into the LPMEOH™ reactor.

The in-situ catalyst activation procedure was completed on 24 August 2001. Although the overall procedure was completed without incident, the resultant catalyst activity was lower than expected. This catalyst performance was later determined to be a function of the higher than desired temperature of the catalyst slurry tank used to store the catalyst slurry prior to activation. This over-temperature issue is not an inherent problem with the in-situ activation; a change in operating procedure was made to correct the problem.

Catalyst Physical Properties. Table 43 lists the physical properties for the batch of alternative catalyst used in this run (sample K0108-3, oxide form), freshly reduced, and spent catalyst samples from Kingsport Catalyst Campaign 3. With the exception of sample K0108-2, XRD analysis for all slurry samples indicated the expected phases of Cu and ZnO. Initial copper crystallite sizes were larger than anticipated, implying that some unexpected initial sintering had occurred (see below). However, only a minor increase in copper crystallite size was observed over the 213 day period prior to catalyst addition/withdrawal (Figure 15).

The sample identified as taken following the completion of the in-situ activation, K0108-2, exhibited very unusual properties. The solid isolated from the slurry had a light brown color compared to the normal black of the as received, freshly reduced, or spent catalyst. XRD analysis revealed that Cu_2O was the major phase, ZnO the normal minor phase, and low minor/trace CuO, Cu_4O_3 and perhaps Cu phases. These phases can be compared with CuO found in the as received catalyst and elemental Cu in the catalyst from a normal activation. It is very unlikely that K0108-2 is the product of the in-situ activation since Cu_2O would certainly be reduced to elemental Cu; rather, and as discussed below, the sample was very likely taken prior to its reduction.

The initial sample, K0108-2, had a copper surface area significantly lower than expected for the freshly reduced catalyst. Subsequent values over the next 54 days were reasonably constant with an average relative copper surface area of 0.654. Between 68 and 110 days on stream, there was a general decrease in relative copper surface area followed by a period, 138 to 194 days, in which it increased with time. The relative copper surface area of the final sample examined (213 days) had decreased to 0.392. An increase in copper surface area with time on stream is, of

Table 43. Physical properties of catalyst samples from Kingsport Catalyst Campaign 3.

sample	description	TOS days	crystallite size, Å		surface area m^2/g	relative Cu surface area[a]	wt% solids, as recd. slurry
			Cu	ZnO			
K0108-2	in-situ reduced		-	-	69	0.613	-
K0108-3	oxide form	-	-	-	101	1.33[b]	-
K0109-1	reactor slurry	12	177.7	89.8	78	0.667	20.28
K0109-2	reactor slurry	19	188.0	87.8	na	na	33.90
K0109-3	reactor slurry	26	184.9	158.8[c]	85	0.638	6.212
K0110-1	reactor slurry	40	180.7	77.6	82	0.659	15.12
K0110-2	reactor slurry	54	203.2	98.3	82	0.652	26.86
K0110-3	reactor slurry	68	197.2	45.2	78	0.589	23.45
K0111-1	reactor slurry	82	200.0	79.6	80	0.461	20.30
K0111-3	reactor slurry	98	203.7	79.4	82	0.480	23.20
K0112-1	reactor slurry	110	256.3	76.6	74	0.431	24.59
K0201-1	reactor slurry	138	211.6	77.5	50	0.466	19.06
K0201-2	reactor slurry	152	206.7	120.9	76	0.525	10.49
K0202-1	reactor slurry	166	210.8	83.5	76	0.539	11.51
K0203-1	reactor slurry	194	219.5	71.1	75	0.534	16.12
K0203-2	reactor slurry	202	216.4	101.5	-	-	20.94
K0203-3	reactor slurry	208	214.8	142.9	24	-	-
K0203-4	reactor slurry	213	218.3	100.5	51	0.392	34.35
K0204-1	reactor slurry	223	212.6	86.7			
K0204-2	reactor slurry	230	205.6	117.3			
K0204-3	reactor slurry	244	210.5	97.9			

a. Relative Cu SA = observed Cu surface area/Cu surface area of freshly reduced catalyst.

b. Following reduction in Cu surface area apparatus, 10% H_2/N_2, ambient to 180 °C at 1 °C per minute.

c. Suspect value.

na = not available.

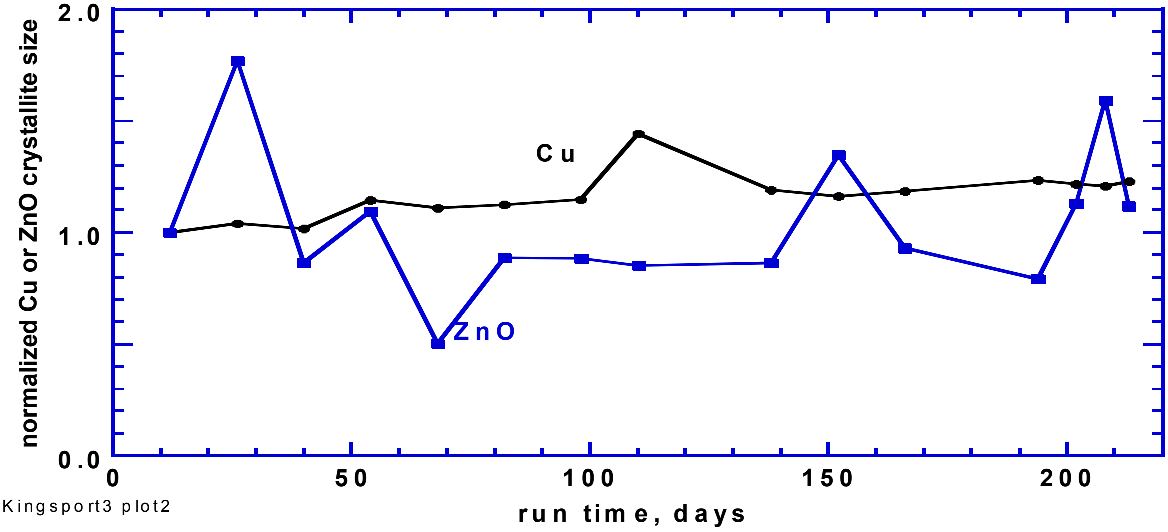

Figure 15. Normalized Cu and ZnO crystallite sizes for Kingsport Catalyst Campaign 3 slurries. The following initial crystallite sizes were used for normalization: Cu, 177.7 Å; ZnO, 89.8 Å.

course, contrary to the expectation that gradual sintering will result in loss of surface area. It is believed that this was an artificial increase resulting from iron deposited on the catalyst as described in section 1.7.

Catalyst Composition. Elemental analysis and XRF data for spent catalyst samples are listed in Table 44. Also included is data for the batch of catalyst (oxide form) used for this run, sample K0108-3. Over the entire run only two contaminants were found on the catalyst: iron and arsenic. Iron concentrations increased at substantial rate while the increase in arsenic was much more modest (Figure 16). The final sample contained 534 ppmw Fe. Arsenic concentrations reached a maximum of only 318 ppmw and 203 ppmw for the final sample analyzed (213 days). Sulfur was below its limit of detection (160 ppmw or lower) throughout the run. Although a direct comparison of data from Campaigns 2 and 3 is complicated by differences in total syngas exposure, some conclusions can be drawn. The arsenic loading on the catalyst from Campaign 2

Table 44. Elemental composition of solids from Kingsport Catalyst Campaign 3 slurries.

	TOS	concentration, ppmw[b]				
sample[a]	days	As	S	Fe	Ni	Cl
K0108-3	0	≤34	<40	50	<30	nd
K0109-1	12	≤73	<140	48	≤19	nd
K0109-3	26	≤70	<140	52	<10	nd
K0110-1	40	65	≤85	71	<10	nd
K0110-2	54	83	≤100	97	<10	40
K0110-3	68	139	≤120	147	<10	nd
K0111-1	82	138	≤130	191	<10	50
K0111-3	98	150	≤140	241	<10	30
K0112-1	110	260	≤80	293	≤20	nd
K0201-1	138	192	≤95	355	<10	30
K0201-2	152	152	≤57	363	≤10	nd
K0202-1	166	138	≤91	390	<10	nd
K0203-1	194	210	<40	428	<10	nd
K0203-2	202	318	<160	477	<10	nd
K0203-3	208	314	<160	508	≤12	nd
K0203-4	213	203	<160	534	<10	40

a. K0108-3 is catalyst in oxide form; others are solids from reactor slurry samples.
b. Cl by XRF.
na = not available; nd = not detected.

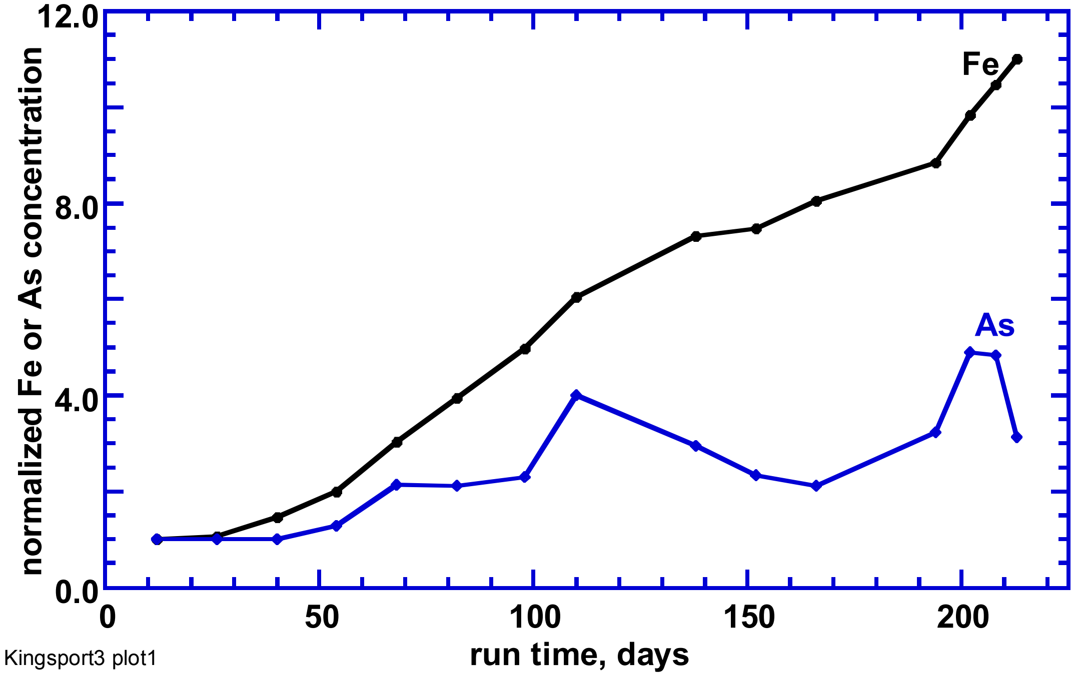

Figure 16. Normalized Fe and As concentrations on Kingsport Catalyst Campaign 3 samples. Initial concentrations (12 days) of 48 ppmw Fe and 65 ppmw As were used for normalization.

was significantly higher, 1,045 ppmw after 200 days than for the Campaign 3 catalyst, only 318 ppmw after 202 days. Similarly for these run times, the Campaign 2 catalyst contained 277 ppmw sulfur while no sulfur was detected on the Campaign 3 catalyst. However, Fe on the Campaign 2 catalyst was only 89 ppmw.

One result of note was the substantial increase in Fe on the catalyst with time. The most likely and possibly the only source of iron contamination is $Fe(CO)_5$. The volatile carbonyl present in the syngas feed can enter the LPMEOH™ reactor if breakthrough of the adsorbent in the 29C-40 catalyst guard bed occurred. This is thought to be very unlikely. A laboratory evaluation of the Cu/C adsorbent showed it has a very high $Fe(CO)_5$ removal capacity. Furthermore, results from gas sampling performed on 23 April 2002 found < 8 ppb $Fe(CO)_5$ in the 29C-40 catalyst guard bed inlet and outlet. Another possibility is that $Fe(CO)_5$ was generated within the reactor or the associated recycle loop hardware. Based on laboratory experiments, this also seems unlikely. The equivalent of a carbonyl burnout was conducted in a laboratory reactor by exposing mineral oil to syngas with a H_2/CO ratio of approximately 0.5 at 250 °C and 750 psig. Initially, a burst of 100 ppb $Fe(CO)_5$ was found in the reactor outlet but the $Fe(CO)_5$ concentration quickly decreased to 4 ppb after 20 hours and to 3 ppb after 33 hours. Such generated $Fe(CO)_5$ concentrations are insufficient to account for the large iron concentrations on the catalyst. Although this iron contamination was unfortunate and likely affected the catalyst activity, it is not related to poor adsorbent performance in the catalyst guard bed or to some problem with the in-situ reduction process.

It was subsequently determined that the most likely source of the iron was the incorrect installation of carbon steel parts inside the reactor during a maintenance outage in April of 2001. The correct stainless steel parts were installed after the conclusion of Kingsport Catalyst Campaign 3 in June of 2002. A hot function test was completed following the replacement of the carbon steel parts in June of 2002. During this procedure, sampling of the reactor feed gas stream was performed; during the three-day period, the measured levels of $Fe(CO)_5$ dropped gradually to approximately 30 ppb.

3.4 Kingsport Catalyst Campaign 4

During the third Kingsport run, it was found that storage of the fresh catalyst in the presence of mineral oil at elevated temperatures prior to reduction was the cause of the lower than expected catalyst activity. For the fourth catalyst campaign, the operating steps in the procedure were modified so that the fresh methanol synthesis catalyst would not be exposed to temperatures in excess of 100 °C prior to the introduction of dilute syngas. In this procedure, batches of fresh catalyst were added directly into the LPMEOH™ reactor after mixing in the catalyst activation vessel. The entire contents of the reactor were then reduced, or activated, using dilute Balanced Gas in N_2.

The in-situ catalyst activation procedure was completed on 27 June 2002. Results of the second in-situ activation were excellent with a reducing gas uptake of 98% of the theoretical value calculated based on analytical data and measured flowrates.

Catalyst Composition. Elemental analysis and XRF data for spent catalyst samples are listed in Table 45. No significant quantities of any of the contaminants analyzed were found during the first three months of this catalyst campaign.

Table 45. Elemental composition of solids from Kingsport Catalyst Campaign 4 slurries.

	TOS	concentration, ppmw[b]				
sample[a]	days	As	S	Fe	Ni	Cl
K0206-1	0	<20	<40	<23	<10	<100
K0109-1	12	< 2	<19	28	< 7	na
K0109-3	26	4.2	<25	44	< 7	na
K0110-1	40	5.4	<39	40	< 6	na
K0110-2	54	19	<47	58	< 7	na

a. K0206-1 is catalyst in oxide form; others are solids from reactor slurry samples.
b. Cl by XRF.
na = not available.

4. LPMEOH™ Demonstration Unit Contaminant Removal Configurations and Trials

4.1 Impurity Removal Upstream of the LPMEOH™ Demonstration Unit

A description of the Eastman upstream gas cleanup systems was covered in the topical report entitled "Project Data on Eastman Chemical Company's Chemicals-from-Coal Complex in Kingsport, TN"[30]. These systems include a Rectisol gas clean-up plant located downstream of the Texaco coal gasification system and a catalyst guard bed (equipment number 10C-30), which was installed by Eastman upstream of the fixed-bed methanol plant. Figure 17 shows the location of this equipment in relation to the syngas generation system and to both the fixed-bed methanol plant and the LPMEOH™ Demonstration Unit. The Rectisol unit was primarily designed to remove sulfur compounds from the syngas stream. The Eastman catalyst guard bed was installed to remove trace contaminants (in particular, compounds of sulfur and arsenic) which adversely impact the long-term performance of methanol synthesis catalysts.

Table 46 details the adsorbents used in the Eastman catalyst guard bed during the operating phase of the LPMEOH™ Demonstration Project. Table 47 provides a list of the trace components exiting from the Eastman catalyst guard bed that have been measured in syngas streams or calculated from uptake on the surface of catalyst samples taken from the LPMEOH™ reactor. Variations in the reported values are most likely attributed to either changes in the concentrations of species in the coal feed to the gasification plant, changes in operation of the Rectisol syngas clean-up plant, or changes in performance of the Eastman catalyst guard bed. Based upon the latter occurrence, the adsorbent material in the Eastman catalyst guard bed has been changed three times during the operation of the LPMEOH™ Demonstration Unit. During the first change (September 1997), the existing materials for removal of sulfur and arsenic compounds were replaced with the same quantities of fresh adsorbent. In June 1999, this charge of adsorbent was removed and replaced only with the material targeted for removal of arsenic compounds. In October 2002, the adsorbent was removed and again replaced only with the material targeted for removal of arsenic compounds.

4.2 LPMEOH™ Demonstration Unit Catalyst Guard Bed (29C-40) Configuration

The 29C-40 catalyst guard bed is a fixed adsorbent guard bed that protects methanol synthesis catalyst in the LPMEOH™ reactor against possible upsets of contaminants from the upstream gas cleanup units. The unit is 4 feet in diameter with an active bed length of 12 feet. Normal process flow is downward; upward flow is used for thermal regeneration of the adsorbent.

The original design of the 29C-40 catalyst guard bed was for the removal of iron and nickel carbonyl contaminants. Iron and nickel carbonyl was targeted for removal based on pre-testing of the syngas feed streams during the design phase of the LPMEOH™ Demonstration Project. An activated carbon adsorbent operating at ambient conditions was chosen for the removal of these carbonyl contaminants. Activated carbon is an effective physical adsorbent for the removal of carbonyls. The original design for the catalyst guard bed also included a thermal regeneration system to reclaim performance of the guard bed adsorbent following saturation with $Fe(CO)_5$[31].

After operation of the LPMEOH™ Demonstration Project started up in April 1997, it was determined that levels of iron and nickel carbonyl were not present to the level of detection (typically 10 ppb or less) in the syngas feed. Furthermore, while there was an initial increase in iron observed on the reactor catalyst, this stabilized after about 30 days and was later attributed to construction debris in the reactor.

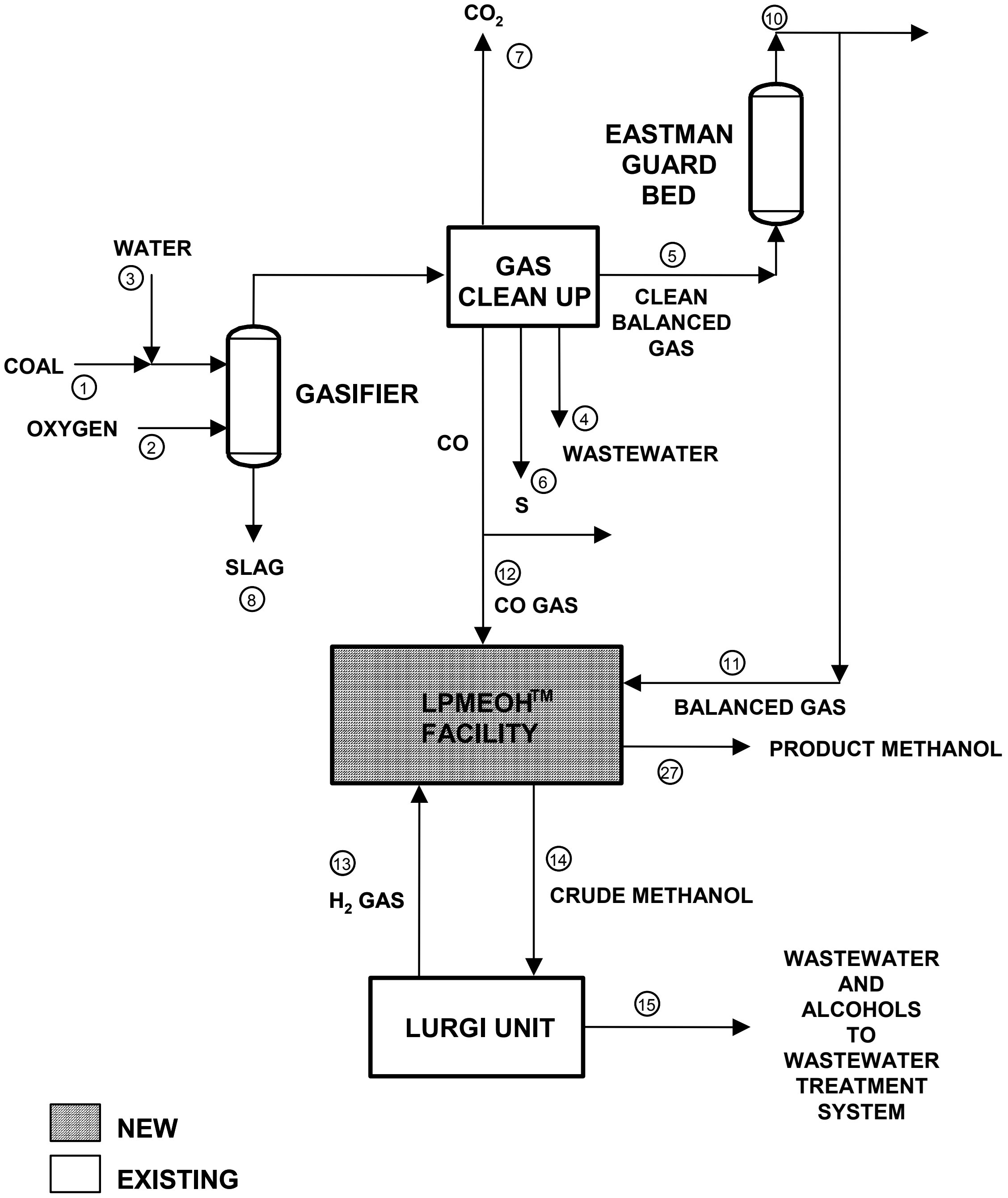

Figure 17. Integration of existing Eastman facilities with LPMEOH™ Demonstration Unit.

Table 46. Adsorbents used in 10C-30 catalyst guard bed during operation of LPMEOH™ Demonstration Unit.

Adsorbent Material	Targeted Catalyst Poison	Time in Service
(1) Zinc Oxide (155 cubic feet) (2) Manganese Dioxide (75 cubic feet)	(1) Sulfur (2) Arsenic	1995 – September 1997
(1) Zinc Oxide (155 cubic feet) (2) Manganese Dioxide (75 cubic feet)	(1) Sulfur (2) Arsenic	October 1997 – June 1999
Manganese Dioxide (230 cubic feet)	Arsenic	June 1999 – October 2002
Manganese Dioxide (230 cubic feet)	Arsenic	October 2002 – 31 December 2002 (continuing)

Table 47. Summary of trace impurities leaving Eastman 10C-30 catalyst guard bed.

Date	Syngas Stream(s)	Species	Steady-State Concentration (ppb)	Sample Material
May 1996 (AFFTU) ***after Eastman catalyst guard bed***	Balanced Gas, CO Gas	Arsenic	27	Spent Catalyst
		Arsenic	40	Spent Adsorbent
		COS	7-15	Syngas
		H_2S	1-6	Syngas
June 1997 (Plant) ***after LPMEOH catalyst guard bed***	Balanced Gas	Arsenic	87	Spent Catalyst
December 1997 - January 1998 (AFFTU) ***after LPMEOH catalyst guard bed***	Balanced Gas	Arsenic	> 31	Spent Adsorbent
		COS	10-20	Syngas
		H_2S	< 2	Syngas
		Total S	37	Spent Catalyst
January 1998 (Plant) ***after LPMEOH catalyst guard bed***	Balanced Gas	Arsenic	8	Spent Catalyst
June 1999 (Plant) ***before Eastman catalyst guard bed***	Balanced Gas	Arsenic	39	Syngas
September 1999 (Plant) ***before Eastman catalyst guard bed***	Balanced Gas	Arsenic	53	Syngas
July 2000 (Plant) ***before Eastman catalyst guard bed***	Balanced Gas	Arsenic	64	Syngas

4.3 Catalyst Guard Bed Adsorbent Trial

Levels of arsenic and sulfur began increasing on the reactor catalyst after operations commenced. The concentration of arsine upstream and downstream of the 29C-40 catalyst guard bed was periodically monitored during operations and is summarized in Table 47. As shown in the table, the level of arsenic was consistently greater than the design limit of 10 ppb. It was necessary to change the adsorbent in the catalyst guard bed to target the removal of arsenic to improve performance. A summary of all the adsorbent materials used in the 29C-40 catalyst guard bed is given in Table 48.

Table 48. Adsorbents used in 29C-40 catalyst guard bed during operation of LPMEOH™ Demonstration Unit.

Adsorbent Material	Targeted Catalyst Poison	Time in Service
Activated Carbon (6,300 pounds)	Iron, Nickel	April 1997 – November 1997
Activated Carbon (6,553 pounds)	Iron, Nickel	December 1997 – June 1999
(1) Manganese Dioxide (2,900 pounds) (2) Activated Carbon (2,200 pounds)	(1) Arsenic (2) Iron, Nickel	June 1999 – July 2000
Copper-impregnated Activated Carbon (4,892 pounds)	Arsenic, Sulfur, Iron, Nickel	August 2000 – July 2001
Copper-impregnated Activated Carbon (5,336 pounds)	Arsenic, Sulfur, Iron, Nickel	August 2001 – February 2002
Copper-impregnated Activated Carbon (5,073 pounds)	Arsenic, Sulfur, Iron, Nickel	March 2002 – June 2002
Copper-impregnated Activated Carbon (5,810 pounds)	Arsenic, Sulfur, Iron, Nickel	June 2002 – October 2002
Copper-impregnated Activated Carbon (5,225 pounds)	Arsenic, Sulfur, Iron, Nickel	October 2002 – 31 December 2002 (continuing)

4.4 Catalyst Guard Bed Analysis

Analysis of spent guard bed adsorbents not only supplies information about adsorbent performance but also about the contaminants present in the syngas feed. This information can then be used to focus efforts regarding which contaminants are methanol catalyst poisons and, therefore, determine which must be removed from the syngas feed. Based on the information reported below, contaminants containing the following elements are present in the Balanced Gas: As, S, N, Fe, Ni, F. Arsenic, as described above, is most reasonable as AsH_3 and S as H_2S and COS. Nitrogen is present as HCN in rather substantial quantities but perhaps also as NH_3 or amines. The volatile metal carbonyls, $Fe(CO)_5$ and $Ni(CO)_4$, provide a likely source of Fe and Ni. Fluorine could arise from HF or from various organo-fluorine compounds. Over the course of the Kingsport Catalyst Campaign 2, several catalyst guard bed arrangements were used and these are described below. None of these proved effective for removal of As and S-containing species and these are viewed as the most likely source of downstream catalyst contamination.

Catalyst Guard Bed Arrangement Prior to June 1999. The 29C-40 catalyst guard bed contained activated carbon. Spent adsorbent was removed from the bed on 07 June 1999 after approximately 20 months of service. XRF and elemental analysis results for spent carbon from the catalyst guard bed are detailed in Tables 49 and 50. The fresh adsorbent contained substantial concentrations of S, N, and Fe and thus an accurate accounting of these elements in the spent samples was difficult. In particular, the fresh adsorbent sulfur concentration was too high to obtain meaningful sulfur loadings on the bed. XRF and elemental analysis indicated a fairly uniform As concentration throughout the bed implying that activated carbon was largely ineffective for removal of arsenic-containing contaminants. Iron, nickel, and chlorine were not detected in concentrations above those found in the fresh adsorbent. Both Zn and Mn were detected and these might originate from the upstream Eastman catalyst guard bed. Nitrogen concentrations were lower on the spent versus fresh adsorbent implying that no significant adsorption of N-containing species occurred. Fluorine was also below its limit of detection on the bed inlet sample.

Table 49. XRF analysis results for spent activated carbon from the 29C-40 catalyst guard bed (6/99).

		Concentration, ppmw[a]						
Sample	description	S	As	Fe	Ni	Cl	Mn	Zn
AGB-57	fresh adsorbent	11,400	<16	3,700	60	8	10	nd
AGB-42	bed inlet	8,300	1,500	3,100	30	10	160	220
AGB-46	5' from bed inlet	8,600	1,400	3,200	nd	nd	160	240
AGB-50	12' from bed inlet	11,050	1,800	2,200	nd	nd	80	210

a. Also detected but at concentrations ≤ value for fresh adsorbent: Si, Al, Ca, K, Na, Mg, P, Sr, V, Cu, Cr, Co, Y; nd = not detected.

Table 50. Elemental analysis results for spent activated carbon from the 29C-40 catalyst guard bed (6/99).

		elemental concentrations, ppmw, vs fresh adsorbent[a]								
sample no.	description	As	S	N	Zn	Mn	Fe	Ni	Cr	Cu
AGB-57	fresh adsorbent	6.0	5,930	5,000	2.6	10.7	2,010	39.6	5.0	18.6
AGB-42	bed inlet	1,630	≤360	2,400	225	141	nd	nd	nd	nd
AGB-46	5' from bed inlet	1,570	≤330	-	213	135	nd	nd	nd	nd
AGB-50	12' from bed inlet	1,990	≤430	3,400	122	79	nd	nd	nd	nd

a. For spent adsorbent, elemental concentrations were corrected for concentrations on fresh adsorbent; nd = not detected.

Catalyst Guard Bed Arrangement after June 1999. During the 07 June 1999 changeout of adsorbent, the Eastman catalyst guard bed was filled completely with MnO_2/Al_2O_3 and the 29C-40 catalyst guard bed was charged with about 50 % (by volume) MnO_2/Al_2O_3 followed by activated carbon downstream. The use of $ZnO/CaAl_2O_4$ was discontinued in the Eastman catalyst guard bed. After approximately two months of operation (11 August 1999), samples were removed from the 29C-40 catalyst guard bed. For the three MnO_2/Al_2O_3 samples (see Table 51), XRD showed MnO_2 as the major phase with trace Mn_2O_3. Table 51 lists the concentrations of elements greater than those in the fresh adsorbent. Arsenic was found throughout the MnO_2 portion of the bed but sulfur above that on the fresh adsorbent was found only on the inlet sample.

Table 51. XRF analysis results for fresh and spent MnO_2/Al_2O_3 from 29C-40 catalyst guard bed, 8/11/99.

		conc., wt%		concentration, ppmw								
sample	description	Al	Mn	As	As[a]	S	S[a]	Mg	Zn	Mo	Ga	Ba
	fresh adsorbent	36.2	24.4	<46	6.3	150	210	180	nd	nd	nd	nd
AGB81199-1	top	34.2	22.2	940	200	280	410	270	90	40	nd	nd
AGB81199-3	2 ft down	34.6	21.7	800	130	80	260	<300	nd	nd	30	nd
AGB81199-6	5 ft down	34.4	21.9	580	66	90	250	240	40	nd	nd	120

a. Concentration determined by elemental analysis; nd = not detected.

For the activated carbon portion of the bed, XRF and elemental analysis data for arsenic were in excellent agreement and showed arsenic concentrations greater than that of the fresh adsorbent throughout the bed with a gradient from inlet to outlet (Table 52). This implies that AsH_3 had broken through the bed. Background sulfur concentrations were too high to draw meaningful conclusions concerning sulfur adsorption.

Table 52. XRF analysis results for fresh and spent carbon from the 29C-40 catalyst guard bed, 8/11/99.

		concentrations in ppmw								
Sample	description	S	S[a]	As	As[a]	Na	Mn	Mo	Ba	Zr
	fresh adsorbent	11,400	370[b]	<16	2.1	400	12	nd	nd	nd
AGB 81199-9	8' down, top C	10,700	400[b]	1,000	1,000	700	40	10	130	40
AGB 81199-11	10' down, middle C	9,800	330[b]	240	260	800	30	10	130	30
AGB 81199-13	12' down, bottom C	8,300	320[b]	320	410	300	50	10	80	nd

a. Concentration determined by elemental analysis.

b. Large errors because of high background S; nd = not detected.

The most direct way to determine what syngas contaminants are entering the LPMEOH™ reactor is sampling and analysis of the syngas streams. Unfortunately, on-line capabilities to continuously monitor contaminants were not available and more laborious periodic gas phase sampling was required. Samples were collected by passing gas through charcoal canisters to trap contaminants and these were subsequently analyzed at Air Products. Two locations (the inlet to and outlet of the 29C-40 catalyst guard bed) were selected for sampling. This testing was intended primarily for quantification of arsenic in the feed gas. The background levels of other contaminants, specifically sulfur and iron, on the carbon used were too high to obtain gas phase concentrations of these. An important point is that the analysis determined the quantity of elemental arsenic in the gas and not its form. Arsine is the most reasonable gas phase species based on the syngas composition.[32] The concentrations reported in Table 53 assume that all the arsenic found on the carbon adsorbent resulted from gaseous arsine. These results show that, beyond an initial period during June of 1999, the adsorbents used in the 29C-40 catalyst guard bed were not effective for arsenic removal until the reduced copper-impregnated activated carbon was used.

Catalyst Guard Bed Arrangement after April 2001. Because of the ineffectiveness of the above guard bed arrangements for contaminant removal, particularly AsH_3, the 29C-40 catalyst guard bed was emptied and loaded with copper oxide impregnated activated carbon (CuO/C) during the end of Kingsport Catalyst Campaign 2. Laboratory testing had shown that the adsorbent was very effective for removal of AsH_3 from syngas. Unfortunately, exposure of the adsorbent in the 29C-40 catalyst guard bed to Balanced Gas resulted in a significant increase in the bed temperature that was traced to an unexpected (at ambient temperature) exothermic reduction of CuO to metallic Cu. The bed was subsequently reduced in a controlled manner using a dilute syngas feed and brought back on-line. After 89 days, the bed was emptied and samples were forwarded to Air Products for analysis (Table 54).

Table 53. Gas phase analysis results, Kingsport Catalyst Campaign 2, 6/14/099 to 7/12/00.

analysis dates	sampling location	ppb AsH_3	average conc., ppb
6/14/99 – 6/16/99	29C-40 catalyst guard bed inlet	16, 13, 26	18
	29C-40 catalyst guard bed outlet	not detected*	not detected*
9/22/99 – 9/24/99	29C-40 catalyst guard bed inlet	50, 47, 50	49
	29C-40 catalyst guard bed outlet	23, 21, 31	25
9/24/99 -10/1/99	29C-40 catalyst guard bed outlet	41	41
10/1/99 - 10/11/99	29C-40 catalyst guard bed outlet	40	40
10/11/99 - 10/17/99	29C-40 catalyst guard bed outlet	37	37
7/10/00 - 7/12/00	29C-40 catalyst guard bed outlet	53, 52, 46, 47	49

* Approximate limit of detection was 1 ppb.

The arsenic concentrations at the bed inlet and outlet were 2,690 and 1,000 ppmw, respectively. Arsenic concentrations for the intermediate samples varied in an irregular manner, perhaps because of the damage caused by elevated temperatures. The high background sulfur concentrations on the adsorbent precluded meaningful sulfur quantification on all but the inlet sample. The inlet sample S concentration was 4,900 ppmw after correction for the background. Similarly, the Fe concentration on the spent samples could not be distinguished from the Fe background. Curiously, 610 ppmw Mo was found on the inlet sample and this, perhaps, could be related to the elevated bed temperature.

Table 54. Elemental analysis of spent Cu/C adsorbent from 29C-40 catalyst guard bed (7/24/01).

		concentration, ppmw						
sample no.	description	As	S*	Fe	Ni	P	Cr	Mo
18141-87-1	inlet	2,690	4,900	≤1,400	≤27	≤150	≤9.4	610
18141-87-2	2nd from inlet	706	nd	≤1,400	≤27	≤150	≤17	≤140
18141-87-4	4th from inlet	1,690	nd	≤1,400	≤27	≤150	≤12	≤140
18141-87-6	6th from inlet	731	nd	≤1,400	≤27	≤150	≤23	≤140
18141-87-9	outlet	1,000	nd	≤1,400	≤27	≤150	≤16	≤140
18141-87-10	fresh adsorbent	≤11	-	≤1,400	≤27	≤150	≤8.9	≤140

* Concentration corrected for background on the fresh adsorbent.

Copper surface area measurements for fresh and spent adsorbent samples proved to be quite illuminating. Fresh CuO/C adsorbent following laboratory reduction with dilute H_2 had a copper surface area of 24.3 m^2/g. The spent inlet sample exhibited no measurable copper surface. This may be the result of damage from overheating upon syngas exposure. Based on the apparent damage to the adsorbent because of high bed temperatures, it was not surprising that the adsorbent was also largely ineffective for AsH_3 removal. Listed in Table 55 are the AsH_3 concentrations in the 29C-40 catalyst guard bed inlet and outlet. After only 5.7 days on line, AsH_3 was above its detection limit at the bed outlet.

Table 55. Inlet and outlet arsine concentrations for the 29C-40 catalyst guard bed containing Cu/C.

sampling location	Approx. run time, days[a]	AsH_3 conc, ppb	estimated error
Inlet	4.7	41	
Inlet	5.1	39	
Inlet	5.7	39	
Outlet	4.7	<2	
Outlet	5.1	<2	
Outlet	5.7	6.7	
Outlet	10.8	18	9.0
Outlet	39.9	11	5.0
Outlet	40.9	12	6
Outlet	41.9	12	6
Outlet	45.9	16	8
Inlet	74.9	37	8
Outlet	80.0	32	7
Outlet	82.7	23	5
Outlet	84.8	28	6
Outlet	87.8	29	6

a. Time to end of sampling period.

For Kingsport Catalyst Campaign 3, the 29C-40 catalyst guard bed contained CuO/C adsorbent. The adsorbent was reduced to Cu/C in a controlled manner using dilute syngas. The bed was on-line for 180 days. The adsorbent had undergone two “regeneration” cycles in which the bed was purged with heated N_2. As described below, this treatment is believed to increase the copper surface available for reaction with AsH_3. No actual desorption of AsH_3 occurs during this thermal treatment process.

The copper surface area of the inlet sample was 21.3 m^2/g, comparable to that for the freshly reduced adsorbent, 24.3 m^2/g, indicating that the controlled reduction resulted in no significant loss of copper surface. The arsenic concentration varied in a regular fashion down the bed with 9,260 ppmw and 2,280 ppmw at the inlet and outlet, respectively (Table 56). Sulfur concentrations were corrected for that of the fresh adsorbent and, because of high background sulfur concentration, the level of sulfur could be calculated only for the inlet sample. Similarly, high background iron precluded quantification of iron adsorption. No other contaminants were found on the spent adsorbent samples.

Table 56. Elemental analysis of spent Cu/C adsorbent from 29C-40 catalyst guard bed, 20 February 2002.

		concentration, ppmw						
sample no.	description	As	S[a]	Fe	Ni	P	Cr	Mo
18141-88-1	inlet	9,260	5,900	≤1,400	≤27	≤150	<8	≤140
18141-88-3	3rd from inlet	8,720	nd	≤1,400	≤27	≤150	<8	≤140
18141-88-6	6th from inlet	5,100	nd	≤1,400	≤27	≤150	<8	≤140
18141-88-9	9th from inlet	4,250	nd	≤1,400	≤27	≤150	<8	≤140
18141-88-12	12th from inlet	3,240	nd	≤1,400	≤27	≤150	<8	≤140
18141-88-16	16th from inlet	3,150	nd	≤1,400	≤27	≤150	<8	≤140
18141-88-19	outlet	2,280	nd	≤1,400	≤27	≤150	<8	≤140

a. Concentration corrected for background on the fresh adsorbent; nd = not detected.

The effectiveness of the 29C-40 catalyst guard bed was followed by monitoring AsH_3 concentrations in the catalyst guard bed outlet. Samples were collected by passing gas through an activated carbon trap followed by subsequent analysis for arsenic. Run times listed in Table 56 are cumulative times to the end of each sampling period. For example, the inlet sample listed as day 6 was obtained by collecting gas over a 48-hour period, day 4 to day 6. During the first 27 days, the outlet AsH_3 concentration was less than 4 ppb while the inlet arsine concentration was 52 ppb (6 days) and 63 ppb (28 days). Thus, the bed was effective for AsH_3 removal.

The outlet concentration was next determined on the 68th day and found to be 5.6 ppb, indicating that some breakthrough had occurred. With the exception of a determination on Day 98, the outlet concentration approximately increased with time on stream and reached 30 ppb by Day 102, indicating substantial breakthrough. Two thermal "regenerations" were conducted by purging the bed with heated N_2. As shown in Table 57, the AsH_3 outlet concentration was below its limit of detection following both treatments. Thus, these thermal treatments extended the usable life of the adsorbent.

The thermal treatment described above is not a regeneration in the traditional sense. No AsH_3 desorption occurs because the Cu-AsH_3 reaction is irreversible. As noted earlier in this report, the rate limiting step in the reaction of Cu/C with AsH_3 is theorized to be diffusion of bound arsenic away from the Cu surface and into the bulk. It was reasoned that a "purge" of 120 °C N_2 would warm the bed sufficiently to increase the rate of surface arsenic diffusion into the bulk and thus provide fresh copper surface for AsH_3 adsorption. Based on the experimental results, the thermal treatment was successful, supplying additional AsH_3 removal capacity.

The data in Table 57 indicates that AsH_3 breakthrough occurred sometime between 27 and 68 days. If the breakthrough time (t_i) is taken to be 50 days and the time to reach half the inlet AsH_3 concentration in the outlet is 102 days (t_m), the calculated arsenic capacity is 0.571 wt% and the mass transfer coefficient (k) is $4.45x10^{-4}$ min^{-1}. The calculated mass transfer zone length was 6.1 feet, which is about half of the length of the 12 foot long catalyst guard bed.

Table 57. Arsine concentrations in 29C-40 catalyst guard bed inlet and outlet. Two sequential charges of Cu/C adsorbent.

1st adsorbent charge	sampling location	approx. run time, days*	AsH_3 conc, ppb	2nd adsorbent charge	sampling location	approx. run time, days*	AsH_3 conc, ppb
fresh adsorbent, reduced		0		fresh adsorbent, reduced		0	
	Inlet	6	52 (15)		Inlet	5.0	55 (12)
	Outlet	19	<4		Outlet	11.2	<3
	Outlet	21	<4		Outlet	17.0	<3
	Outlet	24	<4		Inlet	45.4	52
	Outlet	27	<4		Inlet	46.2	48
	Inlet	28	63 (18)		Inlet	47.0	54
	Outlet	68	5.6 (1.3)		Inlet	47.1	45
	Outlet	75	14 (3)		Outlet	23.9	<2
	Outlet	84	23 (5.1		Outlet	28.2	4.5
	Outlet	90	20 (4.3		Outlet	46.0	12
	Outlet	98	8.8 (1.9		Outlet	46.2	8.9
	Outlet	102	30 (6.6)		Outlet	47.0	9.1
	purge with heated N_2, 2 d	105					
	Outlet	109	<6				
	Outlet	111	<6				
	Outlet	126	<5				
	Outlet	131	≤5.3				
	Inlet	133	66 (14				
	Outlet	140	≤5.4				
	Outlet	147	14 (3				
	Outlet	154	8.7 (3.5				
	Outlet	164	7.1 (2.9				
	Inlet	157	66 (28				
	purge with heated N_2, 2 d	167					
	Outlet	173	<3				
	Outlet	178	≤4.2				

5. Effect of Trace Contaminants on Catalyst Life at the LPMEOH™ Demonstration Unit

5.1 Overview of Trace Contaminant Issues at the LPMEOH™ Demonstration Unit

One of the key technical issues at the LPMEOH™ Demonstration Unit during the over five years of operation has been catalyst life. The determination of the impact of trace contaminants in the coal-derived syngas on the performance of the methanol synthesis catalyst was a key objective of the LPMEOH™ Demonstration Project. It was important to develop methods for the identification and removal of these contaminants to achieve acceptable catalyst deactivation rates.

Early in the design phase of the LPMEOH™ Demonstration Project, iron and nickel carbonyls were considered as the most likely contaminants in the coal-based syngas. This was based on historical data with other coal-derived gases as well as initial analytical data for the syngas gathered at the Eastman site. This consideration culminated in the design of a single fixed guard bed operating at ambient temperature for the removal of carbonyls.

The original design of the carbonyl removal guard bed (catalyst guard bed 29C-40) was based on activated carbon as the adsorbent. As previously mentioned in this report, the removal of carbonyl contaminants using activated carbon is a physical adsorption process that proceeds at ambient temperature. A thermal treatment system was incorporated into the design to regenerate the activated carbon in order to extend its useful life.

After initial operation, it soon became evident that carbonyls were not significantly present in the syngas. As described in Section 3 of this report, nickel was never appreciably measured on the catalyst surface and, although iron was initially measured in large quantities in the catalyst samples after start-up, iron carbonyl was not measured in the feed syngas. The presence of the iron after start-up was later attributed to construction debris.

Levels of arsenic and to a lesser extent sulfur were found to be increasing on the catalyst samples over time. The arsenic was also measured in the syngas entering the 29C-40 catalyst guard bed and has a historical range of 40 to 60 ppb. As shown in Section 1 of this report, arsenic, most likely in the form of arsine, was found to be a significant methanol synthesis poison. It also became evident that the activated carbon adsorbent in the 29C-40 catalyst guard bed was not effective for arsenic contaminant removal.

As described in Sections 2 and 4 of this report, adsorbents to remove arsine were evaluated for use in the LPMEOH™ Demonstration Unit. A significant challenge was the fact that the adsorbent used in the existing 29C-40 catalyst guard bed would be required to operate at ambient temperature due to the existing equipment configuration; many potential adsorbents were found to be kinetically controlled and, therefore, would function effectively only at elevated temperatures.

Table 48 in Section 4 of this report summarizes the adsorbent trials conducted in the LPMEOH™ Demonstration Unit. The effect of the use of the various adsorbents in the 29C-40 catalyst guard bed on the catalyst performance was evaluated two ways: 1) by gas phase analysis of the 29C-40 catalyst guard bed inlet and outlet streams for arsenic and 2) by considering the variations in catalyst deactivation in the absence of known changes to process conditions.

5.2 Catalyst Performance: Catalyst Campaign 1

Initial catalyst life data indicated an accelerated catalyst deactivation occurred; whereas, the remaining operation from June 1997 through November 1997 matched the typical activity loss measured in the laboratory. Figure 18 shows performance results from the LPMEOH™ reactor during the first several months of operation. The data are reduced to a ratio of rate constant pre-exponential factors (actual vs. design value for fresh catalyst), using an in-house kinetic model, to eliminate the effects of changing feed composition or operating conditions. Typical exponential decay will appear as a straight line on a log-plot, as shown. The curve fit to data from a 4-month test at the LaPorte PDU in 1988/89 and laboratory autoclave data from 1996 are included for reference.

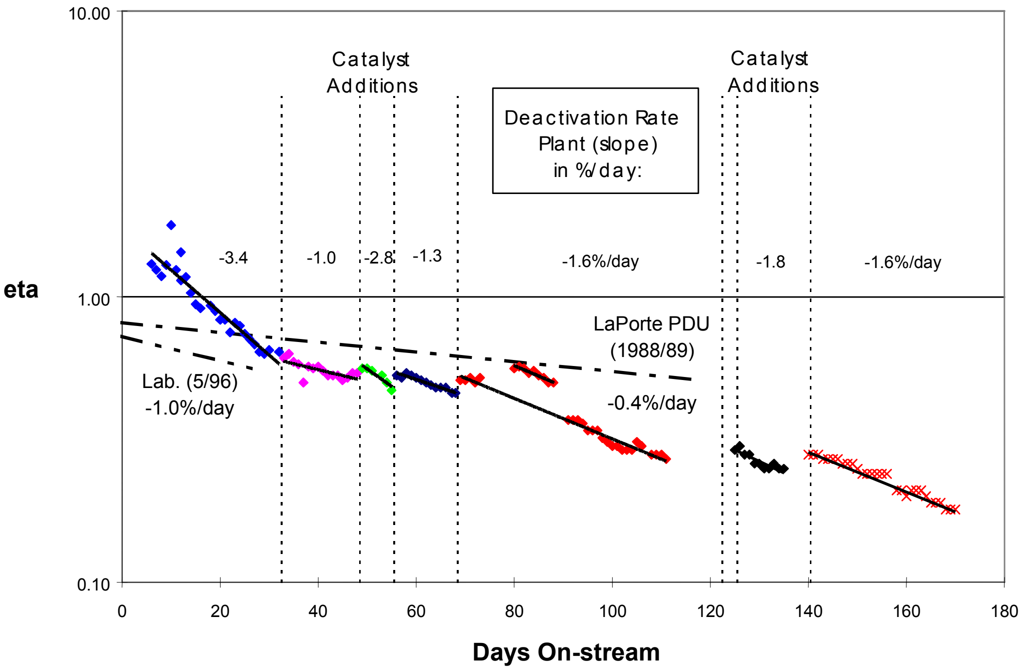

Figure 18. Kingsport LPMEOH™ catalyst life (Catalyst Campaign 1).

As reported previously in this report, analyses of catalyst samples from Kingsport Catalyst Campaign 1 had indicated a step-change increase in the concentration of iron on the catalyst surface during the initial month of operation, which could not be correlated to the presence of iron carbonyl in the feed gas streams. This finding is most likely related to the detection of post-construction debris (iron) within various parts of the facility. During this period, higher than expected levels of arsenic were also found on the catalyst samples.

During Catalyst Campaign 1, deactivation rates were higher than expected based on experience from the LaPorte AFDU (catalyst deactivation rate of –0.4% per day). In fact, the catalyst life was similar to the baseline deactivation results obtained during laboratory autoclave testing (catalyst deactivation rate of –1.0% per day). Ignoring the catalyst performance results for the first month due to catalyst hyperactivity and the presence of iron construction debris, the average deactivation rate for this campaign was -1.3% per day. This was based on operation with the activated carbon adsorbent in the 29C-40 catalyst guard bed and a LPMEOH™ reactor temperature of 250 °C. After an initial operating period of seven months, the reactor was drained and another partial charge of fresh catalyst was activated during December of 1997 (Catalyst Campaign 2).

5.3 Catalyst Performance: Campaign 2

Catalyst Campaign 2 was the longest run of the operating program at 1,325 days. During most of this catalyst campaign, the operating temperature in the LPMEOH™ reactor was lowered to 235 °C. By using the lowest possible temperature necessary to achieve the required methanol production rate, the life of the methanol synthesis catalyst was expected to be extended.

At the start of this campaign in December of 1997, a partial charge of fresh catalyst was activated and added to the reactor system. The adsorbent in the 29C-40 catalyst guard bed was also replaced with fresh activated carbon. During the first half of this campaign, the activated carbon remained in the catalyst guard bed while data was collected on operating performance. During this time, alternate adsorbents would also be identified and evaluated. Figure 19 shows the catalyst performance for the first year of operation.

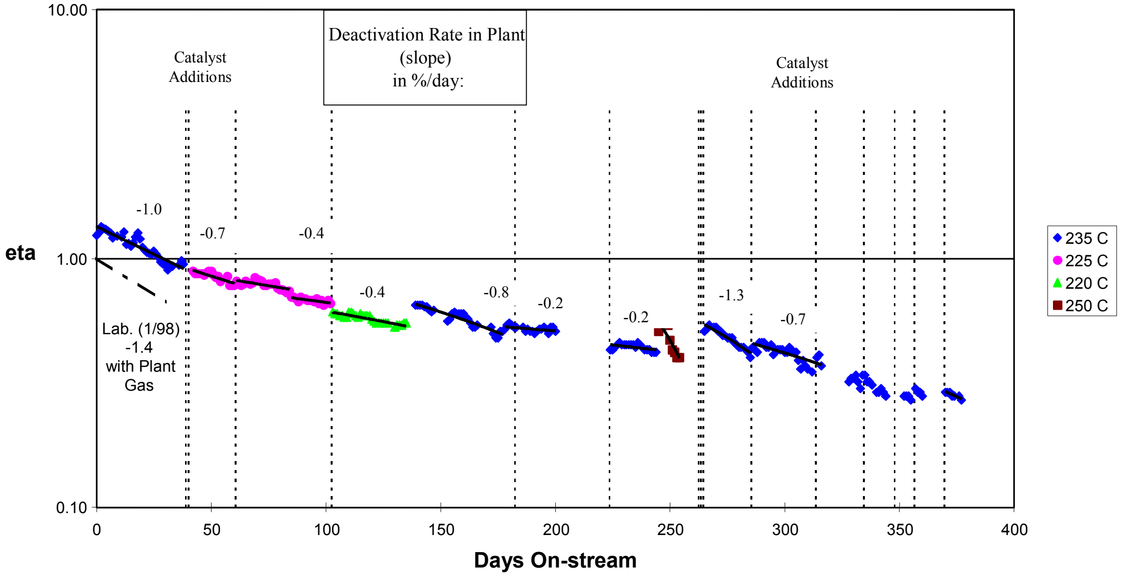

Figure 19. Kingsport LPMEOH™ catalyst life (Catalyst Campaign 2: 1997-1998).

At Day 604 of the campaign, an alternate manganese dioxide adsorbent was charged to half of the 29C-40 catalyst guard bed. This selection was based on vendor input as to the effectiveness of the adsorbent for arsenic and sulfur removal. The other half of the catalyst guard bed was charged with activated carbon to remove any metal carbonyl compounds. Based on analysis of arsenic in the catalyst guard bed inlet and outlet streams, the manganese dioxide adsorbent was initially effective in removing the arsenic from the syngas. However, breakthrough of arsenic, as indicated by gas phase analysis of the syngas in and out of the catalyst guard bed, was determined to occur in approximately one month on stream. It was later determined that the manganese dioxide was kinetically limited and would be expected to perform acceptably only at elevated temperatures. Catalyst life data during this portion of Catalyst Campaign 2 is shown in Figure 20.

A copper-oxide impregnated activated carbon was identified during this campaign as a suitable adsorbent for the removal of arsenic and sulfur. However, it was not fully implemented in the 29C-40 catalyst guard bed until Catalyst Campaign 3. The catalyst deactivation data for the period following the manganese dioxide adsorbent trial is shown in Figure 21.

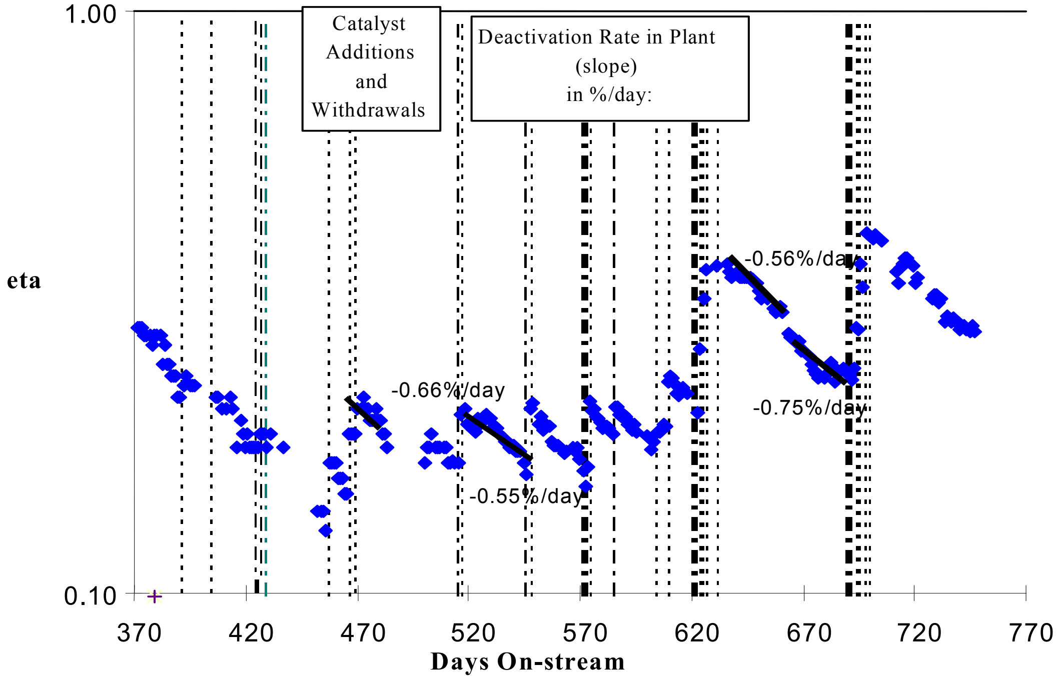

Figure 20. Kingsport LPMEOH™ catalyst life (Catalyst Campaign 2: 1999). Reactor temperature = 235 °C.

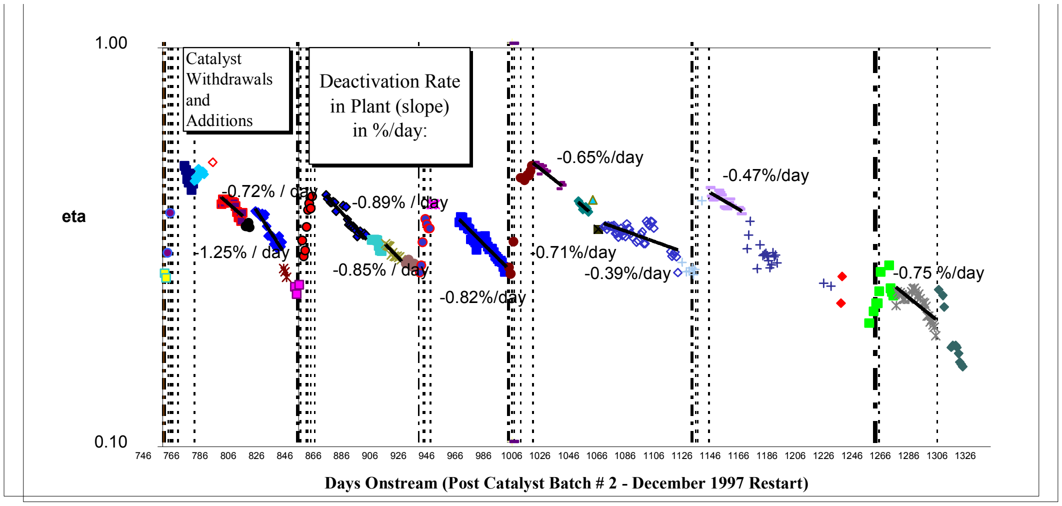

Figure 21. Kingsport LPMEOH™ catalyst life (Catalyst Campaign 2: 2000-2001).
Reactor temperature at 235 °C until Day 1304, when temperature was gradually increased to 250 °C.

5.4 Catalyst Performance: Catalyst Campaign 3

Catalyst Campaign 3 involved the first demonstration of an in-situ catalyst activation concept. A full charge (40,000 pounds) of fresh methanol synthesis catalyst was placed into the LPMEOH™ reactor and reduced at one time. This was in contrast to the batch-wise reduction of smaller catalyst quantities (2,000 pounds each) used earlier in the demonstration program.

The initial activity of the methanol synthesis catalyst for Catalyst Campaign 3 was less than expected when compared with data from the laboratory. The activity problem was later determined to be caused by over-temperature in the slurry storage tank prior to reduction. These conditions allowed a reaction between the inert mineral oil and the fresh catalyst to occur, which resulted in the lower catalyst activity. This is not an inherent problem with the in-situ activation and was ultimately corrected through simple procedural changes to avoid higher temperature storage of the fresh catalyst slurry.

Figure 22 shows the catalyst life plot for the third campaign. During this campaign, reduced copper oxide-impregnated activated carbon (Cu/C) was used exclusively in the 29C-40 catalyst guard bed. A controlled reduction procedure was developed based on laboratory data and the use of the existing catalyst guard bed configuration. This procedure was then used to prepare the adsorbent for service.

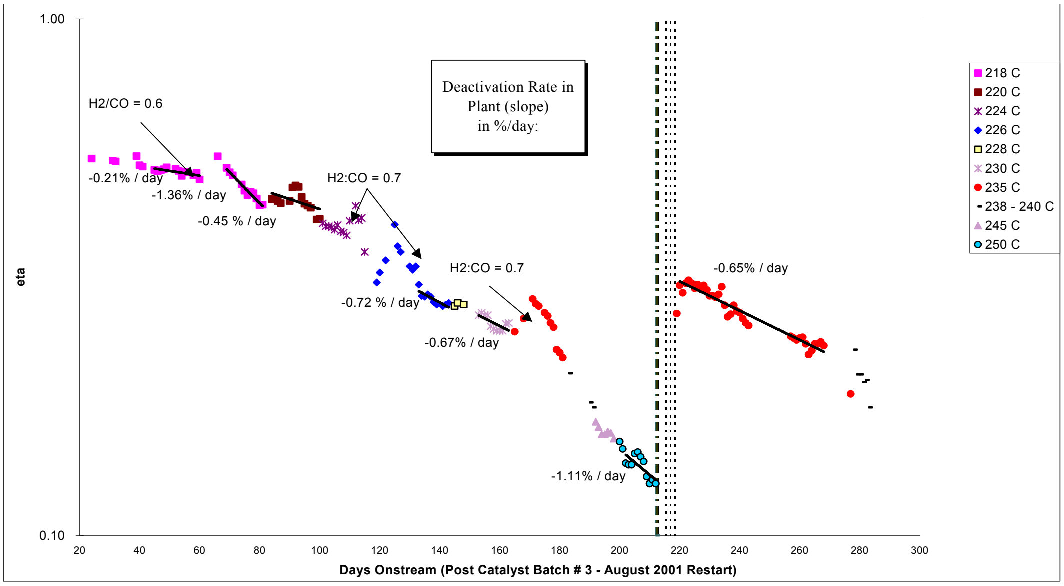

Figure 22. Kingsport LPMEOH™ catalyst life (Catalyst Campaign 3).

The Cu/C adsorbent was effective in reducing arsine concentrations in the feed gas to the LPMEOH™ Demonstration Unit. Gas phase analysis of the syngas stream entering and exiting the 29C-40 catalyst guard bed showed that the guard bed reduced the inlet arsine concentration from approximately 50 to 60 ppb down to the level of detection of 3 to 6 ppb. The results of this testing is shown in Table 57 (Section 4 of this report).

As noted in Section 4 of this report, a thermal treatment step was developed for the Cu/C adsorbent. This treatment allowed for additional service time for the adsorbent. Figure 23 gives an overview of the 29C-40 catalyst guard bed adsorbent operations undertaken during Catalyst Campaign 3. Two thermal treatments were used with the original charge of adsorbent following the in-situ activation. Based on gas phase analysis for arsine, it was determined that the original charge of copper oxide-impregnated activated carbon had an effective operating period of two months and the thermally treated material had an effective operating period of one month.

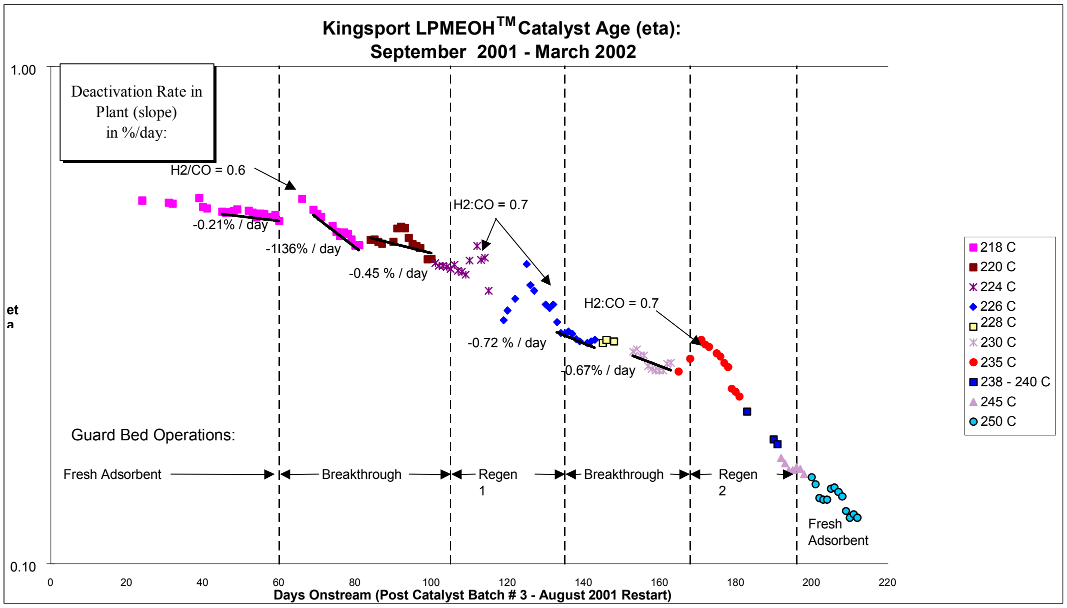

Figure 23. Operations associated with 29C-40 catalyst guard bed during Catalyst Campaign 3.

5.5 Catalyst Performance: Campaign 4

Based on the lower than expected activity achieved during the first in-situ catalyst activation, it was decided to perform another in-situ activation with a revised procedure. This revised procedure was developed to eliminate the step that resulted in the storage of the fresh catalyst slurry at elevated temperatures.

The second in-situ activation was undertaken in late June 2002. At the same time, a fresh charge of copper oxide impregnated activated carbon was reduced and placed into service in the 29C-40 catalyst guard bed. Performance of the LPMEOH™ reactor following the second in-situ catalyst activation is presented in Figure 24. As shown in the figure, catalyst performance was excellent with an approximate catalyst deactivation rate of 0.1 to 0.2 % per day during the first 6 months of operation. In addition, during this time, the initial LPMEOH™ reactor temperature of 215 ^{o}C was not changed. This improved result may have been related to the performance of the adsorbent in the 29C-40 catalyst guard bed, to the removal of carbon steel components from the

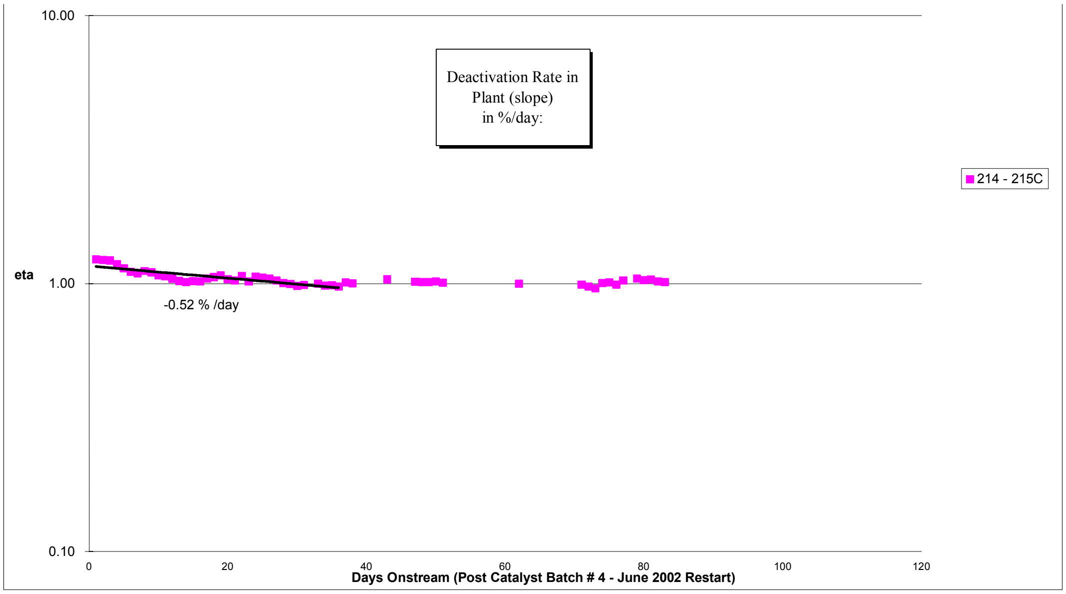

Figure 24. Kingsport LPMEOH™ catalyst life (Catalyst Campaign 4).

reactor internals, and to the operation of the LPMEOH™ reactor at reduced temperature (temperature programming).

C. Conclusions

1. A wide variety of syngas contaminants were evaluated to determine their effect on methanol synthesis catalyst activity in the laboratory. Included were contaminants containing arsenic, phosphorus, sulfur, nitrogen, halides, iron, and nickel. Of these, arsine, phosphine, carbonyl sulfide, carbon disulfide, thiophene, methyl thiocyanate, methyl chloride, methyl fluoride, iron carbonyl, and nickel carbonyl were found to increase the rate of catalyst deactivation and, thus, are catalyst poisons. If these poisons are not removed from the syngas feed to a methanol synthesis reactor, a decrease in catalyst activity will occur. The nitrogen containing contaminants methyl amine, hydrogen cyanide, and acetonitrile were found to have no effect on catalyst activity and, thus, removal of these contaminants from the syngas feed is not required. Based on the results of this study, the following ranking of methanol synthesis catalyst poison strength was obtained: $Ni(CO)_4 > Fe(CO)_5 >$ thiophene $\cong AsH_3 > CH_3Cl > CH_3SCN > CS_2 > COS > PH_3 > CH_3F$.

2. Ten adsorbents were screened for effectiveness for arsine removal and for safe usage under syngas. The adsorbents consisted of various metal oxides supported on alumina or carbon and, in one case, carbon alone. All with the exception of those containing PbO exhibited an affinity for AsH_3. The ineffectiveness of PbO-based adsorbents was unexpected and traced to formation of inactive surface $PbCO_3$ in the presence of carbon

dioxide containing syngas. A reduced copper oxide impregnated activated carbon (reduced CuO/C or Cu/C) adsorbent was judged to be the most suitable adsorbent and it was evaluated more thoroughly.

3. The arsine affinity of CuO/C was very high with a minimum capacity of 3.0 wt% arsenic. Both the CuO and C regions of the adsorbent appear to react with AsH_3. The reduced adsorbent, Cu/C, was much less effective for AsH_3 removal and at 30 °C its capacity was 1.74 weight % but it effectiveness was substantially better at elevated temperature with a minimum arsenic capacity of 4.31 wt% at 140 °C. A novel thermal treatment procedure to restore the capacity of the adsorbent for arsine was developed.

4. The Cu/C adsorbent was slightly less effective for PH_3 removal at 140 °C than for AsH_3. Removal of other common syngas contaminants was not satisfactory at 140 °C. The sulfur-containing contaminants thiophene, COS, and CS_2 were only partially removed from a syngas feed and breakthrough was observed for each. The adsorbent had almost no affinity for CH_3Cl. It is likely that these results reflect a kinetic limitation and higher bed temperatures will be required for effective thiophene, COS, CS_2, or CH_3Cl removal. The Cu/C adsorbent was very effective for removal of $Fe(CO)_5$ and $Ni(CO)_4$ at 30 °C but less effective at 140 °C. This implies that metal carbonyls are removed by being adsorbed on the carbon portion of the adsorbent rather than by reaction with metallic copper.

5. Enhanced (non-catalytic) activated carbon was examined as an alternative to Cu/C because it contained no metals and, hence, its use was not complicated by safety or performance issues associated with reduction. The arsenic adsorption profiles for the enhanced carbon and Cu/C were quite similar at 30 °C. However, because the Cu/C performance at 140 °C was far superior to that of enhanced activated carbon at 30 °C, the enhanced carbon would be a possible alternative to Cu/C only for applications limited to ambient temperature guard beds.

6. Conclusions regarding the catalyst properties for Kingsport Catalyst Campaign 2 were complicated by additions of freshly reduced catalyst and withdrawals of aged catalyst during the run. Copper surface area decreased with time on stream. Three significant contaminants were found on spent catalyst samples – arsenic, sulfur, and iron - with arsenic being the most abundant. The total arsenic and sulfur loading on the catalyst correlated with an exponential decrease in eta, a measure of catalyst activity. Nitrogen, cyanide, or halides were not detected on the catalyst. XAS studies showed that a phase most similar to Cu_3As was formed on the catalyst. Mineral oil from the liquid phase reactor was found to contain some unsaturated hydrocarbons not present in the fresh oil but concentrations were approximately constant with run time and were judged not to contribute to catalyst deactivation. Gas phase analysis clearly showed the presence of an arsenic containing species in the syngas feed and, based on the reducing nature of syngas, most likely arsine, AsH_3.

7. An in-situ activation of the catalyst in the oxide form and mineral oil was performed for Catalyst Campaign 3 using dilute syngas. Catalyst additions/withdrawals were not used

until the very end of the run. The initial characterization of catalyst samples from the LPMEOH™ Demonstration Unit showed unexpectedly low methanol synthesis activity and unexpected properties. Initial copper crystallite sizes were larger than expected, implying that some sintering occurred. Only a minor increase in copper crystallite size was observed over the 213 days prior to catalyst addition/withdrawal. The catalyst surface area, average pore diameter, and pore volume varied modestly. The initial copper surface area was significantly lower than expected but it remained constant. XRF and elemental analysis indicated the present of only two contaminants, iron and arsenic, over the entire run. Iron concentrations increased at substantial rate with a final value of 534 ppmw. The increase in arsenic concentration was much more modest with a maximum of 318 ppmw. Sulfur was below its limit of detection, 160 ppmw, throughout the run. The substantial increase in Fe concentration was unexpected and troubling. Analysis showed <8 ppb $Fe(CO)_5$ in the 29C-40 catalyst guard bed inlet and outlet. Furthermore, a laboratory evaluation showed that the $Fe(CO)_5$ removal capacity of the Cu/C adsorbent was very high. Thus, breakthrough of $Fe(CO)_5$ to the reactor was very unlikely. It was later determined that the incorrect addition of carbon steel parts to the LPMEOH™ internals most likely was the source of the unexpected iron contamination.

8. The 29C-40 catalyst guard bed was designed for ambient temperature operation and to target the removal of carbonyl contaminants. With the exception of two instances of the accidental introduction of iron to the system in Catalyst Campaign 1 (construction debris) and Catalyst Campaign 3 (incorrectly installed carbon steel parts in the LPMEOH™ reactor), iron and nickel carbonyls have never been a major issue associated with the performance of the methanol synthesis catalyst. In addition, iron carbonyl has never been significantly measured in the gas entering the 29C-40 catalyst guard bed. Arsenic, and to a lesser degree sulfur, have been the main contaminants analyzed on the samples of catalyst slurry taken from the LPMEOH™ reactor. Two adsorbents to target arsenic and sulfur were evaluated during Catalyst Campaigns 2 through 4. During Catalyst Campaign 2, the 29C-40 catalyst guard bed was charged with 50% by volume manganese dioxide and 50% activated carbon. The manganese dioxide adsorbent displayed affinity for arsenic removal but the adsorbent bed broke through (based on gas phase arsine analysis) in approximately one month of service. During Catalyst Campaigns 3 and 4, a copper oxide-impregnated activated carbon adsorbent was reduced and placed into service. This adsorbent was effective in arsine removal as determined by gas phase analysis and catalyst sample results. During these campaigns, the AsH_3 concentration was reduced from 50 to 60 ppb to < 5 ppb AsH_3 downstream of the 29C-40 catalyst guard bed. The freshly reduced copper oxide-impregnated activated carbon had a service life of about two months at the LPMEOH™ Demonstration Unit. An innovative thermal treatment was employed to extend the service life of the adsorbent by two additional months.

9. Catalyst Campaign 4 at the LPMEOH™ Demonstration Unit was the second campaign to use an in-situ activation procedure. Catalyst performance during this campaign was excellent with an approximate catalyst deactivation rate of 0.1 – 0.2 % per day during the first 6 months of operation. The initial LPMEOH™ reactor temperature of 215 ^{o}C was not increased during the first six months of operation due to the very low catalyst

deactivation rates and consistent reactor productivity during this campaign. This improved result may have been related to the performance of the Cu/C adsorbent in the 29C-40 catalyst guard bed, the removal of carbon steel components from the reactor internals, and the operation of the LPMEOH™ reactor at reduced temperature (temperature programming).

10. Although several different adsorbents were evaluated in the LPMEOH™ Demonstration Unit, it was difficult to positively correlate catalyst performance, as measured by catalyst activity or eta, with the adsorbent performance. This was due to the presence of other variations in operation not related to the adsorbent, such as upstream gas composition, which can result in variations in the kinetic model predictions of eta. The copper oxide-impregnated activated carbon was found to be effective for arsenic removal at ambient temperature based on results from gas phase arsine analysis (in and out of the 29C-40 catalyst guard bed) and also based on analysis of catalyst samples from the LPMEOH™ reactor.

D. References

1. Diamond, B.W.; Heydorn, E.C.; Tijm, P.J.A.; Street, B.T.; Kornosky, R.M. "Commercial-Scale Demonstration of the Liquid Phase Methanol (LPMEOH™) Process: Operating Experience Update", Seventh Annual Clean Coal Technology Conference, Knoxville, TN, June 1999.
2. Beishon, D. S., Hood, J., Vierrath, H. E., Proceedings of the 6th Annual International Pittsburgh Coal Conference, Pittsburgh, PA, USA, 25-29 September 1989, p. 539-547.
3. "X-Ray Absorption: Principles, Applications, techniques of EXAFS, SEXAFS, and XANES", D. C. Koningsberger, R. Prins, Eds., Wiley-Interscience, New York, 1988.
4. Thermodynamics calculated were performed using "HSC Chemistry for Windows" version 2.03, Outokumpu Research.
5. Saleh, J. M., J. Chem. Soc. Faraday Trans, , **68**, 1520-1527. (1972)
6. US patent 6,063,349 (2000) as an example. There are numerous references to HCN as a FT catalyst poison in the patent literature.
7. Kung, H. H., Catalysis Today, **1992**, 11, 443-453.
8. Twigg, M. V.; Spencer, M. S. Appl. Cat. A., **212**, 161-174 (2001).
9. Young, P. W.; Clark, C. B. Chem. Eng. Progress, **69**, 69-74 (1973).
10. Grant, A. W.; Ranney, J. T.; Campbell, C. T.; Vans, T.; Thornton, G. Catalyst Let., **65**, 159-168 (2000)
11. Lacher, J. R.; Emery, E.; Bohmfalk, E.; Park, J. D. J. Phys. Chem., **60**, 492-495 (1956).
12. The Chemist's Companion, Gordon, A.J., Ford, R.A. eds., John Wiley & Sons. p. 113 (1972)
13. Roberts, G. W., Brown, D. M., Hsiung, T. H., Lewnard, J. J. Chem. Eng Sci. **45**, 2713-2720 (1990).
14. Roberts, G. W., Brown, D. M., Hsiung, T. H., Lewnard, J. J. Ind. Eng. Chem. Res., **32**, 1610-1621, (1993),
15. Golden, T. C.; Hsiung, H.; Snyder, K. E. Ind. Eng. Chem. Res., **29**, 502-507 (1991).
16. Stirling, A. J. Am. Chem. Soc. **124**, 4058-4067 (2002).
17. Menendez, J.A.; Phillips, J.; Xia, B.; Radovic, L.R. Langmuir **12**, 4404-4410 (1996) for example.
18. Carr, N.L.; Stahlfeld, D.L. Hydrocarbon Processing 100-102, May 1985
19. Carr, N.L.; Massoth, F. E.; Stahlfeld, D.L.; Young, J.E. US patent 3,782,076 (1974)
20. Carr, N.L.; Stahlfeld, D.L. US patent 3,789,581 (1974)
21. Watanabe, T.; Imai, H.; Suzuki, T. J. Electrochem. Soc., **143**, 2654-2657 (1996).
22. Mellor, J. W. A Comprehensive Treatise on Inorganic and Theoretical Chemistry, Volume IX, John Wiley & Sons, Inc. p. 62-64 (1960).
23. Comprehensive Inorganic Chemistry, Trotman-Dickenson, A.F., exec. ed., Pergamon Press, Vol. 2,p. 415 (1973).
24. Lange's Handbook of Chemistry, ed. Dean, J.A., McGraw-Hill Book Co., p. 3-127 (1985).
25. Bhatt, B.L.; Golden, T.C.; Hsiung, T.H. Sep. Sci. Tech. 26, 1559-1574 (1991)
26. Blankenship, S.A.; Voight, R.W. US patent 5,990,372 (1999)
27. Sun, J. T.; Metcalfe, I.S.; Sahibzada, M. Ind. Eng. Chem. Res. **38**, 3868-3872 (1999).
28. Robinson, W.R.A.M.; Mol, J.C. Appl. Cat. **63**, 165-179 (1990).
29. Robinson, W.R.A.M.; Mol, J.C. Appl. Cat. **60**, 73-86 (1990).
30. "Project Data on Eastman Chemical Company's Chemicals-From-Coal Complex in Kingsport, TN", Topical Report, Cooperative Agreement No. DE-FC22-92PC90543, March 2003.
31. Commercial Scale Demonstration of the Liquid Phase Methanol Process, Public Design Report (Final Report, Volume 1: Public Design), January 2000
32. Beishon, D. S., Hood, J., Vierrath, H. E., Proceedings of the 6th Annual International Pittsburgh Coal Conference, Pittsburgh, PA, USA, 25-29 September 1989, p. 539-547.

Appendix A. Experimental Techniques

1. Experimental methods

1.1. Effects of syngas contaminant on catalyst activity experiments. The apparatus used has been described in detail previously.[2] Reactions were performed in a 300 cc stirred reactor. Each contaminant was evaluated using the following procedure. Methanol synthesis catalyst powder, ~10 g (oxide form), in ~120 g mineral oil was reduced using 2 vol% H_2 in N_2 at 100 psig, 200 standard cubic centimeters per minute (sccm) flow. The reactor temperature was gradually ramped from 100 ^{o}C to 240 °C. The reduced catalyst slurry was then exposed to syngas at ~750 psig and ~6,000 GHSV and the temperature was increased to 250 °C. Exposure to clean syngas was continued, usually at least 150 hours, until a baseline deactivation rate could be calculated. The desired contaminant was introduced into the syngas feed by blending with a pre-mixed secondary feed. Each pre-mixed cylinder gas contained ppm levels of contaminant in 5 vol% CO and 95 vol% H_2. Contaminant exposure was continued until a deactivation rate could be obtained (usually <100 hours). The secondary feed flow was stopped and exposure of the catalyst to clean syngas was continued until a deactivation rate was obtained again. Upon completion of a run, the catalyst slurry was removed and saved for analysis.

1.2. HCN reactivity at low temperature. A bed consisting of three layers of methanol synthesis catalyst pellets separated by thin plugs of quartz wool was reduced with 2 vol% H_2 in N_2 and a manually controlled temperature ramp, 100 to 190 °C. The reduced catalyst at 30 ^{o}C was then exposed to Kingsport Gas containing 51.3 ppm HCN over 2.0 days. The average exit composition over the run was 68.20 vol% H_2, 22.79 vol% CO, 4.58 vol% CO_2 and 4.08 vol% N_2. Water concentration varied from 0.13 vol% initially to 0.027 vol% by end of run. No methanol or other organics were observed in the bed exit. The spent bed was analyzed for cyanide.

1.3. $Fe(CO)_5$ formation in the absence of catalyst. Prior to use, the reactor was cleaned using the normal procedure (Ultrasonic cleaner, soapy warm water for several hours). The reactor was loaded with 120 g fresh mineral oil and heated to 250 °C under helium (He) at 100 psig. Flow of Shell Gas (tube trailer) was begun at ~1,000 sccm and the reactor was quickly pressurized to 750 psig. GC analysis showed the reactor inlet was free of $Ni(CO)_4$ and $Fe(CO)_5$. The reactor exit was then monitored using the carbonyl GC and the $Fe(CO)_5$ concentration over the 33 hour run.

1.4. Adsorbent testing. Adsorbents were tested using a 1.66 cm diameter bed. Layers of adsorbent were separated by thin plugs of quartz wool. A trap was placed downstream of the adsorbent and consisted of either activated carbon or additional adsorbent separated from the test material by a large plug of quartz wool. The test bed was heated to the desired using a heating mantle and heating was controlled by a thermocouple on the external wall of the bed. In many experiments, the internal bed temperature was monitored by thermocouples placed at the bed inlet, middle, and outlet; alternatively, one thermocouple was placed in the middle of the bed. Prior to syngas exposure, the bed was purged with N_2 to insure residual O_2 was removed. With the bed pressurized to 750 psig, syngas flow was begun. The syngas feed was most often Kingsport Gas, approximate composition: 68 vol% H_2, 23 vol% CO, 5 vol% CO_2, 4 vol% N_2. For runs involving PbO-based adsorbents, an in-line microporous filter was placed downstream of the bed to trap any dust particles. EDS analysis found no detectable quantities of Pb, Al, As, or Mn on the spent filters, although some particles consistent with stainless steel or rust were found. One run involving the PbO/Al_2O_3 adsorbent used a CO_2-free syngas obtained by blending the H_2, CO, and N_2. For experiments involving Cu/C, the CuO/C form of the adsorbent was reduced using 2.06 vol% H_2 in N_2, 100 psig, 350 GHSV. A heating ramp was generated by manually raising the temperature: 100 °C for 2.5 hours; 125 °C for 1 hour; 150 °C for 1 hour; 160 °C for 15 hours; 180 °C for 1 hour; 220 °C for 2 hours. Gases exiting the bed were analyzed by GC.

The CuO/C adsorbent was also exposed to syngas at higher temperatures, 40, 60, and 80 °C. In these experiments, test beds containing 5 g samples of powdered CuO/C were initially purged with N_2 and pressurized to 80 psig. Syngas (Kingsport gas) was introduced and the pressure was increased to about 750 psig over 24 minutes. Upon completion of each run, the spent adsorbent was unloaded under N_2 and the solids were placed under mineral oil to inhibit air oxidation during analysis.

Following the initial exposure to syngas and return to the initial bed temperature, the desired contaminant was introduced by blending syngas with a secondary feed. For example, the arsine secondary feed was obtained from a cylinder containing 15-17 ppm AsH_3 and 5 vol% CO in H_2. Contaminant feed concentrations were calculated from the measured flow rates of the syngas and of the secondary feed. In the case of metal carbonyl exposure, GC analysis of the secondary feed cylinder indicated it contained 0.729 ppm $Ni(CO)_4$ and a $Fe(CO)_5$ peak too large to quantify. The $Fe(CO)_5$ concentration was based on other experimental results and calculated as 81.3 ppm. Reported Fe and Ni concentrations on spent Cu/C were corrected the background concentrations of these metal on the clean adsorbent. Another metal carbonyl exposure experiment was conducted using a test bed consisting of 5.927 g Cu/C in four layers separated by thin plugs of quartz wool was evaluated at 30 °C and 750 psig. The bed feed was Shell Gas from a tube trailer blended with cylinder H_2 to give approximately Kingsport Gas (average comp. 73.6 vol% H_2, 23.6 vol% CO, 1.1 vol% CO_2, 0.4 vol% N_2; GHSV 6,531). The Shell Gas contained volatile carbonyls, 912 ppb $Fe(CO)_5$ and 437 ppb $Ni(CO)_4$ by GC. Following blending with H_2, GC analysis showed that the initial feed contained 567 ppb $Fe(CO)_5$ and 115 ppb $Ni(CO)_4$. Volatile carbonyl concentrations were found to vary over the run (outside temperature, different tube on tube trailer) but the average inlet concentrations (by GC) were 580 ppb $Fe(CO)_5$ and 112 ppb $Ni(CO)_4$.

1.5. Methanol synthesis activity of Cu/C. A test bed containing CuO/C pellets was reduced as described above. The H_2 uptake was consistent with 12.8 wt% Cu versus the expected 10 wt%. Flow of Kingsport Gas at 753 psig and GHSV of 3,017 h^{-1} was begun. The bed temperature was increased from 100 to 250 °C in 25 °C increments. The composition of the bed outlet gas, including methanol or other organics, were determined at each temperature. Upon completion of the run, the spent Cu/C was unloaded under a N_2 atmosphere and placed under mineral oil to inhibit air oxidation during subsequent analysis.

1.6. Reduction of CuO/C with dilute syngas. A test bed containing 24.272 g CuO/C was exposed to 1.09 vol% syngas (CO+H_2) in N_2 (65.0 psig, 159.2 sccm total feed, GHSV 394 h^{-1}) at an internal bed temperature of 100 °C. Dilute syngas was obtained by blending N_2 with cylinder Kingsport Gas - 69.4 vol% H_2, 21.1 vol% CO, 4.5 vol% CO_2, 5.0 vol% N_2. In a second experiment, 24.397 g CuO/C was exposed to 1.09 vol% ($CO+H_2$) in N_2 (65.0 psig, 159.2 sccm total feed, GHSV 392) at 80 °C. Both beds were unloaded under N_2 and the solids were placed under mineral oil to inhibit air oxidation during analysis.

1.7. Experiments involving MnO_2/Al_2O_3. To evaluate its potential reduction, a test bed containing 17.603 g MnO_2/Al_2O_3 at 40 °C was exposed to Kingsport Gas at 745 psig, 1,462 sccm, 3,210 h^{-1} for 73 hours. In a second experiment, 5.161 g MnO_2/Al_2O_3 was heated to 100 °C and exposed to Kingsport Gas at 750 psig; 400 sccm; 2,995 h^{-1} for 72 hours. The spent adsorbents were unloaded under N_2 and the solids were placed under mineral oil to inhibit air oxidation during analysis.

2. Analytical methods

2.1. Catalyst sample preparation. Prior to sample preparation, the solid loading of the well mixed slurry was determined by TGA. The sample was heated to 800 °C at 10 °C per minute under a 100 sccm N_2 purge. Weight loss, which began at about 110 °C, was monitored as a function of temperature. The weight remaining at 600 °C was taken to be the solid content of the slurry.

Depending on the analysis to be performed, either a catalyst slurry or a dry, solid catalyst was required. For analysis requiring a slurry, a portion of the slurry sample was centrifuged to separate the solid and oil phases. The sample was transferred into a N_2-purged dry box where most of the oil was poured off and discarded or used for further analysis (see below). Concentrated slurry was used for XRF, XRD, and particle size distribution analysis. Other analysis required a dry solid sample. Solids were obtained from the concentrated mineral oil-catalyst slurries by a cyclohexane extraction. A portion of concentrated slurry was transferred to a Whatman 33x80 mm cellulose extraction thimble and placed in a Soxhlet extraction apparatus fitted with a 500 milliliter (mL) round bottom flask and a reflux condenser. About 300 mL cyclohexane was placed in the flask and heated to reflux over an 8 hour period. Usually, this procedure was repeated with a fresh charge of cyclohexane. The extraction thimble and contents were removed from the extraction apparatus, excess cyclohexane was poured off, and the remaining solid dried by standing overnight in the N_2-purged dry box. The resulting solid was dried under vacuum for at least several hours. The dry solid is potentially pyrophoric because of air oxidation of metallic copper to Cu_2O or CuO and, hence, it must be stored and handled under an inert atmosphere.

2.2. UV analysis of mineral oil samples. For some catalyst slurry samples, the separated mineral oil (see above) was characterized by UV spectroscopy. A small amount of mineral oil was filtered through a 25 μm syringe filter to remove particulates. The filtered mineral oil was diluted with cyclohexane to a 1 to 2 wt% solution. UV/visible spectra were recorded against a cyclohexane baseline. Absorbances were normalized by dividing the absorbance by the mineral oil concentration in weight %.

2.3. XRD/XRF. Average crystallite sizes were calculated using the Scherrer equation which utilizes profile breadths corrected to an external standard (NBS 676, alumina). Samples were scanned as mineral oil slurries on a glass slide using the Siemens/Bruker D5000 from 20 to 80°

using parallel beam optics, a 0.02° step size and 1.5 second count time. Additional analysis was performed on the PW1480 Spectrometer using plastic cups covered with Prolene film in a He atmosphere. XRF concentrations were obtained using the semiquantitative program UNIQUANT which provides estimates of all elements, Na to U. Elemental concentrations were corrected for the weight of mineral oil present and were reported based on dry catalyst.

2.4. BET surface area, pore size distribution, and pore volume. A N_2 adsorption/desorption isotherm at –196 °C was measured using ASTM method D-4222. Pore size distribution was calculated from desorption data using the method developed by Barret, Joyner, and Helenda based on the Kelvin equation. Prior to the isotherm, the sample was outgassed at ambient temperature under vacuum for several hours.

2.5. Particle size distributions. The particle size distributions of spent catalyst slurries were determined using a Horiba LA-910 laser scattering particle size distribution analyzer. Drakeol-10 mineral oil was used to dilute slurry samples to a concentration suitable for analysis. The technique can determine particle size ranging from 0.022 to 1,020 μm.

2.6. Elemental analysis. Samples were opened in a glove bag under N_2. For arsenic, iron, nickel, sulfur, and other trace elements analysis, 0.25 g sample and 10 mL of high purity nitric acid in a sealed microwave digestion vessel were placed in a microwave oven under high power for a few minutes. Following cooling, the sample solution was diluted with high purity deionized water. Standard and blank solutions were prepared in the same matrix. All standard, blank, and sample solutions were analyzed by Inductively Coupled Plasma Atomic Emission Spectroscopy (ICP-AES). For copper, zinc, and aluminum analysis, 0.20 g solid, 25 mL of high purity nitric acid and 10 mL of high purity sulfuric acid were combined in a 500 mL Erlenmeyer flask. The flask was placed on a hotplate with high heat until only the sulfuric acid portion of the acid digest remained. After cooling, 10 mL of high purity nitric and hydrochloric acids are added and the solution was diluted with high purity deionized water. Standard and blank solutions were prepared in the same matrix. All standard, blank, and sample solutions were analyzed by ICP-AES. For silicon, aluminum, and halides, 0.4 g solid and 5 mL of a high purity solution composed of 50% potassium hydroxide, 5% potassium nitrate, and deionized water were placed in a 50 mL nickel crucible. The crucible was heated to 600 °C for 2 hours in a muffle furnace. After cooling, the product was dissolved in deionized water slightly acidified with nitric acid and diluted with additional deionized water. Standard and blank solutions were prepared in the same matrix. All standard, blank, and sample solutions were analyzed by ICP-AES. For non-routine chloride analysis, sample solutions were analyzed using chloride ion selective electrode. Additional analyses were performed at Galbraith Laboratories, Knoxville, TN. These included standard C, H analysis by combustion, carbonate, cyanide, total fluorine, total halogen as chlorine, and nitrogen by the Kjeldahl method.

2.7. Copper surface area measurements. Copper surface areas were determined by a N_2O titration of the solid catalyst. Samples were loaded into a quartz U-tube in argon (Ar) dry box. Each sample was reduced under a flow of 10 vol% H_2 in Ar and a temperature ramp of 1 °C per minute to 180 °C for 30 minutes followed by cooling to 60 °C under an Ar purge. Pulses of N_2O were injected into the sample vessel by blending 500 μl 10 vol% N_2O in He with an Ar purge where reaction occurred with surface copper atoms to form Cu_2O and gaseous N_2. Relative concentrations of N_2 and N_2O were monitored using a Pfeizer mass spectrometer. The total N_2O consumption (or N_2 formation) was used to calculate the available copper surface area. One problem of note was identifying an appropriate reference for calibration purposes. Use of freshly reduced methanol synthesis catalyst was plagued by large variations in repetitive measurements and, therefore, large percent errors. More reproducible results were obtained for an aged catalyst sample that had been run for about 1,000 hours. Six repetitive measurements for the aged catalyst gave an average value of 24.7 m^2/g with an error of 4.49%. Prior to N_2O titration, solids were routinely prereduced with dilute H_2. For one sample (K0004-1), the copper surface area without a pre-reduction was found to be lower, 10.65 vs. 12.87 m^2/g, indicating the presence of some oxidized copper surface, either due to air contamination or formation during the catalytic cycle.

2.8. XPS, AEM, XAS. X-ray photoelectron spectroscopy (XPS) results were acquired on the PHI 5000LS ESCA spectrometer with a base operating pressure of $1x10^{-9}$ torr. A standard MgK_α x-ray source was used under the following conditions: 15 keV accelerating voltage, 400 W, 800 μm spot-size, and 45° take-off angle. Analytical electron microscopy (AEM) elemental mapping was performed at Lehigh University using VG HB603 STEM. X-ray absorption spectroscopy (XAS) results were obtained at the Stanford Synchrotron Radiation Laboratory**.**

2.9. Gas phase arsenic analysis. Gas phase arsenic concentrations in a syngas feed were determined using a modified version of NIOSH Method 6001 "Arsine" in which arsenic was trapped on a column of activated carbon. The limit of detection was 1 ppb arsenic (as arsine).

2.10. Thermal analysis of adsorbents. TGA/IR/DSC analysis was obtained using a TA 2960 SDT. Samples were heated from room temperature to 1,000 °C at 10 °C per minute. Weight changes, thermal changes, and IR of evolved gases were obtained under N_2 or 3 vol% H_2 in N_2 flowing at 100 cc per minute. The evolved gases were passed through a 10 cm IR gas cell and spectra were recorded at 4 cm^{-1} resolution on MIDCA IR. For PbO-containing adsorbents, TGA/IR/DSC data was also collected using a 100 cc per minute CO_2 flow.